TABLE OF CONTENTS

LIST OF TABLES

Page

LIST OF FIGURES

Page

Clicours.COM

LIST OF ABREVIATIONS

A	Power absorbed
AC	Alternating current
A_{eff}	Effective absorbance
AEM	Ethylene acrylic elastomer dipolymer
CB	Carbon black
CF	Carbon fiber
CNT	Carbon nanotube
COOH–SWCNT	SWCNT chemically functionalized with COOH
COPA	Polyamide thermoplastic elastomers with polyamide hard segments and soft segments based on aliphatic polyesters or aliphatic polycarbonates
COPE	Copolyether-ester block thermoplastic
CR	Polychloroprene
CSM	Chlorosulfonated polyethylene
CuNW	Copper nanowire
DBSA	Dodecylbenzene sulfonic acid
DC	Direct current
ECC	Electrically conductive composites
ECE	Electrically conductive elastomers
ECPC	Electrically conductive polymer composites

EM	Electromagnetic
EMA	Ethylene methyl acrylate
EMC	Electromagnetic compatibility
EMI	Electromagnetic interference
ENR	Epoxidized natural rubber
EG	Expanded graphite
EVA	Poly (ethylene-vinyl acetate)
FKM	Fluoroelastomer
I	Incident radiation
ICP	Intrinsically conducting polymers
IEC	International Electrotechnical Commission
IIR	Butyl rubber
G	Graphite
GHz	Giga Hertz
GnP	Graphene nanoplatelets
GNR	Graphene nanoribbon
LDPE	Low density Polyethylene
MA	Maleic anhydride
MWCNT	Multi-walled carbon nanotubes
NPs	Silver nanoparticles
NR	Natural rubber

PAni	Polyaniline
PAni.DBSA	Polyaniline doped with dodecylbenzene sulfonic acid
PC	Polycarbonate
PDMS	Polydimethylsiloxane
PMMA	Poly(methyl methacrylate)
PP	Polypropylene
PPy	Polypyrrole
PS	Polystyrene
PTT	Polytrimethylene terephthalate
PVA	Polyvinyl alcohol
R	Power reflected
RAM	Radar absorbing material
RET	Reactive ethylene terpolymer
RFI	Radio frequency interference
SAE	Styrene acrylic emulsion
SBC	Styrenic block copolymers
SBR	Styrene–butadiene rubber
SBS	Styrene–butadiene–styrene triblock copolymer
SCF	Short carbon fiber
SE	Shielding effectiveness
SE_A	Shielding by absorption
SE_M	Shielding by multiple reflections

SE_R	Shielding by reflection
SEBS	Poly (styrene-b-ethylene-ran-butylene-b-styrene)
SEBS-MA	SEBS grafted maleic anhydride
SG-CNT	“Super-growth” single-walled CNTs
Si	Siloxane rubber
SMP	Shape-memory polymer
S-parameters	Scattering parameters
SWCNT	Single-walled carbon nanotubes
T	Power transmitted
TPE	Thermoplastic elastomers
TPO	Polyolefin-based thermoplastic elastomers
TPU	Thermoplastic elastomers based on polyurethanes
TPV	Thermoplastic elastomers based on dynamically vulcanized elastomer-plastic blends
TRG	Thermally reduced graphene nanosheets
USD	United States Dollars

LIST OF SYMBOLS

f	Weight fraction of additive in the insulating matrix
f_p	Weight fraction of the conductive additive in the percolation threshold
G’	Storage modulus
G’’	Loss modulus
rad	Radian
rpm	Revolutions per minute
S	Siemens
s	Second
^{t}	Critical exponent
t	Thickness
tanδ	Loss tangent or dissipation factor
T_g	Glass Transition
T_m	Melt Transition
ω	Angular frequency
ε	Complex dielectric permittivity
ε’	Real part of dielectric permittivity
ε’’	Imaginary part of dielectric permittivity
η*	Complex viscosity
λ	Thermal conductivity
ρ	Electrical resistivity
σ	Electrical conductivity

σ_c	Electrical conductivity of the conductive phase

INTRODUCTION

0.1 General background

The extraordinary ongoing development in electrical and electronic fields are boosting the progress and improvement of electromagnetic interference (EMI) shielding materials. The miniaturization of the systems and equipment, and the higher power levels and higher frequencies used in these technologies are demanding the development of multifunctional materials in order to reduce interference inconveniences, meet mechanical performance requirements, and respect electromagnetic compatibility regulations.

The development of conductive shielding enclosures is one of the most important approaches to control EMI. In this case, the EMI shielding is a "box or housing" and works by isolating the EMI emitter or receiver (Tong, 2009). The most often used materials for EMI shielding enclosure applications are metal, magnetic materials, plastic cover with conductive layers, or conductive composites (Geetha, Satheesh Kumar, Rao, Vijayan, & Trivedi, 2009; Markham, 1999; Tong, 2009).

For the best shielding effectiveness, the ideal shielding enclosure would be a hollow sphere made of thick metal, with no seams or openings (Tong, 2009). However, obviously, it is not possible to use such an enclosure to protect electronic devices, since it would prevent the use of power cords, data cables, displays, or ventilation systems (Tong, 2009). In a more realistic perspective, a better choice for a material for shielding enclosure considers the balance between shielding effectiveness, mechanical requirements, weight, convenience, esthetic, manufacture, and cost. Consequently, as electronic systems become more complex, electrically conductive polymer composites (ECPCs) could be an excellent option for shielding gaskets and enclosures due to their good ratio between performance and benefits.

Effective materials for EMI shielding present as basic prerequisites some characteristics, such as moderately high electrical conductivity (usually around 1 $S.m^{-1}$) and/or high dielectric

constant (Z. Liu et al., 2007; Thomassin et al., 2013; Udmale V, 2013), and the minimum shielding effectiveness (SE) required is, in general, equal or higher than 20 dB (Cao, Wang, Cao, & Yuan, 2015; Maiti, Shrivastava, Suin, & Khatua, 2013; Yonglai, Mool, & Kenneth, 2007). Factors such as the distance between the source and shielding material, material's thickness, the frequency in which analysis is performed, polymer matrix, and processing parameters strongly influence the EMI-SE values (Al-Saleh, Saadeh, & Sundararaj, 2013; Singh, Ohlan, & Dhawan, 2012; Udmale V, 2013). Moreover, in the case of composite materials, the EMI shielding effectiveness (SE) also depends on the aspect ratio, defects, alignment, dispersion and distribution of conductive fillers (Z. Liu et al., 2007; Thomassin et al., 2013; Udmale V, 2013).

In ECPCs, the change of electrical conductivity from insulator to conductor is due to the formation of an electrical conducting network of conductive fillers: for a given amount of conductive filler in the insulating matrix, known as electrical percolation threshold, the system starts conducting electricity.

At the present time, carbon particles are the most widely used class of conducting additives in polymer composites for EMI shielding (Thomassin et al., 2013). Among the carbon-based additives, nanosized particles, such as carbon nanotubes (CNT) and graphene, have shown to be very efficient for this application (Basu, Singhi, Satapathy, & Fahim, 2013; Kuilla et al., 2010; Peponi et al., 2009). These nanoparticles present, in general, excellent mechanical and optical properties, high thermal and electrical conductivities, enormous specific areas and high aspect ratios (Bansala, Joshi, Mukhopadhyay, Doong, & Chaudhary, 2017; Basu et al., 2013; El Achaby et al., 2012; H. Kim, Abdala, & Macosko, 2010; Kuilla et al., 2010; Srivastava & Mittal, 2017). However, due to their high surface energy, carbon nanoparticles also present strong particle-particle interactions, and because of that are difficult to disperse in a nanometer level in polymer matrices (Kuilla et al., 2010; Spitalsky, Tasis, Papagelis, & Galiotis, 2010).

In order to improve the dispersion of carbon nanoparticles, different strategies that include covalent and non-covalent functionalization of the nanoparticles are applied. Generally,

covalent functionalization is very effective to improve dispersion, however, the process can damage the structure of the nanoparticles and reduce their intrinsic electrical conductivities (Choudhary & Gupta, 2011). Therefore, non-covalent functionalization that includes the use of polymers or chemical intermediates to induce physical nanoparticle/matrix interactions are preferred in many cases (Choudhary & Gupta, 2011; Vasileiou, Docoslis, Kontopoulou, Xiang, & Ye, 2013).

In carbon based-polymeric nanocomposites the use of matrices with aromatic rings in their chemical structure may facilitate the dispersion of the nanoadditives. In these systems, it is expected interactions between π electrons of the polymer matrix and π electrons of the carbon additive (Y.-T. Liu, Xie, & Ye, 2011; Loh, Bao, Ang, & Yang, 2010; Maiti et al., 2013; You et al., 2014). These interactions increase the dispersion and distribution of the carbon additives, and consequently decrease the amount of additive required to achieve the desired properties, avoid processing issues, and reduce costs. Besides, the combination of carbon additives of different types and shapes are also showing to be an alternative to improve the conductive network in hybrid nanocomposites and reduce the amount of carbon additives needed (M.-S. Kim et al., 2013; Maiti et al., 2013; Sharma, Gupta, Tandon, & Sachdev, 2016; S. Zhang et al., 2013). Additionally, many authors report the use of modified polymer matrices by grafted functional groups as an approach to promote interactions and to improve the dispersion of the conductive additives without decreasing their properties (Vasileiou et al., 2013). One of the most used multifunctional chemical intermediate is maleic anhydride. Moreover, different works available in the literature also point out that the processing methods commonly used to prepare ECPCs can strongly affect the dispersion of carbon nanoparticles, and, in some cases, induce their orientation inside a given polymeric matrix, which, consequently, intensely affect the properties of the final material (Arjmand, Apperley, Okoniewski, & Sundararaj, 2012; Panaitescu et al., 2014; Vasileiou et al., 2013).

The choice of the most suitable polymer matrix depends on each specific application. For example, in many applications it is extremely important to ensure the shielding quality of the joints of a shielded enclosure, otherwise the whole EMI protection could be impaired, while

Clicours.COM

in others is important ensure the coating protection of flexible wires to avoid leakage of information transmitted by EM waves. In these applications, flexible properties are highly desired and electrically conductive elastomers (ECE) are, in general, considered one of the best option as polymeric matrices. Therefore, ECE are being used as EMI shielding materials in many areas, such as electronic, electrical, telecommunications, housing, medical, and automotive industries (Tong, 2009). However, the manufacture of conventional elastomers generally involves many steps, vulcanization process, environmental issues due to the use of solvents, and consequently high time and cost of production. Therefore, thermoplastic elastomers (TPEs) are being used as an alternative to replace conventional elastomers.

TPEs are, in general, phase-separated systems that present a hard phase acting as thermoreversible cross-links, and a soft phase that provides flexibility and elasticity. Because of that, these materials present the huge advantage of being manufactured as thermoplastics at the same time that exhibit mechanical behavior similar to conventional vulcanized elastomers Among many different classes and types of TPEs, one of the most widely used is the poly (styrene-b-ethylene-ran-butylene-b-styrene) (SEBS) (Drobny, 2007a). SEBS is basically a block copolymer that exhibits morphology generally constituted by three interconnected blocks, two rigid blocks of polystyrene in the ends and another rubbery of poly (ethylene-butylene) in the middle (Drobny, 2007c). Besides, due to its styrenic blocks, which present aromatic rings in their molecular structure, the use of SEBS as a polymeric matrix in carbon-based nanocomposites may be a huge advantage to obtain EMI shielding materials of high performance.

0.2 Motivations

Several studies in the literature discuss about interactions of low frequency radiations to biological systems. The studies investigate the possible effects of non-ionizing electromagnetic radiation on human health including problems mainly related to reproduction and fertility (Genuis, 2008; Merhi, 2012; Nazıroglu, Yuksel, Kose, & Ozkaya, 2013), nervous system dysfunctions (Benson et al., 2013; Genuis, 2008; Gherardini, Ciuti, Tognarelli, & Cinti, 2014;

Hardell & Sage, 2008; Hossmann & Hermann, 2003), and cancer (Benson et al., 2013; Genuis, 2008; Hardell & Sage, 2008; McColl et al., 2015). The impact of electromagnetic radiation in human health is still not conclusive. However, despite the challenges in establishing irrefutable scientific proof of health problem related to non-ionizing electromagnetic radiation, epidemiological analyses suggest considerable potential of injury because of the exposure (Genuis, 2008). From the industrial point of view, EMI are related to technical problems. Most electronic devices in operation emit electromagnetic waves and all electronic devices are prone to EMI problems (Tong, 2009), and as a result, ensuring electromagnetic compatibility becomes necessary (Tong, 2009). In order to ensure the performance requirements, EMC regulations have been established and standards set by international organizations (Tong, 2009). These standards must be satisfied for commercial electronics and one way to achieve the EMC required level is making use of shielding materials.

Therefore, in a global context, it is clear the interest in investments for the development of advanced materials capable of, for example, reflect and/or absorb electromagnetic radiation in order to overcome the crescent electromagnetic pollution. Consequently, lots of researches are being conducted seeking the development of multifunctional shielding materials that may present suitable mechanical properties, lower density, good processability, and, at the same time, fully satisfy esthetics parameters. In general, composites based on conventional thermoplastic polymers and carbon nanoparticles appear as candidates to meet most of these advanced requirements. However, for some applications EMI shielding materials must also mandatorily present flexible properties.

Currently, composites based on conventional rubbers and traditional carbon particles are the most used flexible EMI shielding materials. However, these composites present some significant drawbacks mainly related to the curing process and the need of high amount of conducting fillers. Therefore, the development of materials that combine the outstanding properties of thermoplastic elastomers and carbon nanoparticles may be a promising option to the development of a new generation of high performance flexible EMI shielding materials.

0.3 Objectives

The main objective of this thesis is to develop an efficient flexible EMI shielding material based on SEBS and different carbon nanoparticles.

In order to understand the relationship between morphology, properties, and processing conditions for superior performances, the research project was divided in 3 phases, and the specific objectives of each phase were defined as following:

i) First phase

- Assess the interactions, dispersion and distribution of CNT in the SEBS matrix;
- Analyse the microstructure and evaluate the electrical conductivity and electromagnetic shielding effectiveness of the nanocomposites.

ii) Second phase

- Assess the interactions, dispersion and distribution of graphene nanoplatelets (GnP) in the SEBS matrix;
- Analyse how the microstructure, electrical conductivity and electromagnetic shielding effectiveness of the nanocomposites depend on the carbon nanoadditive used in hybrid nanocomposites of SEBS/CNT/GnP;
- Investigate the existence of synergic effects on the properties of the hybrid nanocomposites compared to the binary nanocomposites (SEBS/CNT and SEBS/GnP).

iii) Third phase

- Assess the influence of maleic anhydride in the matrix on the microstructure and properties of the nanocomposites;
- Analyse how the processing method used to obtain the nanocomposites of SEBS/CNT affects the microstructure, mechanical and electrical properties, and performance of the nanocomposites for EMI shielding

0.4 Thesis design

This thesis is divided in 6 chapters that present a brief literature review regarding carbon-based polymeric composites for EMI shielding, the articles related to each phase of the project, a brief discussion and summary of the results, conclusions and recommendations, according to the following:

i) Chapter 1: literature review

ii) Chapter 2: "Electromagnetic interference shielding and electrical properties of nanocomposites based on poly (styrene-b-ethylene-ran-butylene-b-styrene) and carbon nanotubes" published in Polymer European Journal. This article presents the results from the first phase of the project regarding nanocomposites of SEBS/CNT for EMI shielding.

iii) Chapter 3: "Hybrid Nanocomposites of Thermoplastic Elastomer and Carbon Nanoadditives for Electromagnetic Shielding" published in Polymer European Journal. This article concerns the results from the second phase of the project regarding nanocomposites of SEBS/GnP and hybrid nanocomposites of SEBS/GnP/CNT for EMI shielding. Synergic effects on the hybrid nanocomposite are highlighted.

iv) Chapter 4: “Morphology, mechanical properties, and electromagnetic shielding effectiveness of SEBS/CNT nanocomposites: effects of maleic anhydride, CNT loading, and processing method” submitted to Polymer International. This article is based on the results from the third phase of the project regarding SEBS/CNT and SEBS-MA/CNT nanocomposites prepared by two different molding techniques. A balance between EMI shielding and mechanical properties is also presented.

v) Chapter 5: Discussion and summary of the results

vi) Conclusions and recommendations

Lastly, additional information is provided in Appendix I.

CHAPTER 1

POLYMER NANOCOMPOSITES FOR EMI SHIELDING APPLICATIONS

In this chapter, the concept of polymer composites for EMI shielding is presented, with a focus on the carbon-based polymer nanocomposites. The influence of several parameters such as the effect of particles size, shape, dispersion, and orientation on the EMI shielding effectiveness of some polymer composites present in the literature is reviewed. Definitions and the key properties for multifunctional EMI shielding materials is presented as well. Finally, a review of flexible materials for EMI shielding is reported.

1.1 Electromagnetic compatibility: definition, general information, and market

The astonishing development of electrical systems and electronic devices in the current information age is not just promoting undeniable advances in all technological fields, but also boosting problems and concerns related to electromagnetic pollution. The expansion of devices that operates in higher levels of power and frequencies, allied to the need of light materials, low cost, suitable mechanical properties, easy shaping, and the importance of esthetic aspects are increasingly demanding the development of multifunctional materials.

Electronic devices may either cause electromagnetic interferences to other electronic systems in the environment or suffer from interferences coming from these pieces of equipment. Because of that, all sorts of electronic devices are subject to electromagnetic compatibility (EMC) standards for commercial applications. EMC is the capability of an electronic system to work efficiently without disrupting or being affected by other surrounding devices, and is controlled by different regulations and legislations ("Electromagnetic Compatibility (EMC) Shielding Market - Global Industry Analysis, Market Size, Share, Trends, Analysis, Growth and Forecast, 2013 - 2019," ; Tong, 2009) The International Electrotechnical Commission (IEC) is the major organization responsible for preparing and establishing International

Standards for all electrical, electronic and related technologies ("International Electrotechnical Commission," ; Tong, 2009).

The miniaturization of electronic systems and all the technical requirements needed for high technological applications are amplifying the complexity of ensuring EMC, and, as expected the EMC market is increasing. Mainly driven by explosive sales in the consumer electronics, the global market related to EMI and radio frequency interference (RFI) shielding has grown from US$5.6 bn in 2015 to around US$6 bn in 2016 ("EMI/RFI: Materials and Technologies," 2016). The expected Compound Annual Growth Rate (CAGR) is ≈ 7 % from 2017 to 2023, which means an increase to ≈ US$10 bn by 2023 ("EMI Shielding Market (Materials Type - Conductive Polymers, Conductive Coatings and Paints, Metal Shielding Products, and EMI/EMC Filters; End-use Industry - Telecommunication and IT, Healthcare, Aerospace and Defense, Automotive, and Consumer Electronics) - Global Industry Analysis, Size, Share, Growth, Trends, and Forecast 2017 - 2025," 2017; "EMI Shielding Materials - Global Market Outlook (2017-2023)," 2017).

The EMC market consists of a diverse class of EMI and RFI shielding products, based on different materials such as conductive polymers composites as conductive coatings and paints, metal shielding products, EMI/EMC filters, and others ("EMI Shielding Market (Materials Type - Conductive Polymers, Conductive Coatings and Paints, Metal Shielding Products, and EMI/EMC Filters; End-use Industry - Telecommunication and IT, Healthcare, Aerospace and Defense, Automotive, and Consumer Electronics) - Global Industry Analysis, Size, Share, Growth, Trends, and Forecast 2017 - 2025," 2017). However, EMI shielding materials for non-metal surfaces, mainly provided by conductive coatings and paints, held the largest market share in 2016 ("EMI Shielding Market by Component (EMI Shielding Tapes & Laminates, Conductive Coatings and Paints, Metal Shielding Products, Conductive Polymers, EMI Filters), Method (Radiation, Conduction), Industry (Consumer Electronics, Telecom & IT, Automotive, Healthcare, Defense & Aerospace), and Geography - Global Forecast to 2022," 2017).

As a sub-segment of the EMI and RFI shielding products, shielding materials used for gaskets and enclosures is of critical importance when a complete EM shielded environment is needed. These materials, are mainly applied to medical, aerospace and defense, automotive, consumer electronics, and telecommunications areas, and many companies in the EMC market compete in terms of price, performance, quality, support services, and product innovation. Among the top companies in the global market are Laird Plc., 3M, Chomerics, RTP Company, Marktek Inc., ETS-Lindgren, Tech-Etch, Inc., Omega Shielding Products, HEICO Corporation, and Schaffner Group ("EMI and RFI shielding materials and technologies - a global strategic business report," 2016; "EMI Shielding Market (Materials Type - Conductive Polymers, Conductive Coatings and Paints, Metal Shielding Products, and EMI/EMC Filters; End-use Industry - Telecommunication and IT, Healthcare, Aerospace and Defense, Automotive, and Consumer Electronics) - Global Industry Analysis, Size, Share, Growth, Trends, and Forecast 2017 - 2025," 2017).

A list of some companies that produce and commercialize materials for EMI shielding can be found in Appendix I.

1.2 Multifunctional materials for EMI shielding

1.2.1 Polymer composites and blends

An extensive class of materials is used for EMI shielding purposes. Metals are by far the most used materials, however, with the development of more sophisticated electronic technology, metals are being replaced by multifunctional materials for higher performances.

Shielding materials based on polymers may present a range of advantages compared to metals, such as lower density and cost, and easier processing (Anupama et al., 2013; Z. Liu et al., 2007; Thomassin et al., 2013). However, most polymers are electrical insulators, a property that makes them almost transparent to electromagnetic waves. Thus, an alternative to overcome

this limitation is the development of electrically conductive polymer composites and blends prepared by dispersing properly concentrations of conductive fillers in polymeric matrices.

Polymer composites for EMI shielding can be divided into three main groups, depending on the conductive filler used, metals, intrinsically conducting polymers (ICP), or carbon fillers, and present different aspects concerning to shielding effectiveness, mechanical properties, and processability. In order to choose the most suitable material for a specific EMI shielding application, it is extremely important to do a thorough balance between all those aspects. The three types of polymer composites for EMI shielding are presented below.

1.2.1.1 Metal-based polymer composites

Metal/polymer composites generally present high EMI shielding effectiveness compared to the other groups. One example is presented by Al-Saleh, Gelves, and Sundararaj (2011) who prepared composites of copper nanowire (CuNW) and Polystyrene (PS). According to the authors, these composites exhibited higher EMI-SE than all known conductive polymer composites (at the time of publication). With 1.3 vol.% of CuNW in samples of 210 μm of thickness, the EMI-SE in the X-band frequency range was 27 dB, corresponding to 99.8% of electromagnetic attenuation. Whereas the same level of shielding for multi-walled carbon nanotubes (MWCNT)/PS composites of 1 mm of thickness (five times thicker than the CuNW/PS films) was just achieved from concentrations over 4.3 vol.% of MWCNT (3.3 times more concentrated than the CuNW/PS composites) (Al-Saleh, Gelves, & Sundararaj, 2011). However, metal/polymer composites commonly exhibit some significant drawbacks, for example the decrease of electrical properties due the presence of metal oxides and poor electrical contact between fillers (Gelves, Al-Saleh, & Sundararaj, 2011), and substantial losses of mechanical properties and processability, as high rigidity, high density, and delamination problems. Other metals, e.g. iron, nickel, silver, aluminum, are also used as conductive fillers in ECPCs, and some reports about metal-based polymer composites for EMI shielding can be found elsewhere (Gargama, Thakur, & Chaturvedi, 2016; Jalali, Dauterstedt, Michaud, & Wuthrich, 2011; Jalali, Molière, Michaud, & Wuthrich, 2013; Joseph & Thomas Sebastian,

2013; E. Kim, Lim, Kang, & Yoo, 2016; Madhu et al., 2014; Tanrattanakul & Bunchuay, 2007).

1.2.1.2 Electrically conductive polymer blends

Blends of intrinsically conducting polymers (ICPs) and insulating polymers are another class of materials largely used for EMI shielding. Magioli et al., (2012) studied blends of conductive polyaniline doped with dodecylbenzene sulfonic acid (PAni.DBSA) and styrene–butadiene–styrene (SBS) triblock copolymer in the X-band frequency range. In that research, blends were prepared by melt compounding and in situ polymerization of aniline in the presence of SBS. The maximum EMI-SE was obtained for the blends containing 30 wt.% of PAni.DBSA prepared by in situ polymerization and was between 35 to 40 dB for all the frequency range studied (Magioli, Soares, Sirqueira, Rahaman, & Khastgir, 2012). Despite the fact that good levels of EMI-SE can be achieved by blends of ICPs and conventional polymers, the high quantity of conductive filler necessary is a considerable disadvantage, other drawbacks are the poor processability (Thomassin et al., 2013) and the use of organic solvent for the synthesis of ICPs. Others reports about ICPs, mainly based on PAni and polypyrrole (PPy), used in electrically conductive polymer blends for EMI shielding can be found in (Bhadra, Singha, & Khastgir, 2009; Saini & Arora, 2012; Schettini, Khastgir, & Soares, 2012; Schettini & Soares, 2011).

1.2.1.3 Carbon-based polymer composites: effect of particles size, shape, dispersion, and orientation

ECPC based on carbon particles are the most widely developed class of composites for EMI shielding at the present time (Thomassin et al., 2013). Among the advantages of using carbon particles as conducting additives, it is possible to highlight the low cost of some particles as carbon black and graphite, and the high aspect ratio of carbon fibers, carbon nanotubes and graphene, which contribute to the formation of an electrical conducting systems with lower amount of additive and may contribute to the improvement of the mechanical properties

Cliccours.COM

(Bokobza, 2007; Choudhary & Gupta, 2011). Besides, these composites can be prepared by the conventional processing methods suitable for industry and do not necessarily need the use of organic solvents. However, some disadvantages are the difficulty of dispersing the particles due to their high surface energy, and also the high cost of carbon nanoparticles of high quality (H. Kim et al., 2010; Kuilla et al., 2010; Singh et al., 2012; Spitalsky et al., 2010).

Concerning shielding applications, it is difficult to make a direct comparison of different carbon additives, since the results reported in the n literature are based on composites of different thickness and performed at different frequency ranges (Thomassin et al., 2013). However, Thomassin et al. (2013) presented the general behaviour established by plotting the SE of composites with different kinds of carbon fillers reported on the literature as a function of their loading amounts (Thomassin et al., 2013). Figure 1.1 shows the EMI-SE versus filler content of different composites.

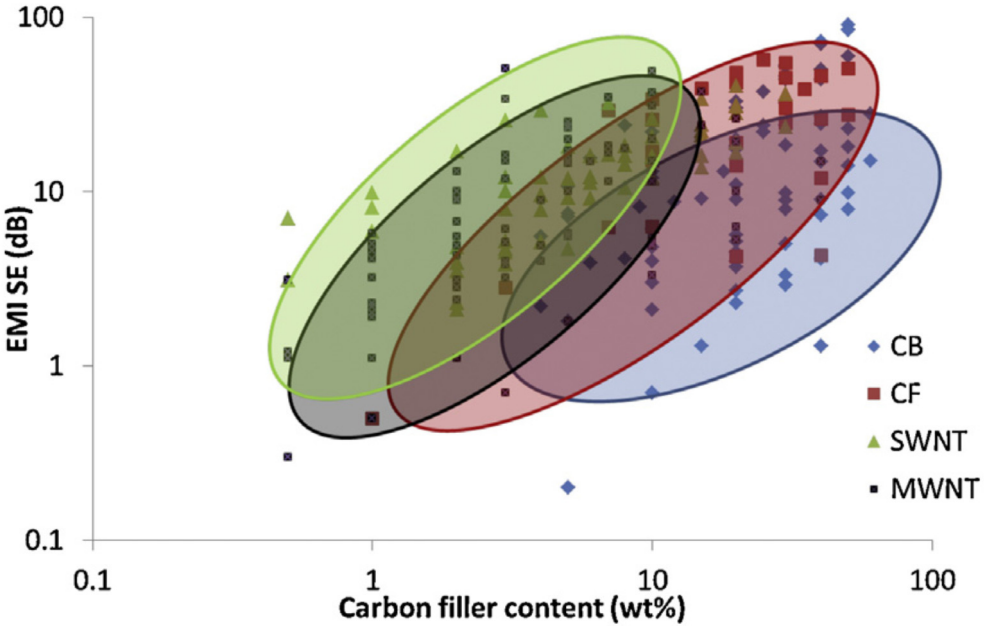

Figure 1.1 - Summary of some EMI-SE reported on the literature regarding different kind of carbon fillers as a function of their loading amount, where SWNTs is single-walled carbon nanotubes, MWNTs is multi-walled carbon nanotubes, CNFs is carbon nanofibers, and CB is carbon black (Thomassin et al., 2013)

As shown at the Figure 1.1, the highest EMI-SE at lower amount of carbon filler are observed for carbon fillers with higher aspect ratio, in general, following the order SWNTs > MWNTs > CNFs > CB. Additionally, experimental results from the literature state that for the same amount of filler, polymer nanocomposites of nanosized carbonaceous fillers present substantial advantages regarding different engineering properties than composites based microsized carbonaceous fillers.

Currently, because of their extraordinary electronic and mechanical properties, and high aspect ratio, CNT are some of the most widely used carbon nanoparticles. Carbon nanotubes are essentially long cylinders of covalently bonded carbon atoms that present diameters from 1 to 100 nm and lengths up to tens of microns, and are basically categorized in two classes, single- and multi-walled CNT (Choudhary & Gupta, 2011; Coleman, Khan, Blau, & Gun'ko, 2006). Single-walled carbon nanotubes (SWCNT) are cylinders with diameter in the order of 1 nm formed by a single graphene sheet rolled up. Multi-walled carbon nanotubes (MWCNT) consist of cylinders formed concentrically and separated by 0.35 nm, similarly to the basal plane separation of graphite. The properties of CNT strongly depend on their number of defects and chirality, that are classified as armchair, zigzag, and chiral, which in turn are dependent on the produce method and synthesis control. In general, CNT can be synthesized upon arc discharge, laser ablation or chemical vapor deposition (CVD) (Dai, 2002; Guanghua, Tahir, & William, 1998; Odom, Huang, Kim, & Lieber, 2000). Among the different methods, CNT obtained upon CVD usually present a considerable amount of defects, which means that their structure is far from ideal, resulting in the damage of their physical and chemical properties. However, the production of CNT by this method is very important, since they can be produced in large scales with relatively low costs (Coleman et al., 2006). More information about structure and properties of CNT can be found in (Choudhary & Gupta, 2011; Coleman et al., 2006; Dai, 2002; Guanghua et al., 1998; Hoenlein et al., 2003; Odom et al., 2000).

Recently, graphene has also attracted special attention as a filler material because of its excellent mechanical and optical properties, high thermal and electrical conductivities, its enormous specific area and high aspect ratio (Basu et al., 2013; El Achaby et al., 2012; H. Kim

et al., 2010; Kuilla et al., 2010). Graphene is considered a two-dimensional carbon nanostructure (2-D) composed of sp2 carbon atoms bonded and densely packed in a hexagonal crystal "honeycomb" structure, formed by a single-layer carbon sheet, or multi-layer carbon sheets (Basu et al., 2013; T. K. Das & Prusty, 2013; El Achaby et al., 2012; H. Kim et al., 2010; Kuilla et al., 2010; Singh et al., 2012). As with CNT, structure, properties and number or defects of graphene deeply depend on the production method. Graphene can be synthetized by different methods including chemical vapor deposition (CVD), arc discharge, epitaxial growth on SiC, chemical conversion, reduction of CO, unzipping carbon nanotubes, and self-assembly of surfactants (H. Kim et al., 2010). Among the diverse methods, graphene produced by CVD and epitaxial growth often present tiny amounts of large-size, defect-free graphene sheets, however these methods are not a suitable source for applications that need a relatively large amount of graphene, e.g. in polymer nanocomposites. In this case, the mechanical cleavage method of preparation is more appropriate (H. Kim et al., 2010). More information can be found in (Castro Neto, Guinea, Peres, Novoselov, & Geim, 2009; H. Kim et al., 2010; Kuilla et al., 2010; Loh et al., 2010; Singh et al., 2012; Soldano, Mahmood, & Dujardin, 2010; Zhu et al., 2010).

For EMI shielding, experimental results show that for the same amount of filler, polymer nanocomposites with nanosized carbon particles present extraordinary electromagnetic shielding effectiveness compared to composites with traditional carbon particles. Al-Saleh and Sundararaj (2009) compared PP composites prepared by melt compounding with 7.5 wt.% of different fillers. For the nanocomposite of PP/CNT, the SE value was 35 dB, while for the composite PP/CB the effectiveness was only 18 dB (Al-Saleh & Sundararaj, 2009). In other study, Anupama et al. (2013) (Anupama et al., 2013) prepared nanocomposites of graphene nanoribbon/polyvinyl alcohol (GNR/PVA) by solution casting. The results showed that the material is very effective for shielding applications even with low amount of additive in very thin samples, although the nanocomposites were frequency dependent on the X-band frequency range. The highest shielding was 62.67 dB at 11.3 GHz, and the average in the X-band frequency range was 45 dB, achieved for a sample of 0.6 mm thick with 0.025 wt% of GNR (Anupama et al., 2013).

Despite carbon-based materials, especially the nanosized ones, represent a class of fillers largely used in polymer nanocomposites nowadays, their utilization is restricted by strong interactions and van der Waals forces between the fillers that form large agglomerates, which hinder their dispersion and consequently, their uniform distribution on the nanometer level (Calisi et al., 2013; Kuilla et al., 2010; Matzeu, Pucci, Savi, Romanelli, & Di Francesco, 2012; Spitalsky et al., 2010). Therefore, the difficulty in disentangling agglomerates is a limiting factor for nanocomposite applications containing CNT and graphene (Choudhary & Gupta, 2011).

Aiming to improve the dispersibility in ECPCs, different strategies are being applied to functionalize carbon nanoparticles, such as covalent modification, and non-covalent functionalization by the use of surfactants or polymer matrices with chemical affinity, or polymer wrapping, as schematically shown in Figure 1.2 (Choudhary & Gupta, 2011).

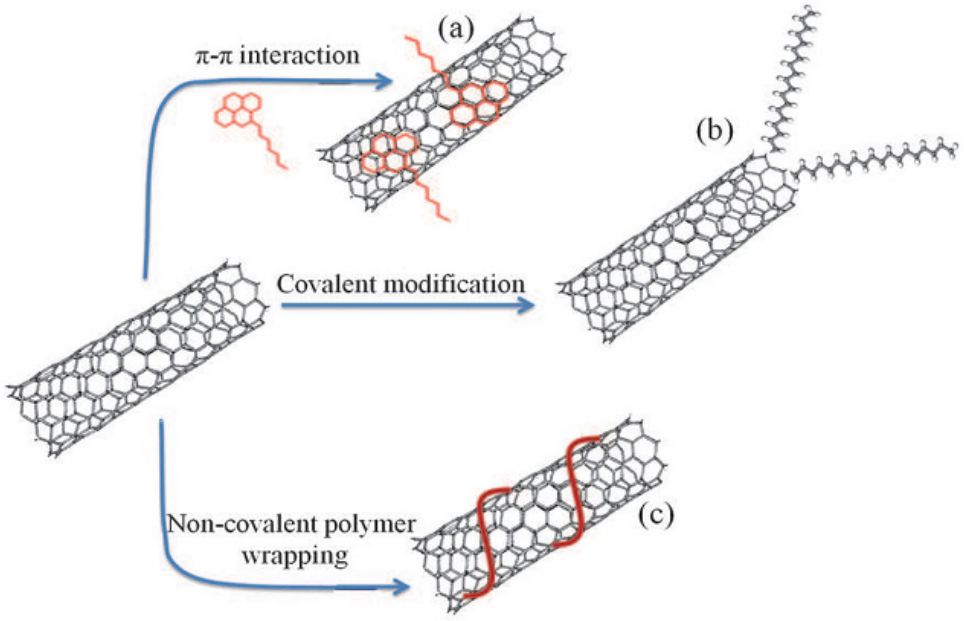

Figure 1.2 - Schematic illustration of possible modifications of CNT, wherein (a) represents π-π interactions, (b) is covalent functionalization with inclusion of functional groups, and (c) is noncovalent functionalization by polymer wrapping (Choudhary & Gupta, 2011)

Among these methods, covalent modification is generally effective, but it also causes deterioration of intrinsic properties of the nanoparticles, which, consequently, decreases their electrical conductivity. Alternatively, non-covalent functionalization methods, including the use of surfactants or matrices that have chemical affinity, may improve carbon nanoparticles dispersion due to the formation of non-covalent interactions, for example, between the π electrons of aromatic groups present, in this case, in both phases (formation of π- π interactions). These methods present the advantage of improving nanoparticles dispersion without decreasing their intrinsic properties (Choudhary & Gupta, 2011; Vasileiou et al., 2013).

Another strategy to improve properties of carbon-based polymer composites is the use of a combination of different carbon additives. These combinations may contribute to the development of multifunctional composites by promoting a better balance between the specific properties desired for each application. Figure 1.3 shows a schematic representation of a hybrid nanocomposite of PS, graphene nanoplatelets (GnP), and CNT. The image also elucidates the non-covalent interactions between the aromatic rings present in the polymer matrix and in the different carbon additives (Maiti et al., 2013).

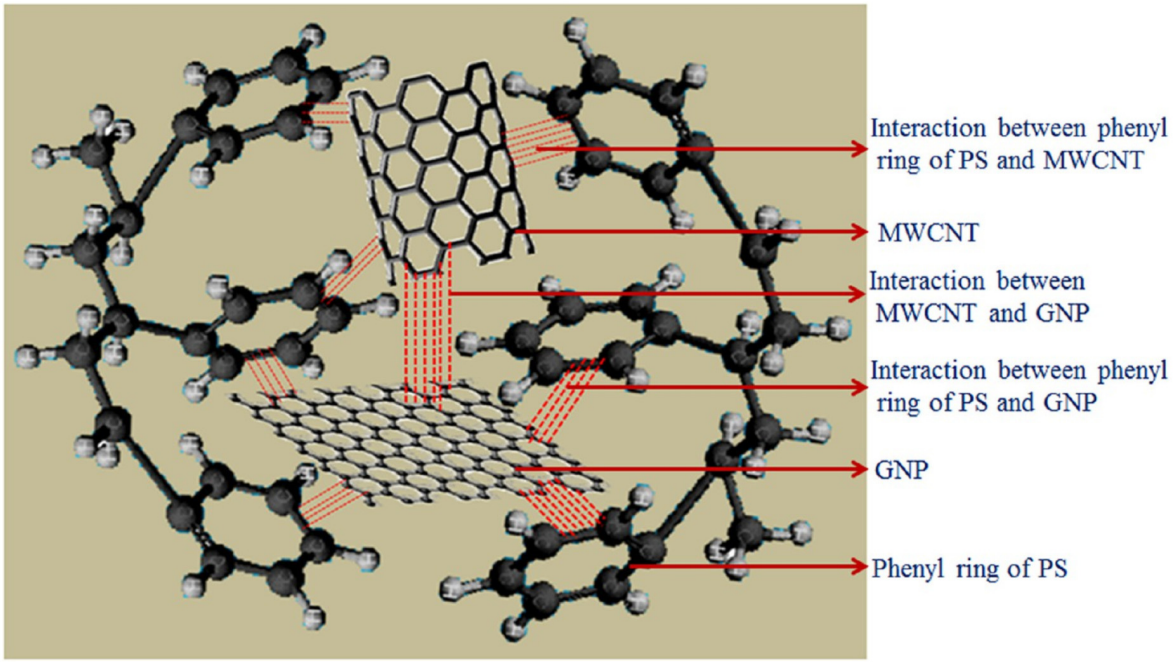

Figure 1.3 - Schematic representation for π-π interactions between GnP, MWCNT, and PS in hybrid nanocomposites of PS/MWCNT/GnP (Maiti et al., 2013)

According to the literature, in carbon-based polymer composites the presence of carbon nanoparticle of different shapes improves the connectivity of the network formed inside the polymer matrix decreasing the necessary filler loading amount (Al-Saleh & Saadeh, 2013; Lin et al., 2016; Sharma et al., 2016), or reducing costs (Al-Saleh & Saadeh, 2013). These combinations may also result in synergistic effects (interactions between two or more substances that when combined present total effects that are greater than the sum of their individual effects).

Reports suggest the combination of carbon nanoparticles for mechanical improvement (Chatterjee et al., 2012; Lin et al., 2016; Yue, Pircheraghi, Monemian, & Manas-Zloczower, 2014; S. Zhang et al., 2013). In this case, the use of nanoparticles with high aspect ratio, as carbon fibers and CNT, facilitate the reinforcement mechanism, while the inclusion of small amounts of particles of dissimilar shapes, such as CB and graphite, increases the surface area of the reinforcement, which promotes better linkage with the polymer matrix (Chatterjee et al.,

2012). This improvement is especially significant for properties like flexural modulus, in which the inter-connected particle network plays a pivotal role (Chatterjee et al., 2012).

Synergic effects are also observed concerning the electrical properties (Maiti et al., 2013; Sharma et al., 2016; Yue et al., 2014; S. Zhang et al., 2013). In this case, the improvement of the connectivity between the carbon additives (due the use of additives of different shapes) enhances the size of conducting network formed inside the polymer matrices, decreasing the electrical percolation threshold and increasing the electrical conductivity of the material. Regarding EMI shielding, synergistic effects, in these cases, are related to the improvement of the electrical conductivity of the system and the geometrical arrangement (microstructure) of the conductive network to interact with the electromagnetic radiation (M.-S. Kim et al., 2013; Maiti et al., 2013; Sharma et al., 2016).

1.2.2 Processing methods and parameters

For the preparation of carbon/polymer nanocomposites, three main methods are used such as in-situ polymerization of monomer in the presence of nanoadditives, solution casting followed by evaporation of solvent, and melt compounding. Reports show that, in general, in situ polymerization and solution casting as very effective methods to properly disperse nanoadditives in polymeric matrices (Choudhary & Gupta, 2011; Coleman et al., 2006; Maiti et al., 2013; Thomassin et al., 2013). However, these techniques involve the use of organic solvents and consequently present some drawbacks in terms of industrial applications and environmental concerns. Consequently, melt compounding is by far the most commonly used method by the industry (Choudhary & Gupta, 2011; Thomassin et al., 2013) and lots of researches in the literature report studies about the melt dispersion process of carbon particles in polymeric matrices and the influence of mixing parameters of different techniques.

Aiming to understand the melt compounding behaviour and improve the dispersion and distribution of the particles some considerations and parameters must be taken into account, such as wetting of initial agglomerates, that depend on the interfacial energy between additive

and matrix; polymer infiltrations; viscosity of the matrix; mixing temperature, time, and speed; and amount of carbon additive (Alig et al., 2012).

The most suitable state of carbon additives dispersion and distribution into the matrix depend on the properties desired for each application. For mechanical reinforcement, carbon additives should be well dispersed throughout the matrix, on the other hand, when electrical conductivity is desired, minor agglomerations or small filler-filler distances are preferred (Alig et al., 2012; Thomassin et al., 2013). Although, some reports available on the literature, state that aiming to improve the electrical conductivity in ECPC, the primary agglomerates of carbon particles should be well disaggregated and distributed into the matrix in a first step, and then a partial re-agglomeration is recommended (Alig et al., 2012; Alig, Skipa, Lellinger, & Pötschke, 2008). The recovery of some portion of agglomeration can be achieved after the mixing process, e.g. during compression molding. The re-agglomeration process, also called secondary agglomeration, ensures inhomogeneous carbon particles distribution and, consequently, smaller distances between them to favour the formation of a connected network (Alig et al., 2012).

The processing method can also have influence on the distribution of carbon particles related to the orientation of the additives inside the polymer matrix (Arjmand et al., 2012; Coleman et al., 2006; Y. A. Kim et al., 2006; Panaitescu et al., 2014; Theilmann, Yun, Asbeck, & Park, 2013). Extrusion, injection, and roll milling can align the particles along the flow direction, which may strongly affect the final properties of the nanocomposites. Panaitescu et al. (2014) prepared nanocomposites of SEBS, with and without maleic anhydride, and graphite using a two-roll-mill to induce orientation. Results showed that the rolling step changed the self-assembling architecture and improve the mechanical behavior of the block copolymers and their composites (Panaitescu et al., 2014). Besides the mechanical properties enhancement, electrical and EMI shielding properties can also be affected by the particles orientation, however in these cases, it is expected the alignment to decrease their efficiencies (Arjmand et al., 2012). Arjmand and co-workers (2012), compared the properties of PS/CNT composites for EMI-SE shielding prepared by injection and compression molding. Results showed that the

injected composites presented lower electrical conductivity, real and imaginary permittivity, and EMI-SE (Arjmand et al., 2012).

1.2.3 Key properties of multifunctional EMI shielding materials: parameters vs. effects

In order to prepare commercial materials for EMI shielding it is necessary to consider a balance between different aspects, such as esthetic parameters, weight, manufacture feasibility, costs, and, above all, the specific properties to ensure the quality of the material and provide an efficient shielding action. Among all the different considerations, electrical conductivity, electromagnetic shielding effectiveness, and mechanical properties are the key parameters to be considered in order to obtain EMI materials of high efficiency.

1.2.3.1 Electrical conductivity: Percolation theory definition

As mentioned in section 1.2.1, conventional polymers are electrically insulating and non magnetic materials and because of that transparent to electromagnetic radiation in their neat form. For EMI shielding applications, although magnetic polymer composites also appear as an option to overcome this condition, main polymeric materials for EMI shielding are formed by ECPCs. In these materials, it is well known that electrical conductivity requires a conducting network formation, while EMI shielding only requires free charge carriers or diploes to interact with the electromagnetic radiation. However, the highest EMI-SE is achieved for a giving composite when a conductive network is present (Chung, 2001; Theilmann et al., 2013).

In ECPCs, the electrical conductivity can be understood considering a formation of a network of multiple microcapacitors, where the conducting particles act as electrodes and the insulating polymeric layer act as a dielectric material (Arjmand et al., 2012; Kumar, Vishnupriya, Chary, & Patro, 2016; Theilmann et al., 2013). In these materials, the nanoparticles must be sufficiently close, but do not necessarily need to touch each other to be able to conduct electricity, in this case the conductivity occurs by tunneling phenomenon (Potts, Dreyer,

Bielawski, & Ruoff, 2011). The change on electrical conductivity from insulators to conductors can be studied by means of the Percolation Theory. According to this theory, from a given amount of conductive filler in the insulating matrix, known as electrical percolation threshold, the system starts conducting electricity. Figure 1.4 schematically shows the variation of electrical conductivity due to the addition of a conductive material in an insulating polymer matrix.

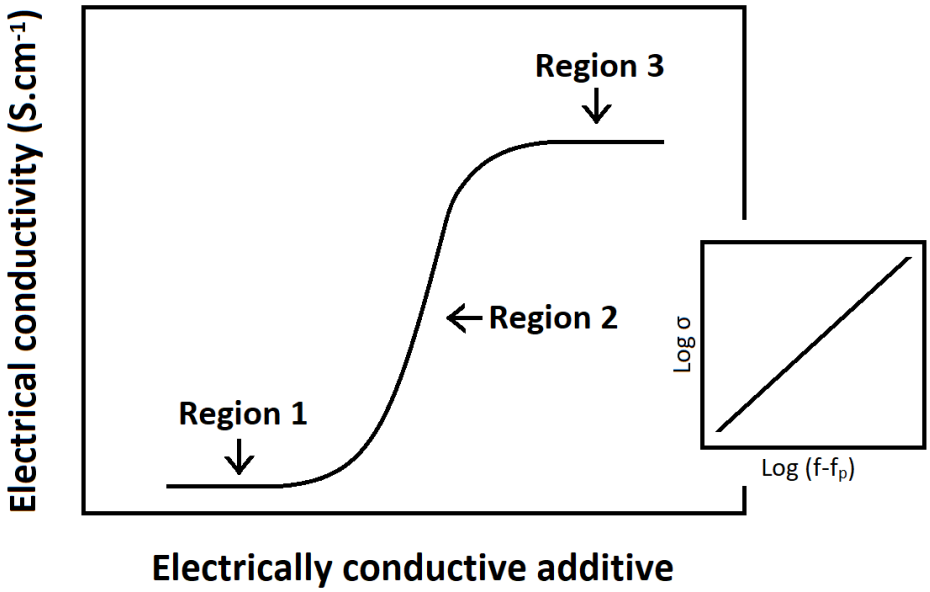

Figure 1.4 - Schematic representation of the variation on the electrical conductivity as a function of the addition of conductive filler in an insulating polymer matrix

As shown in Figure 1.4, at low fractions of conductive additives, the electrical conductivity of the composite is basically the same as the insulating matrix, and the region is called non percolative (region 1). From the addition of a certain amount of additive, the system suffers an abrupt insulating-conductive change, which indicates that the composite reached the electrical percolation threshold. From this percolative region (region 2), the continued loading of nanoadditives induces a gradual increase of the electrical conductivity and the system tends to reach the intrinsic electrical conductivity of additive (region 3) (Estrada Moreno, Díaz Diaz, Mendoza Duarte, & Ibarra Gómez, 2009).

Clicours.COM

According to the Percolation theory, the percolation threshold can be calculated using equation 1.1.

$$\sigma = \sigma_c (f - f_p)^t \quad (1.1)$$

Where, σ is the electrical conductivity of the composite, σ_c is the electrical conductivity of the conductive phase, f and f_p are respectively the fraction of additive in the insulating matrix and the fraction of the conductive additive in the percolation threshold, and t is the critical exponent (Matzeu et al., 2012; Potts et al., 2011; Thomassin et al., 2013; Z. Wu et al., 2014). The fraction of the conductive nanoadditive corresponding to the percolation threshold (f_p) and the critical exponent (t) can be experimentally determined from the plot of $log\ \sigma$ vs. $log\ (f - f_p)$ (Matzeu et al., 2012; Potts et al., 2011; Thomassin et al., 2013; Z. Wu et al., 2014).

According to the percolation theory, the critical exponent is related to the dimensionality of the system. Values between 1.1 and 1.3 can be attributed to two-dimensional systems whereas values between 1.6 and 2 can be attributed to three-dimensional systems (Matzeu et al., 2012; Thomassin et al., 2013). The value of t more widely accepted for three-dimensional systems is 2, although, some studies in the literature present and discuss systems with higher values of t (Lu, Lin, & Chen, 2006; Rubin, Sunshine, Heaney, Bloom, & Balberg, 1999). Deeper information about the electrical conduction of ECPCs and theoretical models are beyond of the purpose of this thesis, but can be vastly found on the literature (Arenhart, Barra, & Fernandes, 2016; Bauhofer & Kovacs, 2009; Kilbride et al., 2002; C. Li, Thostenson, & Chou, 2007; J. Li & Kim, 2007; Maiti et al., 2013; McLachlan et al., 2005; Ounaies, Park, Wise, Siochi, & Harrison, 2003; Stanley, 1977).

In carbon-based polymer composites, the formation of the conducting network is affected by a number of factors related to the type of polymer used as matrix, inherent properties of the conducting additive, and processing method (Bilotti et al., 2013; Potts et al., 2011; Sachdev, Patel, Bhattacharya, & Tandon, 2011; Thomassin et al., 2013). Among these factors, the aspect ratio of carbon additives, the state of dispersion, and the orientation of the particles throughout

the matrix are the ones which have the strongest influence on the final electrical conductivity of the composites, as schematically illustrated in Figure 1.5 (Theilmann et al., 2013).

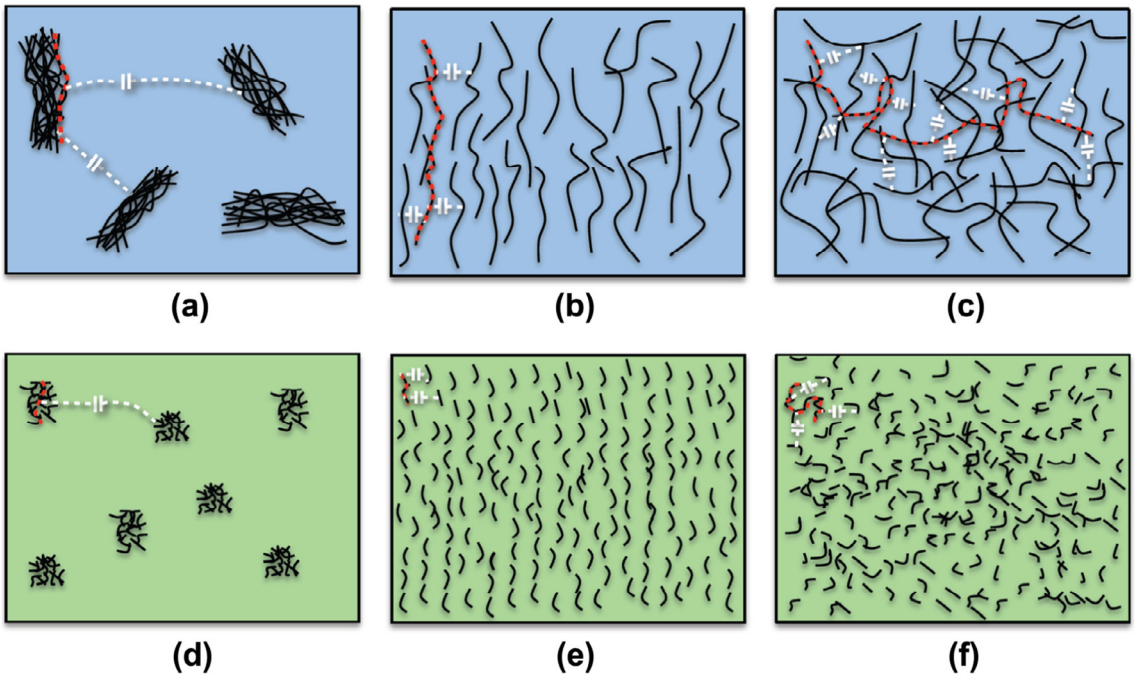

Figure 1.5 - Schematic illustration of a-c) high aspect ratio MWCNT-based PDMS composites considering a) agglomerations of MWCNT, b) aligned distributed MWCNT, and c) randomly distributed MWCNT, and d-f) lower aspect ratio MWCNT-based PDMS composites considering d) agglomerations of MWCNT, e) aligned distributed MWCNT, and f) randomly distributed MWCNT (Theilmann et al., 2013)

As shown in Figure 1.5, in order to maximize the contact between the conducting particles, the clusters of carbon particles (1.5-a and 1.5-d) must be disaggregated and the carbon particles be separated and evenly dispersed throughout the polymer matrix (1.5-b and 1.5-e). In the later case, particles are more likely to come into contact to each other to form a conducting network. Orientation of the particles also considerably affects the conductivity of composites. When particles are randomly distributed the connectivity between them are favored (1.5-c and 1.5-f), compared to when the particles are aligned (1.5-b and 1.5-e) into the matrix. At last, the aspect ratio also plays an important role to improve the electrical conductivity, since in the case of nanocomposites with particles of high aspect ratios (1.5-a, 1.5-b and 1.5-c) lower amounts of

conducting additives are necessary to form the conducting network compared to nanocomposites with particles of lower aspect ratios (1.5-d, 1.5-e and 1.5-f) (Theilmann et al., 2013). Besides, it is also essential to highlight the importance of avoid damaging and reducing the aspect ratio of the particles during the mixing process in order to ensure appropriate electrical conductivity, and, consequently, suitable EMI-SE for shielding applications with the lower possible amount of conducting additives.

1.2.3.2 EMI Shielding effectiveness: definitions, shielding mechanisms, and power balance

In EMI shielding applications, the measure that quantifies the reduction of incident radiation that passes through the attenuating material is known as shielding effectiveness (SE). Mathematically the EMI-SE (given in decibels) can be expressed in a logarithmic scale according to equation 1.2 (Saini & Arora, 2012).

$$\text{EMI-SE(dB)} = 10\log_{10}\left(\frac{P_T}{P_I}\right) = 20\log_{10}\left(\frac{E_T}{E_I}\right) = 20\log_{10}\left(\frac{H_T}{H_I}\right) \quad (1.2)$$

Where P_I (E_I or H_I) and P_T (E_T or H_T) are the energy power (intensity of the electric or magnetic field) of the incident and transmitted electromagnetic waves, respectively.

In materials for EMI shielding, three attenuation mechanisms may happen, where a portion of the incident radiation is reflected from the front surface of the shield, a part is absorbed inside the material, and part is reflected from the rear inner boundary of the material to the frontal inner boundary and so on (Al-Saleh & Sundararaj, 2009; Saini & Arora, 2012; Singh et al., 2012), as schematically exemplified in Figure 1.6 (Al-Saleh & Sundararaj, 2009).

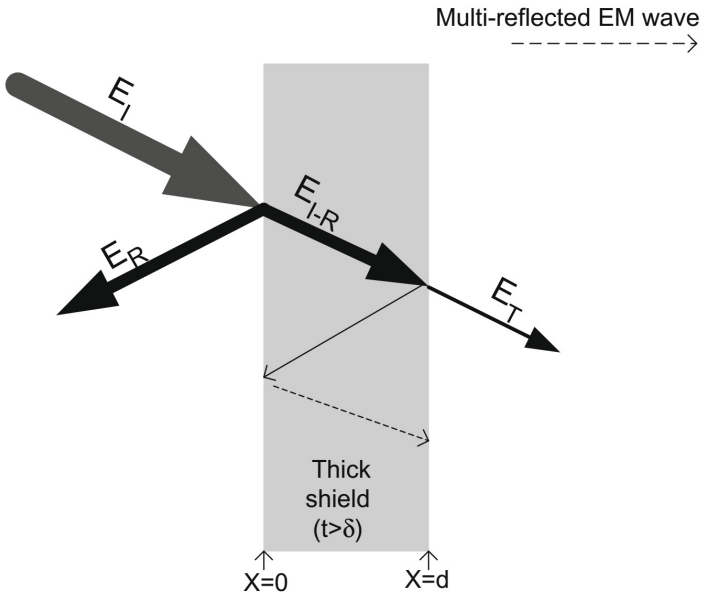

Figure 1.6 - Schematic representation of EMI shielding in ECPCs (Al-Saleh & Sundararaj, 2009)

As shown in Figure 1.6, the total shielding effectiveness is the result of the sum of all electromagnetic shielding mechanisms of the material in accordance with equation 1.3 (Saini & Arora, 2012; Thomassin et al., 2013).

$$EMI\text{-}SE = SE_A + SE_R + SE_M \quad (1.3)$$

Where SE_A, SE_R and SE_M correspond to shielding by absorption, reflection and multiple reflections, respectively. Here, it is worth saying that, in general, the SE_M may be neglected if the SE_A is greater than 10 dB (Al-Saleh et al., 2013; Saini & Arora, 2012; Tong, 2009; Udmale V, 2013).

Experimentally, EMI shielding can be analysed by different methods and instruments, and the most widely used technique include the use of network analyzers. The incident and transmitted waves in a network analyzer is mathematically represented by complex scattering parameters (or S-parameters), for example, S_{11} (or S_{22}) and S_{12} (or S_{21}), which are correlated with the power reflected and the transmitted. In these analyses, when electromagnetic radiation insides

(I) in a shielding material the power absorbed (A), reflected (R), and transmitted (T) totalize 1 (I = 1 = A + R +T) (Saini & Arora, 2012; Thomassin et al., 2013).

The coefficients of R and T are experimentally obtained using S-parameters, according to equations 1.4 and 1.5 (Saini & Arora, 2012; Thomassin et al., 2013).

$$T = [E_T/E_I]^2 = |S_{12}|^2 = |S_{21}|^2 \quad (1.4)$$

$$R = [E_R/E_I]^2 = |S_{11}|^2 = |S_{22}|^2 \quad (1.5)$$

Finally, the SE_R, SE_A, and total EMI-SE are calculated according to equations 1.6, 1.7, 1.8, respectively (Saini & Arora, 2012; Thomassin et al., 2013).

$$SE_R = 10 \log \frac{I}{I-R} \quad (1.6)$$

$$SE_A = 10 \log \frac{I-R}{T} \quad (1.7)$$

$$EMISE = SE_R + SE_A = 10 \log \frac{I}{T} \quad (1.8)$$

Further information about the physical interpretation of EMI shielding and different theoretical models can be found elsewhere (Chung, 2000, 2001; Huang, 1995; M. Y. Koledintseva, 2009; Saini & Arora, 2012; Thomassin et al., 2013; Tong, 2009).

As already mentioned in the previous sections, the shielding effectiveness of a given material depends on many different parameters, and for commercial applications, the minimum EMI-SE commonly required is 20 dB (i.e., equals to or less than 1% of electromagnetic radiation transmission) (Cao et al., 2015; Maiti et al., 2013; Yonglai et al., 2007). Although there are

lots of materials presented on the literature that meet this requirement, a direct comparison of the shielding efficiency of different carbon additives in ECPCs is difficult to make since the samples present different thickness and measurements are done in different frequency ranges. However, for commercial applications, a suitable EMI-SE is generally achieved when the σ_{DC} of the composites is more than 10 $S.m^{-1}$ (Jia et al., 2015; Theilmann et al., 2013). Thus, in order to build a standard that enables comparison, Thomassin et al. (2013) suggested comparing the EMI-SE of different composites considering their electrical conductivities (Thomassin et al., 2013). Figure 1.7 shows a comparison between the EMI-SE of different carbon-based composites and their DC conductivity.

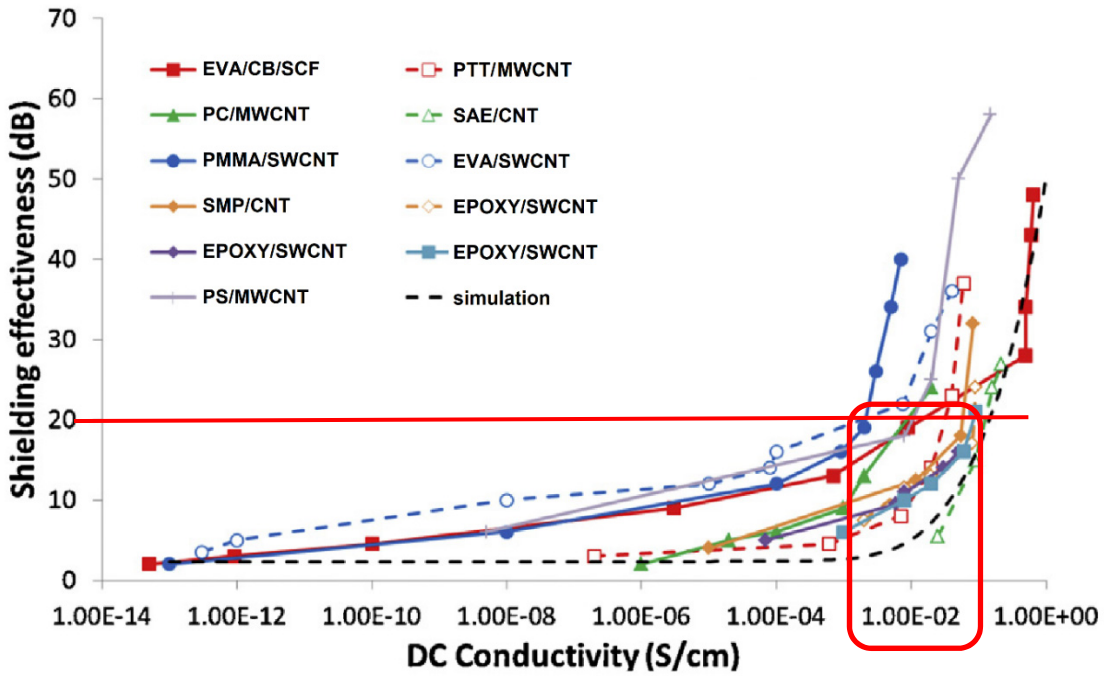

Figure 1.7 - Comparison of the EMI-SE of different carbon-based composites as a function of their DC conductivity (for samples of around 2 mm of thickness at the frequency of 10 GHz). Adapted from (Thomassin et al., 2013)

As shown in Figure 1.7, different composites present a substantial similar behavior when considering their electrical conductivity. It is possible to notice a relation between electrical conductivity and EMI-SE, where the different composites only start presenting the effectiveness required for commercial applications (≥20 dB) when the composites reach a DC

conductivity between around 10E-3 and 10E-1, irrespective of their carbon additive loading (not presented). Another behavior can be observed, just below the percolation threshold the electrical conductivity of the composites drastically increases with the loading of conductive additive, however, the EMI-SE increases only slightly. After the percolation threshold is reached the opposite behaviour happens, and the EMI-SE of the composites becomes very sensible to minor changes in the electrical conductivity, and starts increasing intensely (Thomassin et al., 2013).

For some specific applications, not only the EMI-SE is important, but also the way the radiation is attenuated. In order to compare the shielding mechanisms of different carbon-based composites, Figure 1.8 shows SE_R and SE_A as a function of their electrical conductivity.

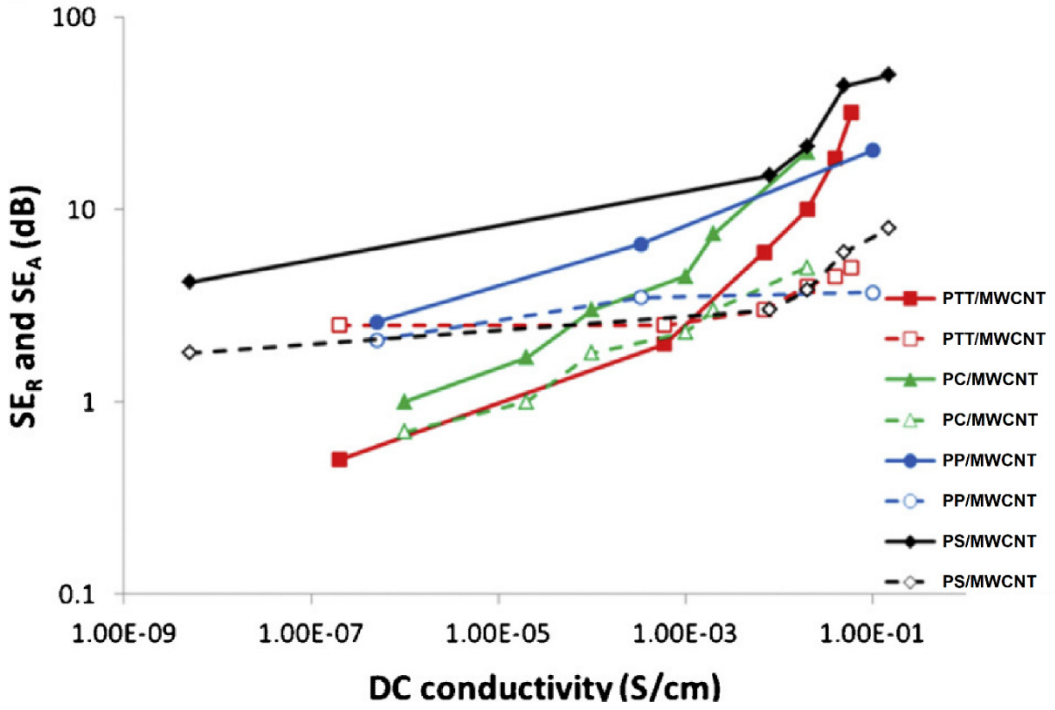

Figure 1.8 - SE_R and SE_A of different MWCNT-based composites as a function of their electrical conductivity (for samples of around 2 mm of thickness at the frequency of 10 GHz). Adapted from (Thomassin et al., 2013)

As it can be observed at Figure 1.8, both SE_R and SE_A contribute to the total EMI-SE in carbon-based composites. Besides, both mechanisms increase with the electrical conductivity of the samples, as expected, and the effect tend to be even more significant in SE_A. However, at this point it is important to highlight the difference between the concepts of shielding mechanisms and power loss. Despite works on the literature showed that some carbon-based nanocomposites present SE_A equal or higher than SE_R, in practice only a small part of power is absorbed by the shielding material (Thomassin et al., 2013). Figure 1.9 present the power balance vs. the electrical conductivity of the same samples presented in Figure 1.8.

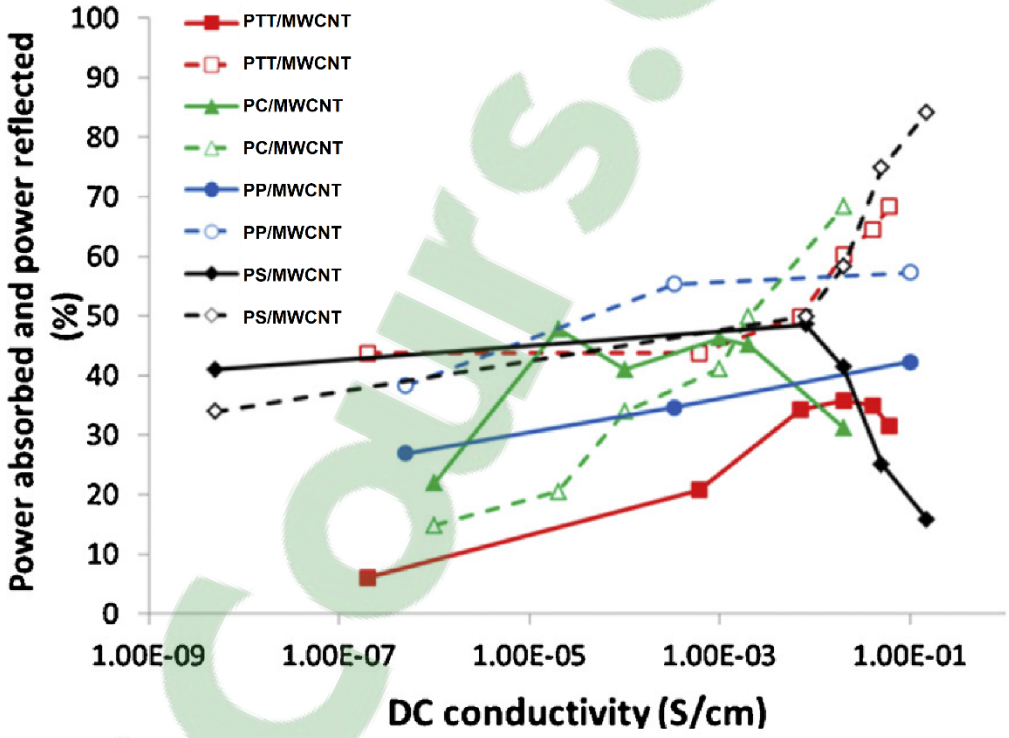

Figure 1.9 - Power balance vs. the electrical conductivity of different MWCNT-based composites as a function of their electrical conductivity (for samples of around 2 mm of thickness at the frequency of 10 GHz). Adapted from (Thomassin et al., 2013)

As shown in Figure 1.9, most part of the radiation is reflected by the shielding materials as the electrical conductivity increases. This behavior can be understood considering that once reflection occurs before absorption, only a small part of the radiation actually remains to be

absorbed by the shielding material (Al-Saleh et al., 2013; Thomassin et al., 2013). Therefore, despite the high values of SE_A of some carbon-based materials and the confusion presented by some reports in the literature, this kind of composites can not be used to absorb EM radiation. In the case of applications that require absorption of the EM radiation different strategies for carbon-based composites are applied, such as the development of multilayers and foams materials with different grades of electrical conductive and/or magnetic additives. In these cases, composites are classified as radar absorbing materials (RAM). However, it is worth emphasizing that the development of RAM materials is not the purpose of this present work.

1.2.3.3 Mechanical properties

For commercial applications, the mechanical properties of EMI shielding materials play an important role. The main parameters that affect their mechanical behaviour include the intrinsic mechanical properties of fillers and matrices, and the aspect ratio, dispersion, and alignment of the fillers inside the matrices (Coleman et al., 2006).

Traditionally, conventional fillers, such as CB and silica, have been used for reinforcement of polymeric materials, however, more recently the use of nanosized fillers, such as carbon nanofibers, CNT, and graphene, are showing to be much more effective. The main advantage of using these nanoparticles remains the fact that fillers of large surface area, when dispersed at a nanoscale level, promote larger contact areas and may favor the wetting and adhesion of the nanofillers in the matrix, which, consequently, enhance the transference of stress from the matrix to the nanofillers (Rath & Li, 2011). On the other hand, the effective dispersion of the fillers is more difficult to achieve in nanosize carbon composites due to large surface area energy and, consequently, strong particle-particle interactions, as already presented in the previous sections (H. Kim et al., 2010; Kuilla et al., 2010; Rath & Li, 2011; Singh et al., 2012; Spitalsky et al., 2010).

One of the biggest challenges in preparing carbon polymer composites for EMI shielding is related to the “ideal” state of mixture for each desirable property. This happens because aiming

to provide electrical properties, it is necessary for the fillers be close to each other to form a conducting network (Arjmand et al., 2012; Arjmand, Mahmoodi, Gelves, Park, & Sundararaj, 2011; Maiti et al., 2013; Thomassin et al., 2013), on the other hand, for the mechanical properties it is desirable the fillers to be completely dispersed in the matrix to avoid aggregation of particles that produces high stress concentration and cause premature failure (Rath & Li, 2011). Another point is that the melt processing techniques commonly used in the industry mainly include extrusion, injection, and the use of rolls, and all these methods can induce the orientation of the particles inside the matrix.

Some works in the literature compare the mechanical properties regarding the alignment of the particles in carbon-based composites along the flow and/or perpendicular to the flow directions, and, in most of the cases, alignment is advantageous to improve the mechanical properties (Erik & Tsu-Wei, 2002; Panaitescu et al., 2014; Yousefi et al., 2014). Panaitescu, et al. (2014), show that highly aligned SEBS and SEBS/G composites presented anisotropic mechanical properties depending on the direction of the alignment (Panaitescu et al., 2014). Figure 1.10 exhibits the mechanical properties (tensile stress vs. tensile strain) of samples that were cut considering the alignment resulted from the induced orientation parallel (II) and perpendicular (L) to the rolling direction (during preparation).

Clicours.COM

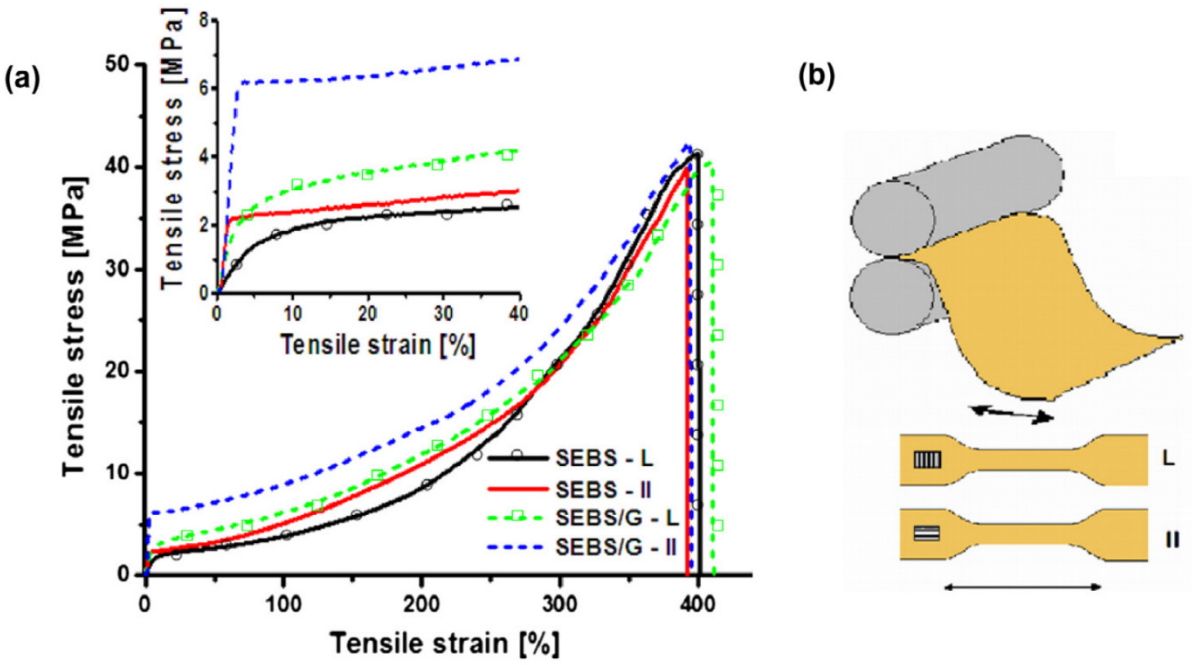

Figure 1.10 - (a) Stress–strain curves for parallel and perpendicular stretching of SEBS and SEBS/G samples, and (b) schematic illustration of specimens cut perpendicular (L) and parallel (II) to the rolling direction. Adapted from (Panaitescu et al., 2014)

As it is presented at Figure 1.10, the authors showed that not just the alignment of CNT was induced by the melting process, but also the polymeric matrix (block copolymer). In this case, the alignment of both the blocks of the copolymer and graphite increased the modulus of the pure matrix and composites.

It is well known that aiming to maintain low cost, reduce processing issues, and avoid the degradation of the mechanical properties of polymer matrices the amount of conducting additive should be the lower as possible. Further, reports on the literature state that from a determined amount of carbon particles, the material start to become more brittle and reduce its failure strain (Rath & Li, 2011; Tanrattanakul & Bunchuay, 2007). However, the amount of the fillers used to improve or avoid decreasing the mechanical properties use to be lower than the loading necessary to achieve high electrical conductivity in polymer composites. Therefore, the balance between mechanical and EMI shielding properties is a critical factor to prepare nanocomposites suitable for commercial applications of EMI shielding materials.

1.3 Flexible materials for EMI shielding applications

As presented in the previous topics, a set of many features must be considered in order to choose the most suitable EMI shielding material for each application. In general, ECPCs based on conventional thermoplastic polymers are able to meet most of the requirements such as low density, aesthetic parameters, and easy processing. However, for some applications in order to avoid leakage of information transmitted by EM waves or ensure a complete environmental sealing e.g., for coating of flexible wires and devices, or for joints of a shielded enclosure, the EMI shielding material must also mandatorily present flexible properties. In these cases, electrically conductive elastomers (ECEs) (a subclass of ECPCs where the polymeric matrix is an elastomer) are considered the most suitable choice (Tong, 2009).

Traditionally, ECEs are being mainly used as EMI gaskets between two metallic surfaces (Gooch & Daher, 2007). For this application, as for other composite materials for EMI shielding, one should keep the loading of conductive additives as low as possible. However, for EMI gaskets this requirement is even more critical, since the amount of conducting additives commonly necessary to achieve suitable EMI-SE significantly decreases the resilience, strength, and ductility of elastomeric matrix. Consequently, the material becomes less effective as a gasket. Therefore, the development of high quality materials for EMI gaskets is commonly more complex than for other EMI shielding materials in general (Chung, 2001).

The selection of the most suitable EMI gasket for each application may consider different criteria, such as shielding effectiveness over a specified frequency range, mounting methods and closure forces, galvanic compatibility with the metallic surfaces, resistance from the external environment, operating temperature range, and costs (Gooch & Daher, 2007). Therefore, among the different flexible materials for EMI shielding, carbon nanoparticles filled ECEs are recently showing to be promising options to the development of EMI shielding materials of high performance.

1.3.1 Review of the ECEs for EMI shielding: general information, effect of dispersion and alignment of carbon particles, and particle-matrix interactions

In this section a review of ECEs for EMI shielding applications and relevant parameters affecting their properties are presented. Special attention is given to carbon particles filled ECEs.

1.3.1.1 Conventional elastomers

ECE gaskets for EMI shielding are conventionally made of a polymer binder, such as silicone, fluorosilicone, or Ethylene Propylene Diene Monomer (EPDM), loaded with different conductive particles, and are used not only to provide EMI protection, but also to function as a pressure and moisture seal (Gooch & Daher, 2007). Generally, most of these composites are prepared by melt compounding in an internal mixer or roll-mill followed by a curing process (Thomassin et al., 2013). The shielding effectiveness and mechanical properties required vary according to the specific application, and are mainly dependent on the elastomeric matrix, type and amount of conductive additive used, filler-matrix interactions, and processing methods. Some examples of ECE for EMI shielding that highlight the influence of these variables are presented below.

ECEs of CB and SCF filled EPDM rubber showed that the composites prepared with SCF presented higher EMI-SE than the samples with CB (≈ 45dB at 8–12 GHz for EPDM/SCF with 50 phr of SCF). As stated by the authors, the explanation for the higher effectiveness of the SCF–filled composites system is related to their higher aspect, since, in this case the formation of the conductive network is favoured with less amount of loading when compared to the particulate additives. Additionally, the samples were also analysed in the 100–2,000 MHz frequency range and results showed that the EMI-SE was dependent on the frequency and greater for the higher frequency range (N. C. Das, Chaki, Khastgir, & Chakraborty, 2001).

Composites of natural rubber (NR), epoxidized natural rubber (ENR), and chlorosulfonated polyethylene (CSM) filled with conductive CB, aluminum powder, and a combination of both were studied to observed the influence of filler-matrix interactions on the EMI shielding and mechanical properties. With respect to additives, CB showed to be more effective to shielding (18–28 dB with 50 phr of CB at 8–12 GHz) than aluminum powder. Interestingly, even though the electrical conductivity was higher for the aluminum powder-based composites, the latter presented lower EMI-SE because of the lower volume fraction and larger grain size of the aluminum powder compared to CB. Regarding the mechanical properties for the composites filled with CB, for samples with 30 phr of CB, the strength increased by approximately 17% for CSM, whereas decreased about 10% and 32% for ENR and NR, respectively. According to the authors, the decrease in tensile strength of NR/CB samples should be due to the nonpolarity of NR and high polarity of the conductive CB. For the composites with 50 phr of CB, the strength decreased for all samples due to the high amount of conducting fillers (Tanrattanakul & Bunchuay, 2007).

In flexible materials for EMI shielding, the balance concerning EMI-SE and mechanical properties plays a critical role, consequently, lots of efforts are being doing in order to improve the relationship between both parameters. Nanocomposites of SG-CNT (long single-walled CNT) and fluorinated rubber prepared by solution casting reached EMI-SE of ≈ 20 dB (at 5.5 - 10 GHz) with 1 wt% of SG-CNT loading. Additionally, the material was stretchable to the double of its original length without cracking (Kato, Horibe, Ata, Yamada, & Hata, 2017). In this work, the authors also showed pictures to exemplify their material working as an EMI shielding enclosure.

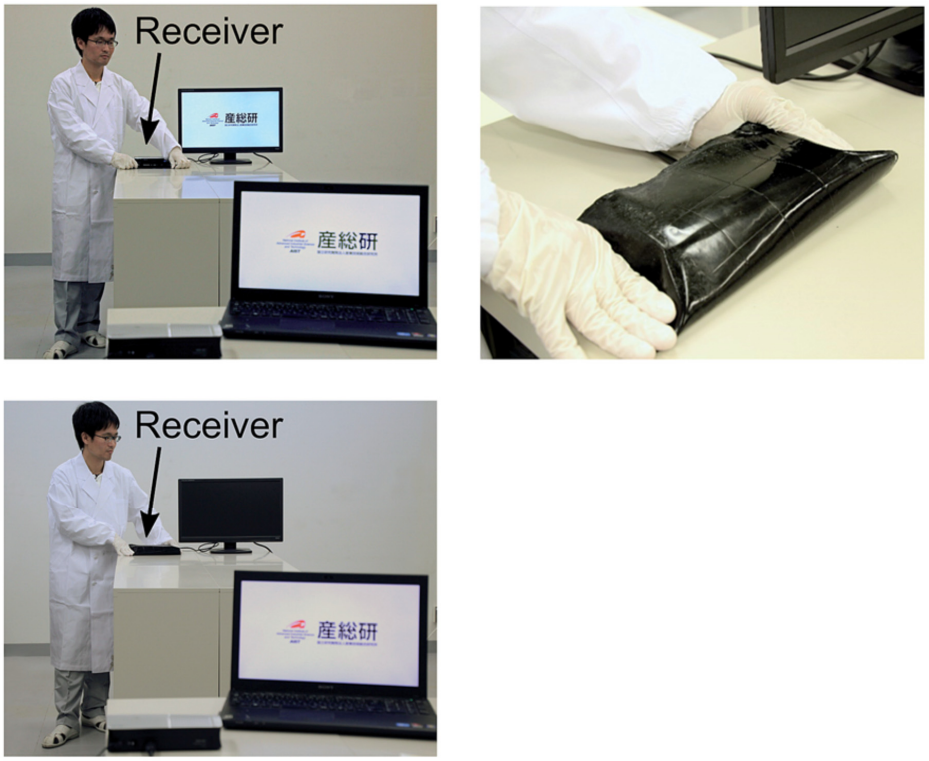

Figure 1.11 - Pictures that exemplify an EMI shielding elastomeric material blocking EM transmission. Adapted from (Kato et al., 2017)

Figure 1.11 shows a receptor of electromagnetic radiation without any shield and with their material wrapping the receptor device. In the first image the receptor worked normally and the screen received the information, and in the second the radiation is blocked and the screen does not show any image (Kato et al., 2017).

Different reports in the literature state that the processing methods commonly used for melt compounding, such as injection, extrusion, and roll milling, can directly affect the properties of ECE due to the orientation of the fillers inside the matrices. This alignment, generally decreases the EMI-SE of the materials compared to composites where the particles are randomly dispersed (Arjmand et al., 2012; Arjmand et al., 2011; Theilmann et al., 2013). Moreover, the EMI-SE of the composites also depend on the direction of the alignment. Composites of EPDM filled with 5 wt.% and 30 wt.% of carbon nanotubes (CNTs) were prepared using a combination of different processing methods (compounding in a mixer,

calendaring, and extrusion) to induce aligned in two distinct directions into the matrix, followed by a curing process. The authors observed that as the amount of CNT in the rubber matrix was increased, the material became more rigid and increased the shear force (melt viscosity), which in turn, collaborated to enhanced the alignment of CNT (Y. A. Kim et al., 2006). The two distinct directions of the CNT alignment is shown in Figure 1.12.

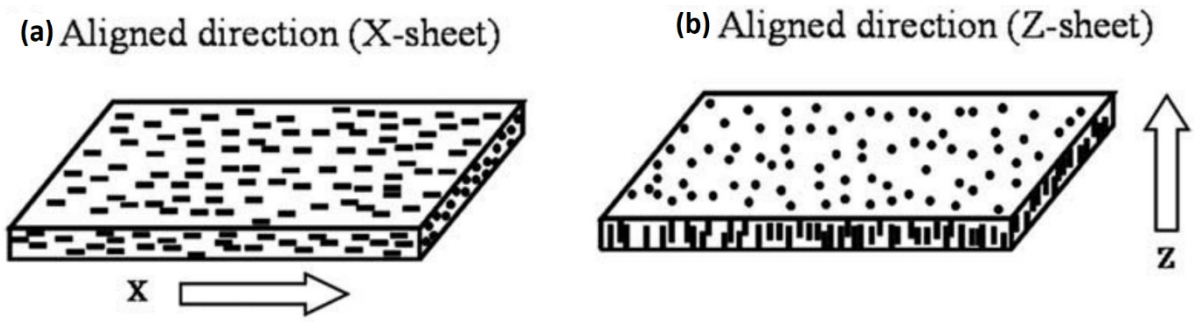

Figure 1.12 - Schematic illustration of different alignment configurations of CNT filled rubber composites upon controlled processing methods. Adapted from (Y. A. Kim et al., 2006)

Results showed that the different orientation of the CNT into the matrix resulted in different improvements in elastic modulus, thermal, and electrical conductivities. Regarding the shielding properties, the maximum EMI-SE was ≈ 60 dB, achieved by the sample with 30 wt% of CNT at the frequency of 1 GHz along the Z-direction (Y. A. Kim et al., 2006).

Besides the examples exhibited above, many others ECEs are presented in the literature for EMI shielding applications. Table 1.1 shows a comparison between different carbon-based rubbers concerning the EMI shielding properties.

Table 1.1 - EMI shielding properties of different carbon-based rubber composites

Sample	**Additive loading**	**Thickness**	**Frequency range**	**EMI-SE**	**Ref.**
EPDM/CB	60 phr	5.5 mm	8–12 GHz	16 dB	(Ghosh & Chakrabarti, 2000)
PDMS/MWNT	5.7 vol%	2 mm	8.2–12.4 GHz	80 dB	(Theilmann et al., 2013)
SBR/CB	60 phr	7 cm	9 GHz	67 dB	(Mohanraj, Chaki, Chakraborty, & Khastgir, 2006)
SBR/CB	60 phr	1.3 cm	10 GHz	≈ 28 dB	(Mohanraj et al., 2006)
SBR/CB	60 phr	0.65 cm	10 GHz	≈ 20 dB	(Mohanraj et al., 2006)
NR/IIR(70/30)/CB	100 phr	2 mm	0.5-5 GHz	≈ 30 dB	(Madani, 2009)
AEM/CB	40 phr	---	8–12 GHz	40 dB	(Sahoo, Naskar, & Tripathy, 2012)
NR/CB	10 phr	≈ 2 mm	1–12 GHz	19–13 dB	(Omar A Al-Hartomy et al., 2013)
IIR/CB	25 phr	---	1 to 15 GHz	≈ 45 dB	(El-Tantawy, 2005)
IIR/LDPE(90/10)/CB	25 phr	---	1 to 15 GHz	≈ 55 dB	(El-Tantawy, 2005)
NR/SCF	30 phr	1.8 - 3.5 mm	100–2000 MHz	≈ 17 dB	(N. C. Das, Khastgir, Chaki, & Chakraborty, 2000)
NR/SCF	30 phr	1.8 - 3.5 mm	8–12 GHz	≈ 27 dB	(N. C. Das et al., 2000)
NR/CB	60 phr	1.8 - 3.5 mm	8–12 GHz	≈ 11 dB	(N. C. Das et al., 2000)
PU/SWNT	20 wt%	2 mm	8.2–12.4 GHz	16–17 dB	(Z. Liu et al., 2007)

Si/CB	40 wt.%	≈ 2 mm	12 GHz	31 dB	(Omar A. Al-Hartomy et al., 2011)
SBR/MWCNT	--	5 mm	18 GHz	40.06 dB	(Abraham et al., 2017)
CR/SCF	40 phr	1.7 mm	100 to 1000 MHz	≈ 37 dB	(Jana, Mallick, & De, 1991)
CR/SCF	40 phr	1.7 mm	8 - 12 GHz	≈ 53 dB	(Jana et al., 1991)
SMP/CNT (Polyesterpolyol series)	6.7 wt.%	3 mm	18–26.5 GHz	≈ 35 dB	(C.-S. Zhang, Ni, Fu, & Kurashiki, 2007)
SMP/CNT (Polyesterpolyol series)	6.7 wt.%	3 mm	33–50 GHz	≈ 48 dB	(C.-S. Zhang et al., 2007)
SMP/CNT (Polyesterpolyol series)	6.7 wt.%	3 mm	50–75 GHz	≈ 62 dB	(C.-S. Zhang et al., 2007)
FKM/CNT	12 wt.%	3.8 mm	8.2–12.4 GHz	≈ 44 dB	(Fletcher, Gupta, Dudley, & Vedeler, 2010)
PU/EG	25 wt.%	2 mm	8.2–12.4 GHz	47.41dB	(Merlini et al., 2017)
PU/xGnP	20 wt.%	2 mm	8.2–12.4 GHz	35.33 dB	(Merlini et al., 2017)
PU/MWCNT	6 wt.%	2 mm	8.2–12.4 GHz	24.14 dB	(Merlini et al., 2017)
PU/CB	30. wt.%	2 mm	8.2–12.4 GHz	28.87 dB	(Merlini et al., 2017)
PU/MWCNT	25 wt.%	100 μm	8–12 GHz	≈ 25 dB	(Anh Son, 2011)

Si/MWCNT	5 wt.%	2 mm	12 GHz	≈ 30 dB	(L. Liu, Kong, Yin, & Matitsine, 2011)
Si/SWCNT	6 wt.%	2 mm	12 GHz	≈ 24 dB	(L. Liu et al., 2011)

Despite the suitable EMI-SE of many carbon-based ECEs for EMI-shielding, the use of conventional rubbers as the elastomeric matrix presents some drawbacks. The main disadvantages of using vulcanized rubbers are related to the curing process, that involves the use of solvents, longer time of fabrication and high energy consumption. Therefore, aiming to overcome these problems, thermoplastic elastomers are showing to be an interesting option to replace conventional rubbers for the development of high performance flexible EMI shielding materials.

1.3.1.2 Thermoplastic elastomers

Thermoplastic elastomers (TPE) is a class of materials that exhibit elastic behaviour similar to conventional vulcanized elastomers, but can be processed as thermoplastics (Drobny, 2007a). TPEs are essentially systems formed by two different phases bonded chemically by block or graft polymerization. In these systems, one phase is hard and solid at ambient temperature and acts as physical cross-links, and the other is an elastomer and provides flexibility and elasticity to the material (Drobny, 2007a).

The main advantages of using TPEs compared to conventional rubbers includes simpler processing, fewer processing steps, shorter fabrication times, lower energy consumption, possibility of using scraps (recyclability), better quality control, and lower fabrication costs. Additionally, since TPEs, in general, have lower density than conventional rubber compounds, their volume cost is often lower (Drobny, 2007a). On the other hand, the fewer disadvantages include melting at elevated temperatures, which consequently reduces the service

temperatures, limited number of low-hardness TPEs, and most TPE materials need to be dried before processing (Drobny, 2007a).

There are different classes of TPEs commercially available, such as styrenic block copolymers (SBC), polyolefin-based thermoplastic elastomers (TPO), thermoplastic elastomers based on dynamically vulcanized elastomer-plastic blends (TPV), thermoplastic elastomers based on polyurethanes (TPU), copolyether-ester block thermoplastic (COPE), polyamide thermoplastic elastomers with polyamide hard segments and soft segments based on aliphatic polyesters or aliphatic polycarbonates (COPA), and others that do not fit into any of the mentioned groups (Drobny, 2007a).

Among these groups, carbon-based TPU composites are recently being widely studied. The interest in TPU as a matrix is mainly due to its polarity, therefore, the use of functionalized carbon particles, is preferred. In these cases, additive-matrix interactions are expected, which normally improves the dispersion of the additives in the matrix. As an example, Bansala et al. (2017) prepared nanocomposites of TPU/thermally reduced graphene nanosheets (TRG) for microwave shielding applications in the frequency range of 12–18 GHz. Results showed that with 5.5 vol% of TRG loading the EMI-SE ranged from 26 to 32 dB in the frequency region for nanocomposites of 2 mm thick. The authors also presented a table in order to compare the SE of different graphene-based/TPU nanocomposites exhibited in the literature (Bansala et al., 2017), which is shown in Table 1.2 (adapted).

Clicours.COM

Table 1.2 - EMI shielding properties of different graphene based-TPU nanocomposites. Adapted from (Bansala et al., 2017)

Filler	Filler loading	Frequency range	EMI SE (dB)	Thickness (mm)
Expanded graphite	20 wt%	8–12 GHz	−20	4
Graphene-like carbon nanostructures (GNS)	25 wt%	8–12 GHz	−26.4	2
Non-covalently modified graphene	7.7 vol%	8–12 GHz	−32	2
Covalently modified graphene	5 vol%	8–12 GHz	−38	2
Polydopamine-coated graphene	4.7 vol%	30 MHz–2 GHz	−17.6	2
Thermally reduced graphene	5.5 vol%	8–12 GHz	−21	3
Functionalized graphene sheets (FGS)	0.35 wt%	8–12 GHz	−9.8	29 × 10
Thermally exfoliated and annealed graphene sheets	5.5 vol%	12–18 GHz	−26 to −29	2

Some others classes of TPEs are being used in EMI shielding composites and blends. As an example, Bhadra, Singha, and Khastgir (2009) prepared blends of polyolefinic thermoplastic elastomer ethylene 1-octene copolymer and polyaniline (PAni) for EMI shielding. According to the authors, blends of 5.4 mm thick with 40 phr of PAni presented an EM attenuation of around 80% in the 7.8–12.4 GHz frequency range (Bhadra et al., 2009). Park et al. (2010) prepared and compared nanocomposites of reactive ethylene terpolymer (RET) and SWCNT and chemical functionalized SWCNT (COOH–SWCNT) for EMI shielding in the 8-12 GHz frequency range. Results showed EMI-SE around one order of magnitude higher for the RET/COOH–SWCNT compared to the RET/SWCNT. The EMI-SE for RET/COOH–SWCNT samples of ≈ 2 mm thick with 2.25 vol % was ≈ 15 dB, and ≈ 5 dB for the RET/SWCNT samples with the same thickness and vol % of conducting additive. The maximum EMI-SE in the study was ≈ 27 dB achieved with 3.5% of SWCNT in RET/ SWCNT nanocomposites (Park, Theilmann, Asbeck, & Bandaru, 2010).

Results of some others composites of TPEs filled with different carbon particles for EMI shielding available on the literature are presented in Table 1.3.

Table 1.3 - EMI shielding properties of different carbon-based TPE composites

Sample	**Additive loading**	**Thickness**	**Frequency range**	**EMI-SE**	**Ref.**
EVA/SCF	30 phr	1.8 - 3.5 mm	100–2000 MHz	≈ 25 dB	(N. C. Das et al., 2000)
EVA/SCF	30 phr	1.8 - 3.5 mm	8–12 GHz	≈ 32 dB	(N. C. Das et al., 2000)
EVA/CB	60 phr	1.8 - 3.5 mm	8–12 GHz	≈ 20 dB	(N. C. Das et al., 2000)
EVA/SWNT	15 wt.%	1.5 mm	12 GHz	22 dB	(Narayan Chandra Das & Maiti, 2008)
EVA/SWNT	15 wt.%	1.5 mm	1 GHz	15 dB	(Narayan Chandra Das & Maiti, 2008)
TPU/MWCNT	10 wt.%	2.5 mm	8.2 - 12.4 GHz	41.6 dB	(T. K. Gupta et al., 2013)
EMA/CB	40 wt.%	5 mm	8.2 - 12.4 GHz	30.8 dB	(Bhawal, Ganguly, Das, Mondal, & Das)
TPU/SWCNT	20 wt.%	2 mm	8.2 - 12.4 GHz	≈ 17 dB	(Z. Liu et al., 2007)
TPU/MWCNT	10 wt.%	1.5 mm	8.2 - 12.4 GHz	≈ 29 dB	(Gupta, Singh, Dhakate, Singh, & Mathur, 2013)
TPU/EG	20 wt%	4 mm	8-12 GHz	20 dB	(Valentini, Piana, Pionteck, Lamastra, & Nanni, 2015)
TPU/CB	15	2 mm	8-12 GHz	≈ 20 dB	(Ramôa et al., 2013)
TPU/CNT	10	2 mm	8-12 GHz	≈ 22 dB	(Ramôa et al., 2013)

Another class of TPEs that may be interesting to produce ECEs for EMI shielding is styrenic block copolymers. As already presented in the previous sections, among other advantages, the use of styrenic block copolymers as matrices in carbon-based composites may promote π-π interactions between both phases, which contribute to improve the dispersion and reduce the

amount of fillers necessary to achieve the required properties without the need using of functionalized carbon particles.

Styrenic block copolymers (SBCs) are TPEs based on alternated blocks of polystyrene and elastomeric segments. When heated, their polystyrene domains soften and the material is capable of flowing and can be processed as a conventional thermoplastic material. On the other hand, at room temperature, the polystyrene block is rigid and acts as cross-links in conventionally vulcanized elastomers, while the elastomeric phase is easily extendable (Drobny, 2007c).

Currently, SBCs is most used class of TPEs worldwide (Drobny, 2007a). However, despite their great potential in conductive composites, only very few works in the literature present SBCs as matrices for EMI shielding materials. Some examples are presented below.

SBS/polyaniline doped with dodecylbenzene sulfonic acid (PAni.DBSA) were prepared and characterized regarding the effect of different processing methods, including melt compounding and in situ polymerization of aniline in SBS, on the EMI-SE of the blends (at 8-12 GHz). With 30 wt% of SBS/PAni.DBSA, the EMI-SE ranged from 35 to 40 dB for the blend prepared by in situ polymerization, and from 20 to 25 dB for the blend prepared by melt compounding (Magioli et al., 2012).

Blends of poly(styrene-b-styrene-butadiene-b-styrene) (STF)/PAni-DBSA were prepared by in situ polymerization and the influence of samples of three different thicknesses, 1, 3 and 5mm, on the EMI-SE was investigated. The higher EMI-SE was achieved for the 5 mm thick sample with 49/51 of PAni.DBSA/STF, respectively, which was 14 dB at 8.20 GHz that correspond to 96% (lower than the minimum SE required for commercial applications). The influence of the thickness was compared for the blend with 35/65 of PAni.DBSA/STF, respectively. The best result, as expected, was achieved with the 5 mm sample, that reached 85% of EMI-SE. According to the authors, the increasing of the sample thickness resulted in higher amount of conducting meshes, which promoted both absorption and internal reflection,

and consequently contributed to increase the final EMI-SE of the blends (Schettini & Soares, 2011).

Hybrid composites of STF filled with PAni-DBSA and CB were prepared by in situ polymerization and the influence of the both additives in the EMI-SE (at 8-12 GHz) was analysed. Results showed that when PAni.DBSA and CB were used at the same time, the EMI-SE of the hybrid composite was not directly proportional to sum of the EMI-SE of both conductive fillers in STF (in composites with just one kind of conducting additive), since the presence of one filler impaired the effectiveness of the other filler to shield EMI radiation and vice a versa. For example, the EMI-SE of the PAni.DBSA/STF with 25 wt% of PAni.DBSA was ≈20 dB, for CB/STF with 25 wt% of CB it was ≈51 dB, and for the hydride composite of PAni.DBSA/CB/STF with 75.2/23.2/1.6 wt% of each phase, respectively, the total EMI-SE was ≈12 dB. In this composites, during the in situ polymerization of Ani into the STF matrix, the addition of electrically conducting CB did not change the electrical properties of the material additively. According to the authors, the presence of CB interfered in the conversion of Ani to PAni regarding the degree of polymerization and in its crystal structure. At the same time, the presence of PAni.DBSA also changed the characteristic properties of CB particles by interacting with the organic groups in their surface and modifying the distribution of the CB particles in the matrix (Schettini et al., 2012).

Composites of silver nanoparticles (NPs)/SBS were prepared and their EMI-SE after 10, 100, 300 times of stretching with ε=0.6 was characterized. The maximum EMI-SE of 69 dB was obtained with 66.5wt% of NPs at frequency range from 8 to 12 GHz (E. Kim et al., 2016). Figure 1.13 exhibits the EMI-SE of the material after cyclic elongation tests.

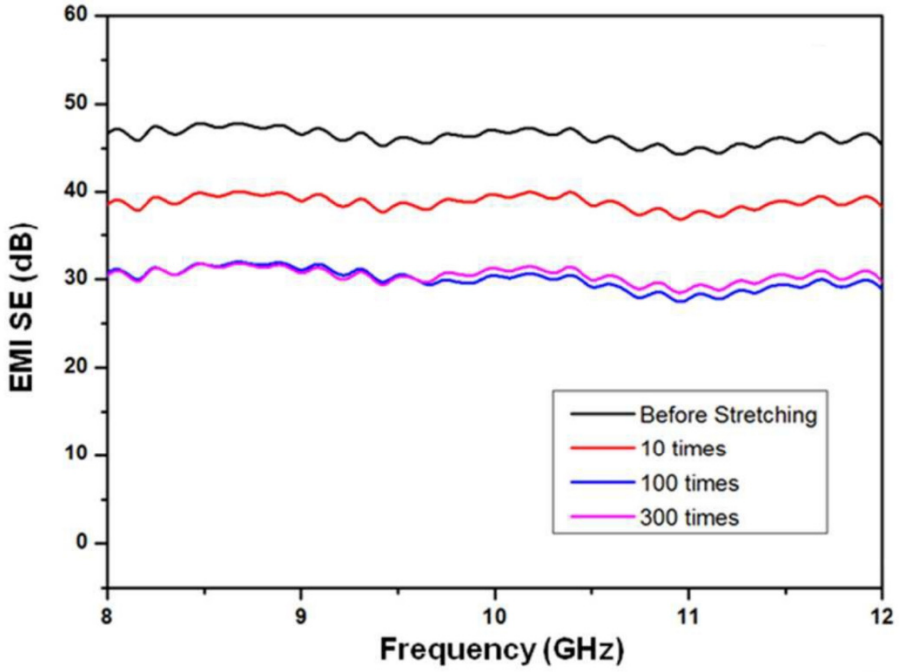

Figure 1.13 - EMI-SE of NPs/SBS composites after 10 to 300 times stretching (E. Kim et al., 2016)

As shown in Figure 1.13, the NPs/SBS composites still maintained suitable EMI-SE (> 20dB) even after cyclic elongation.

Among the whole class of SBCs, although SBS is widely used by industry, this block copolymer is formed by polystyrene and elastomeric segments of polybutadiene and, consequently, it presents an unsaturation in the elastomeric segment that make it more prone to degradation. Therefore, block copolymers such as poly (styrene-b-(ethylene-co-butylene)-b-styrene) (SEBS) are a better option for most applications. SEBS is a styrenic block copolymer obtained upon the hydrogenations of SBS, which due to the absence of unsaturation can be processed at elevated temperatures for longer periods of time without damaging its structure, and also which present excellent chemical resistance, and UV stability (Drobny, 2007c; Holden, 2000). Consequently, composites based on SEBS may be a good option to the development of EMI shielding materials.

Chapters 2, 3, and 4 present specific contributions to the development of a new generation of high performance flexible EMI shielding materials based on nanocomposites of SEBS and carbon nanoparticles.

CHAPTER 2

This chapter presents the article corresponding to the results of the first part of the project. It emphasizes the dispersion and distribution of the conducting additives in the polymeric matrix, additive-matrix interactions, the formation of an electrically conducting network, and the EMI properties of SEBS/CNT nanocomposites for EMI shielding.

ELECTROMAGNETIC INTERFERENCE SHIELDING AND ELECTRICAL PROPERTIES OF NANOCOMPOSITES BASED ON POLY (STYRENE-B-ETHYLENE-RAN-BUTYLENE-B-STYRENE) AND CARBON NANOTUBES

Scheyla Kuester[1,3], Guilherme M. O. Barra[1], José Carlos Ferreira Jr.[1], Bluma G. Soares[2], Nicole R. Demarquette[3]

[1*]Universidade Federal de Santa Catarina, Departamento de Engenharia Mecânica, Florianópolis, SC, Brazil,

[2]Departamento De Engenharia Metalúrgica E De Materiais, Universidade Federal do Rio de Janeiro, Rio de Janeiro, Brazil.

[3#]École de technologie supérieure de Montréal, Mechanical Engineering Department, Montreal, QC, Canada

This article was published in European Polymer Journal, v.77, p.43 -53, 2016.

ABSTRACT

In this work, poly (styrene-b-ethylene-ran-butylene-b-styrene) and carbon nanotube (SEBS/CNT) nanocomposites were prepared by melt compounding for electromagnetic shielding applications. The structural characteristics and the morphology of carbon nanotubes (CNT) and nanocomposites were investigated using Raman spectroscopy and Field Emission Gun Scanning Electron Microscopy. The DC electrical conductivity of the nanocomposites was evaluated by two-probe and four-probe methods, and the electrical percolation threshold

was calculated. Dielectrical properties, shielding mechanisms, and the electromagnetic interference shielding effectiveness (EMI-SE) of the nanocomposites were evaluated for the 8.2-12.4 GHz X-band microwave frequency range. A comparison between theoretical and experimental EMI-SE results was also reported. The nanocomposites studied exhibited a very sharp insulator-conductor transition at a CNT concentration of around 1wt. %, and the electrical conductivity increased by 17 orders of magnitude upon addition of more than 2wt. % CNT. Upon addition of 15 wt. % of CNT, an EMI-SE of 30.07 dB, which corresponds to a reduction of 99.9 % of the incident radiation, was obtained. The results indicate that the nanocomposites studied are promising candidates for electromagnetic shielding applications.

Keywords: Polymer-matrix nanocomposites; Carbon Nanotubes; Electrical properties; Electromagnetic shielding effectiveness

2.1 Introduction

The extensive development of mobile communication in modern society is becoming a serious cause for concern, especially with regards to electromagnetic interferences (EMI). Basically, EMI are undesired signals emitted by electronic equipment that perturb the operation performance of other electronic devices or cause damage to living organisms (Yong Li et al., 2010; Mohammed & Uttandaraman, 2013; Saini & Arora, 2012; Thomassin et al., 2013). In order to avoid these interference problems, significant effort has been dedicated to developing new materials for EMI shielding.

An EMI shielding material is essentially a barrier that attenuates or eliminates the transmission of electromagnetic waves from one region to another, using mobile charge carriers (electrons or holes) or electric and/or magnetic dipoles, which interact with the incident electromagnetic wave (Chung, 2001; Saini & Arora, 2012). In EMI shields, the property that quantifies the ability to attenuate the incident electromagnetic radiation is known as shielding effectiveness (SE), and is given in decibels (dB) (Al-Saleh & Sundararaj, 2009; Ramôa et al., 2013; Saini & Arora, 2012; Thomassin et al., 2013).

EMI-SE results from all shielding mechanisms, according to (Al-Saleh & Sundararaj, 2009; Yong Li et al., 2010; Maiti et al., 2013; Saini & Arora, 2012; Singh et al., 2012):

$$\text{EMI SE} = \text{SE}_\text{R} + \text{SE}_\text{A} + \text{SE}_\text{M}\ (\text{dB}) \tag{2.1}$$

where SE_R, SE_A, and SE_M correspond to shielding mechanisms by reflection, absorption, and multiple-reflection, respectively.

Shielding mechanisms depend on the characteristic of the attenuator material. A shielding mechanism by reflections (SE_R) occurs when the shielding material has mobile charge carriers that interact with the electromagnetic wave. The absorption mechanism (SE_A) is seen when the material has electric and/or magnetic dipoles that interact with the electromagnetic field, and occurs for materials with high dielectric constant and/or high magnetic permeability (Al-Saleh & Sundararaj, 2009; Chung, 2001; Saini & Arora, 2012). The multiple-reflection mechanism (SE_M) happens when the electromagnetic wave is reflected from the second inner boundary to the first being reflected back and forth within the material. However, these internal reflections are absorbed, and consequently, can be ignored when the shielding material is thicker than the distance required to decrease the electromagnetic wave to 1/e or 37% of its original strength. This distance is known as Skin Depth, and can be calculated according to Equation 2.2 (Al-Saleh & Sundararaj, 2009; Chung, 2001; Yong Li et al., 2010; Mohammed & Uttandaraman, 2013; Singh et al., 2012):

$$\delta = \frac{1}{\sqrt{\pi f \mu \sigma}} \tag{2.2}$$

where f is the frequency of radiation (Hz), μ is the magnetic permeability of the shielding material ($\mu = \mu_0\mu_r$, where μ_0 is the permeability of free space $\mu_0 = 4\pi \times 10^{-7}$ H.m^{-1}, and $\mu_r = 1$ for carbon-based materials), and σ is the electrical conductivity. From a practical perspective, SE_M can safely be ignored when $SE_A \geq 10$ dB (Saini & Arora, 2012; Singh et al., 2012).

Clicours.COM

Several theoretical models have been suggested in the literature to predict EMI-SE. According to Al-Saleh and Sundararaj (2009), the SE_R and SE_Acan be calculated according to (Al-Saleh & Sundararaj, 2009):

$$SE_{\mathrm{R}} = 39.5 + 10log\left(\frac{\sigma}{2\pi f\mu}\right) \quad (2.3)$$

$$SE_{\mathrm{A}} = 8.7\frac{t}{\delta} \quad (2.4)$$

where σ is the electrical conductivity, f is the frequency of radiation (Hz), μ is the magnetic permeability of the shielding material ($\mu = \mu_0\mu_r$, where μ_0 is the permeability of vacuum $\mu_0 = 4\pi \times 10^{-7}$ H.m^{-1}, with $\mu_r = 1$ carbon-based materials), t is the shielding material thickness, and δ is the skin depth. It is important to state that Equation 2.3 predicts a negative value for shielding if $\sigma/f\mu$ is less than 7.04×10^{-4}(Al-Saleh & Sundararaj, 2009).

Experimentally, EMI-SE can be evaluated by measuring the amount of power of an incident radiation that is being reflected (R,) and that is being transmitted (T) using complex scattering parameters (Al-Saleh et al., 2013; Al-Saleh & Sundararaj, 2009; Maiti et al., 2013; Ramôa et al., 2013). As the incident radiation power is normally taken as 1 mW, the amount of absorbed (A) radiation can be estimated from Equation 2.5 (Al-Saleh et al., 2013; Maiti et al., 2013; Ramôa et al., 2013; Saini & Arora, 2012):

$$\mathrm{I} = 1 = \mathrm{A} + \mathrm{R} + \mathrm{T} \quad (2.5)$$

From T and R experimental data coefficients, the contribution to EMI-SE by reflection (SE_R) and absorption (SE_A) mechanisms can be determined by (Al-Saleh & Sundararaj, 2009; Maiti et al., 2013; Ramôa et al., 2013; Saini & Arora, 2012):

$$\mathrm{SE_R} = 10\log\frac{\mathrm{I}}{\mathrm{I}-\mathrm{R}} \quad (2.6)$$

$$SE_A = 10 \log \frac{I-R}{T} \quad (2.7)$$

$$EMISE = SE_R + SE_A = 10 \log \frac{I}{I-R} + 10 \log \frac{I-R}{T} = 10 \log \frac{I}{T} \quad (2.8)$$

Traditionally, metals have been the most used materials for EMI shielding applications, mainly due to their high conductivity. However, these materials present some drawbacks, such as high density, propensity to corrosion, and uneconomic processing (Anupama et al., 2013; Saini & Arora, 2012; Thomassin et al., 2013; Yousefi et al., 2014). As an alternative, dielectric materials, such as polymer composites based on conductive carbon particles, are being developed (Anupama et al., 2013; Chung, 2001; Z. Liu et al., 2007; Maiti et al., 2013; Mohammed & Uttandaraman, 2013; Ramôa et al., 2013; Sachdev et al., 2011; Saini & Arora, 2012; Thomassin et al., 2013; Yousefi et al., 2014; C.-S. Zhang et al., 2007).

In electrically conductive polymer composites, the electrical conductivity occurs due to a percolation of the particles imbedded within the polymer matrix. At a certain concentration of fillers, known as the percolation threshold, the composite presents an insulator-conductor transition. (Maiti et al., 2013; Ramôa et al., 2013; Saini & Arora, 2012; Vargas-Bernal, Herrera-Perez, Calixto-Olalde, & Tecpoyotl-Torres, 2013). The percolation threshold depends on a) the nature of the polymer matrix, b) the characteristics of the fillers, such as their geometry, surface area and electrical conductivity, c) the morphology of the composite, characterized by the quality of the distribution and dispersion of fillers, which in turns depends on the d) the matrix-fillers interactions and the processing parameters used to obtained the composite (Alig et al., 2012; Bilotti et al., 2013; Potts et al., 2011; Sachdev et al., 2011; Thomassin et al., 2013).

Considering the relevance of having a low percolation threshold in order to reduce costs and facilitate the processing of composites (Bilotti et al., 2013; You et al., 2014), the use of carbon nanoparticles, such as CNT and graphene, can represent a nice alternative to obtaining polymer composites, which in this case, are known as polymer nanocomposites (Al-Saleh et al., 2013; Alig et al., 2012; Calisi et al., 2013; Maiti et al., 2013; Matzeu et al., 2012; Saini & Arora,

2012; C.-S. Zhang et al., 2007). In particular, experimental results have already shown that the use of CNT is more efficient than the use of the same wt. % of microsized carbon particles (Al-Saleh & Sundararaj, 2009; Alig et al., 2012; L. Liu, Kong, Yin, Chen, & Matitsine, 2010) as far as electromagnetism is concerned.

CNT are long cylinders of covalently bonded carbon atoms which present some relevant mechanical and electrical properties. They also present a high aspect ratio (*p*) (p = L/D, where L is the length ≈ 1- 50 μm, and D is the diameter ≈ 1 - 50 nm) (Alig et al., 2012; Bokobza, 2007; Choudhary & Gupta, 2011; Coleman et al., 2006; Dai, 2002), a characteristic that helps obtain polymer nanocomposites with low electrical thresholds once they are well dispersed and distributed through the polymer matrix (Alig et al., 2012; Thomassin et al., 2013). However, CNT present high surface areas and strong van der Waals interactions between the tubes, which make them prone to forming large agglomerates and hindering their dispersion (Alig et al., 2012; Calisi et al., 2013; Matzeu et al., 2012). Moreover, when CNT are not properly dispersed and distributed in polymer matrices, a higher amount of fillers is necessary to achieve the desired properties (Saini & Arora, 2012).

Seeking to overcome the drawbacks caused by difficulties in dispersing nanosized carbon fillers, some authors have suggested the use of blends of immiscible polymers as matrices. The main advantage in this case is that the CNT may be selectively located in just one of the blend's phases, thus reducing the amount of fillers required (Brigandi, Cogen, & Pearson, 2014; Göldel, Marmur, Kasaliwal, Pötschke, & Heinrich, 2011; Lee, Park, & Lee, 2008; Meier et al., 2011; Sun, Guo, & Yu, 2010; Wode et al., 2012; M. Wu & Shaw, 2006; Zha, Li, Liao, Bai, & Dang, 2013; Q. Zhang, Xiong, Yan, Chen, & Zhu, 2008). However, tailoring the morphology of the blend to achieve the desired electrical properties is not an easy task.

Alternatively, some studies in the literature suggest that the use of block copolymers, such as poly (styrene-b-isoprene-b-styrene) (SIS), poly (styrene-b-butadiene-b-styrene) (SBS), and poly (styrene-b-ethylene-ran-butylene-b-styrene) (SEBS), can be an advantageous substitute of immiscible polymers blends, once the structure of these materials already presents a

morphology of two distinct phases (Lee et al., 2008; Meier et al., 2011). The template morphology of these block copolymers can be used to tailor the location of nanoparticles such as clays (Danilo J. Carastan, Amurin, Craievich, Gonçalves, & Demarquette, 2013, 2014; Helal et al., 2015), as well as carbon nanoparticles (Lee et al., 2008; Meier et al., 2011), although this been done to a lesser degree in the latter case. As examples, Peponi et al. (2009) studied the confinement of functionalized graphene sheets in poly (styrene-b-isoprene-b-styrene) (SIS). According to the results, graphene was confined only in the polystyrene (PS) phase of the block copolymer, due to geometric and chemical affinities between the PS block and the graphene sheets (Peponi et al., 2009). Liu Ye and Xie (2011) studied nanocomposites of poly (styrene-b-butadiene-b-styrene) (SBS) containing modified exfoliated graphene sheets from graphite mixed by solution. According to the authors, these nanocomposites presented π-π interactions between graphene and the PS chains due to the presence of aromatic rings in their structures. Their results indicated a percolation threshold of 0.25 vol. % (corresponding to a conductivity of ($\approx 3.5 \times 10^{-5}$ $S.m^{-1}$), and that upon addition of 4.5 vol.%, a conductivity of 13 $S.m^{-1}$ was reached (Y.-T. Liu et al., 2011).

Li and Shimizu (2009) prepared nanocomposites of SEBS and CNT by melt compounding at very high shear and obtained a maximum conductivity of 5.16 $S.cm^{-1}$ with 15 wt. % of CNT (Yongjin Li & Shimizu, 2009). However, and to the best of our knowledge, composites based on styrenic block copolymers and CNT for electromagnetic shielding applications have thus far never been studied in the literature.

In this work, nanocomposites of SEBS/CNT were prepared by melt compounding for electromagnetic shielding purposes. The structural characteristics and the morphology of CNT and nanocomposites were investigated through Raman spectroscopy and Field Emission Gun Scanning Electron Microscopy. The DC electrical conductivity of the nanocomposites was evaluated by two-probe and four-probe methods, and the electrical percolation threshold was calculated. Dielectrical properties, shielding mechanisms, and the EMI-SE of the nanocomposites were investigated in the 8.2-12.4 GHz X-band microwave frequency range. A comparison between theoretical and experimental EMI-SE results was also reported.

2.2 Experimental

Poly (styrene-b-ethylene-ran-butylene-b-styrene) (SEBS) (Kraton G-1650; number-average molecular weight = 94,000 $g.mol^{-1}$; polystyrene content = 30 wt. %, density 0.91 $g.cm^{-3}$) was obtained from Kraton Polymers do Brasil Ind. Com. Prod. Petr. Ltda. Multiwalled Carbon Nanotube (MWCNT) (Nanocyl™ NC 7000 series, surface area = 250 - 300 $m^2.g^{-1}$; density = 1.30 – 2.00 $g.cm^{-3}$; carbon purity = 90 %; average diameter = 9.5 nm; average length = 1.5 μm), was purchased from Nanocyl S.A.

Nanocomposites were prepared by melt compounding in a torque rheometer (Haake Rheocord) coupled to a mixing chamber (RHEOMIX 600p, 70 cm^3) using roller rotors. The processing parameters were as follows: temperature, 230 °C; rotation speed, 150 rpm, and mixing time, 25 min, defined according to a previous study. Films were compression molded in different geometries (square and circle) and thicknesses (1 and 2 mm), depending on the type of characterization to be performed. The nanocomposites were molded in a Bovenau hydraulic press, model ST P15, at a temperature of 230 °C and pressure of around 20 MPa, for 10 min.

The structural morphology of CNT as-received and once imbedded in the nanocomposite after processing was evaluated by Raman spectroscopy in a CRM (Confocal Raman Microscope) Alpha 300R Witec system with a 532nm laser excitation <100mW and a UHTS 300 (ultra high throughput spectrometer) with gratings of 600 or 1800 g/mm with 500 blaze. The morphology of pristine CNT and SEBS/CNT nanocomposites was studied by field emission gun scanning electron microscopy (FEG-SEM) using a JEOL JSM-6701 F field instrument at an acceleration voltage of 10 kV. For cross-sectional analysis of the nanocomposites, samples were cryogenically fractured in liquid nitrogen and placed in an aluminum sample holder containing a double-sided conductive carbon adhesive tape and coated with gold.

The DC electrical conductivity of neat SEBS and SEBS/CNT nanocomposites with different weight fractions of conductive nanofillers was determined by the two-probe and four-probe methods at room temperature (Heaney, 1999). For neat SEBS and high resistivity

nanocomposites, the electrical conductivity measurements were performed using the two-probe standard method, with a Keithley 6517A electrometer connected to a Keithley 8009 test fixture. The electrical conductivity of the conductive nanofillers and low resistivity nanocomposites was measured using the four-probe standard method, with a Keithley 6220 current source to apply the current and a Keithley 6517A electrometer to measure the difference of potential. Measurements were performed five times, and the average DC electrical conductivity values were registered.

The EMI-SE measurements and the dielectric analysis of the nanocomposites were performed using an Agilent Technology PNA series network analyzer (N5230C Agilent PNA-L, Santa Clara, CA) in the X-band microwave frequency range (8.2-12.4 GHz). EMI-SE measurements were carried out with an X-band waveguide as the sample holder and the thickness of all samples was 2.0 mm.

2.3 Results and Discussion

2.3.1 Morphological analysis

Raman spectroscopy is an interesting tool to access non-covalent π-π interactions between nanotubes and aromatic rings of polymer chains. Figure 2.1 shows the Raman spectra of the pristine CNT and SEBS/CNT nanocomposite with 10 wt. % CNT. The pristine CNT presents the characteristic D peak related to the in-plane vibration of sp^2 carbons atoms at 1335 cm^{-1} and G peak assigned to the stacking orders at 1573 cm^{-1}.It can be seen from Figure 1 that the spectra of the SEBS/CNT nanocomposite presents shifts of 12 cm^{-1} (1347 cm^{-1}) and 19 cm^{-1} (1592 cm^{-1}) in the D-band and G-band peak, respectively providing evidence of non-covalent interfacial interactions between the polymer matrix and the CNTs (Vasileiou et al., 2013).

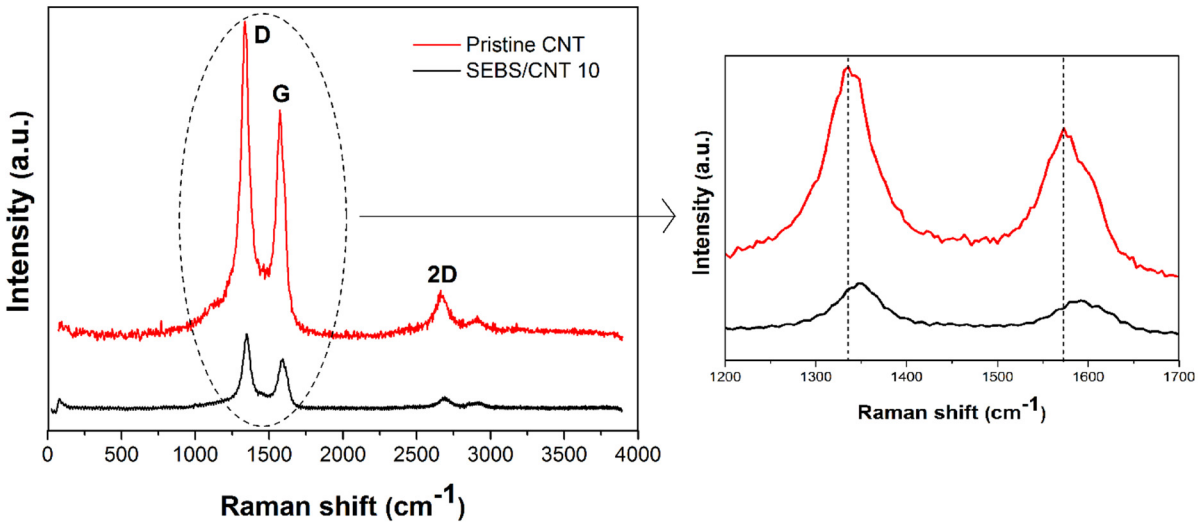

Figure 2.1 - Raman spectra of pristine CNT and SEBS/CNT nanocomposite with 10 wt. % of CNT and blow up of the spectra in the 1200-1700 cm^{-1} region

Furthermore, the intensity ratio of *D* and *G* peaks, I_D/I_G, is often used to evaluate the quantity of defects in the CNT structure (Calisi et al., 2013; Y.-T. Liu et al., 2011; Xiong et al., 2012). According to the spectra analysis, the I_D/I_G of the pristine CNT was 1.40, while the I_D/I_G for the nanocomposite with 10 wt. % CNT loading was 1.45. These results mean that the CNT structure was not significantly damaged during melt compounding.

Carbon nanotubes are usually provided in strong agglomerates. These primary CNT agglomerates make it difficult for the CNT to disperse throughout a polymer matrix. However, according to Alig, Pötschke et al. (2012) the CNT agglomerates can be significantly reduced by polymer infiltration during the melt compounding process (Alig et al., 2012).

The properties of polymer nanocomposites depend substantially on the dispersion and distribution of CNT in the polymer matrix, and the most suitable degree of dispersion varies depending on the desired properties. Figure 2.2 shows the FEG-SEM micrographs of the a) neat SEBS, b) and c) SEBS/CNT with 10 wt. % of CNT at different magnifications.

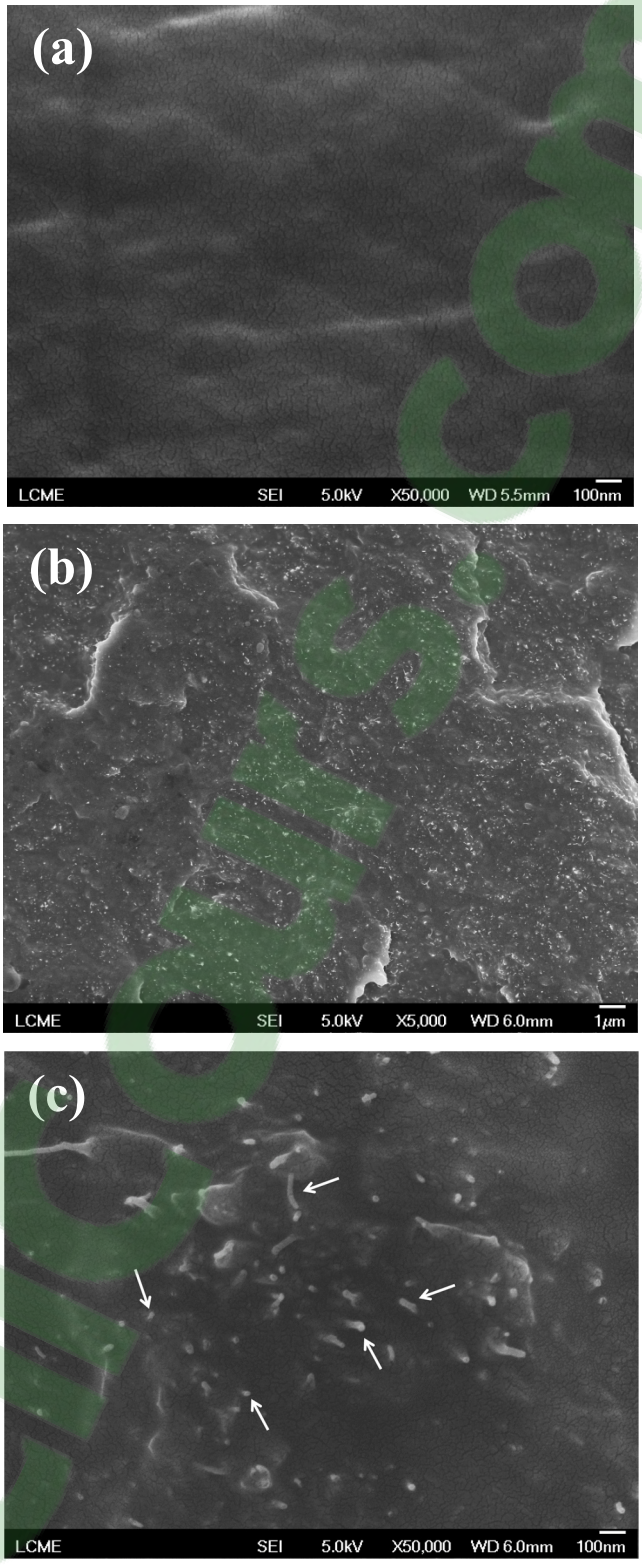

Figure 2.2 - FEG-SEM micrographs of a) neat SEBS, x50000, and SEBS/CNT with 10 wt. % of CNT at different magnifications, b) x5000, c) x50000

The micrograph shown in Figure 2.2 b) indicates that CNT (lighter spots) are uniformly dispersed in the SEBS matrix. In the micrograph at higher magnification presented in Figure 2 c), we can see individualized tubes (indicated by the arrows), which suggest that the CNT clusters were well deagglomerated through the melt compounding process.

2.3.2 Electrical conductivity

Figure 2.3 shows the electrical conductivities of the SEBS/CNT nanocomposites as a function of the weight and volume fractions of CNT. The volume fraction (f) of conductive additives was calculated according to Equation 2.9:

$$f = \frac{w/\rho_a}{w/\rho_a + (1-w)/\rho_m} \tag{2.9}$$

where *w* represents the weight fraction, ρ the density, and the subscripts *a* and *m* are related to the additive and matrix, respectively.

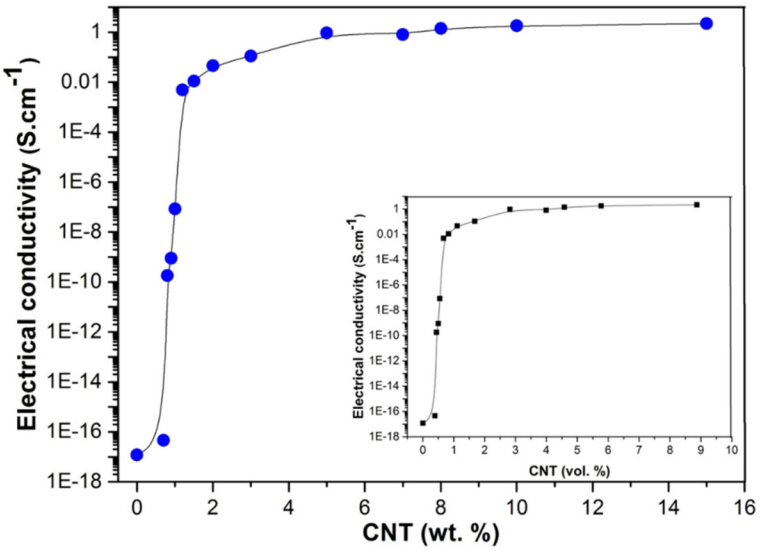

Figure 2.3 - Electrical conductivity of SEBS/CNT nanocomposites at different CNT weight and volume fractions

It can be seen that SEBS/CNT nanocomposites present a sharp transition in the electrical conduction from insulators to conductors as the amount of filler is increased. For extremely low amounts of CNT, the material remains insulating, similarly to the polymer matrix. Starting from 0.8 wt. % of CNT, the electrical conduction starts increasing, and for the nanocomposites between 1.0 and 1.2 wt. % of CNT, the electrical conductivity drastically changes from $8.7x10^{-8}$ to $4.9x10^{-3}$ $S.cm^{-1}$. A much higher increase (of 17 orders of magnitude), with the maximum conductivity around 1 $S.cm^{-1}$, was reached with 8.0 wt. % of CNT for the nanocomposites studied.

In our previous work, composites of SEBS filled with carbon black (CB) and expanded graphite (EG) were prepared by melt compounding under similar conditions (Kuester et al., 2015). However, the composites of SEBS/CB and SEBS/EG presented the maximum electrical conductivity (≈ 2 x 10^{-1} $S.cm^{-1}$) at one order of magnitude lower than the maximum for the nanocomposites obtained in the present work (≈ 1 $S.cm^{-1}$). Moreover, in the case of SEBS/CB and SEBS/EG, more than 15 wt. % fillers were needed to obtain a conductivity in the order of 10^{-1} $S.cm^{-1}$ (Kuester et al., 2015). The differences observed in both studies are in agreement with the results presented by Al-Saleh, Saadeh, and Sundararaj (2013), who studied nanocomposites of acrylonitrile-butadiene-styrene (ABS) with different carbon nanofillers. In the systems obtained, the electrical conductivity of the nanocomposites with the same nanofiller loading could be ranked in the following order: CB< carbon nanofiber (CNF) < CNT. According to the authors, the increase in the electrical conductivity is inversely proportional to the aspect ratio of the nanofillers, and occurs because high aspect ratios favour a nanofiller-nanofiller network formation at lower nanofiller loading (Al-Saleh et al., 2013). In another study, Li and Shimizu (2009) studied nanocomposites of SEBS and CNT prepared by melt compounding at very high shear. According to the authors, an abrupt increase in the conductivity was observed as the MWCNT loading content increased from 1.25 to 2.5 wt. %, and the maximum conductivity was 5.16 $S.cm^{-1}$ for the nanocomposites with 15 wt. % of CNTs (Yongjin Li & Shimizu, 2009).

Clicours.COM

The transition in the nanocomposite's electrical conductivity, known as the electrical percolation threshold, can be calculated according to Equations 2.10 and 2.11 (Vasileiou et al., 2013):

$$\sigma = \sigma_{matrix} \left(\frac{\varphi_c - \varphi}{\varphi_c}\right)^{-s} \qquad \varphi < \varphi_c \tag{2.10}$$

$$\sigma = m \left(\frac{\varphi - \varphi_c}{1 - \varphi_c}\right)^{t} \approx m\,(\varphi - \varphi_c)^{t} \qquad \varphi > \varphi_c \tag{2.11}$$

where σ is the electrical conductivity of the composite, σ_{matrix} is the conductivity of the matrix, φ is weight fraction of the filler, φ_c is critical weight fraction at percolation, s and t are the critical exponents below and above percolation respectively and m is a constant.

The SEBS/CNT nanocomposites presented an electrical percolation threshold of ≈ 1 wt. %, which was lower than the results obtained for SEBS/CNT composites prepared by melt compounding by Li and Shimizu (2009) (between 1.25 and 2.5 wt. %), and by Meier et al. (2011) (2.73 wt. %) (Yongjin Li & Shimizu, 2009; Meier et al., 2011). This percolation threshold is much lower than for carbon fillers, with lower aspect ratios, such as CB, CNF, EG, and graphite (Estrada Moreno et al., 2009; Pavlovsky & Siegmann, 2009; Zucolotto, Avlyanov, & Mattoso, 2004). t was found equal to 1.56. This value corresponds to a three-dimensional system according to the theory of percolation (Thomassin et al., 2013; Z. Wu et al., 2014).

2.3.3 Electromagnetic shielding effectiveness (EMI-SE) and Dielectric properties

Figure 2.4 shows the average incident, reflected, absorbed, and transmitted electromagnetic power for the SEBS/CNT composites at different CNT weight fractions in the 8.2 to 12.4 GHz frequency range. The results indicate that when an incident electromagnetic wave hits the nanocomposites, most of its power is reflected. Further, the amount of power shielded by absorption initially increases with increasing CNT loading, but for the nanocomposites of

higher electrical conductivities, from 8 wt. % of CNT on, the power shielded starts decreasing due the increase of the power blocked by reflection.

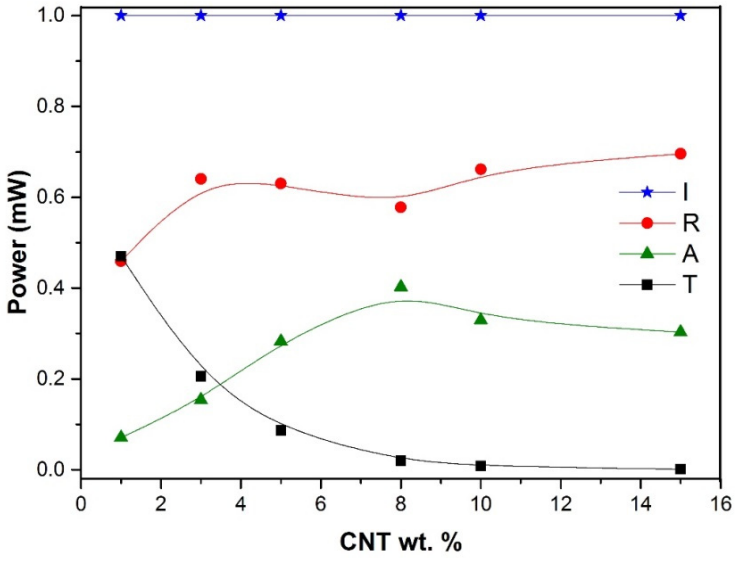

Figure 2.4 - Power balance of the incident (I), reflected (R), absorbed (A), and transmitted (T) electromagnetic power for the SEBS/CNT composites at different CNT weight fractions

Figure 2.5 shows the electromagnetic shielding effectiveness (EMI-SE) experimental results for the SEBS/CNT nanocomposites at different filler weight fractions versus frequency, in the 8.2 to 12.4 GHz range. As expected, EMI-SE increased as the CNT weight fraction in the nanocomposites was increased. Also, for all samples, the SE is practically frequency-independent in the frequency range studied.

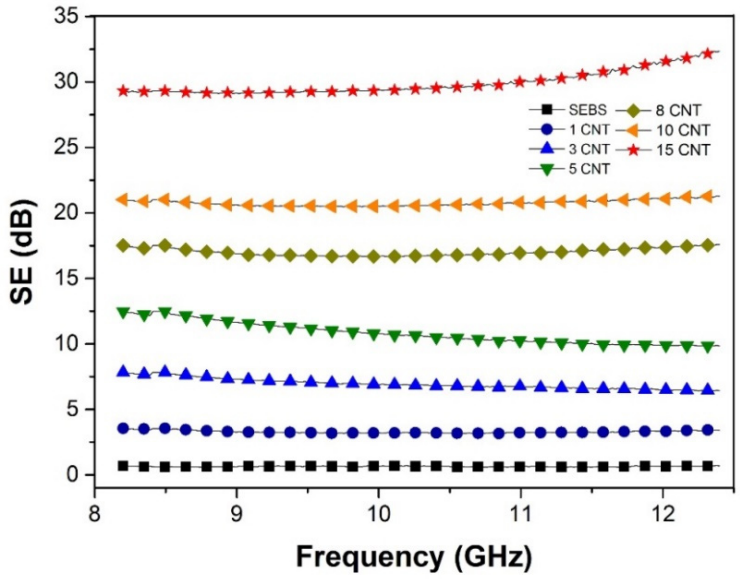

Figure 2.5 - Shielding effectiveness versus frequency of SEBS/CNT nanocomposites at different CNT weight fractions

The SEBS/CNT nanocomposite with 15 wt. % of CNT has an average SE of 30.07 dB. In terms of percentage, this value corresponds to a reduction of 99.9% of the incident power transmitted throughout the material which is much above the minimum required for commercial EMI shielding application. Commercial EMI shielding materials should have a minimum EMI-SE of approximately 20 dB, corresponding to a 99% of attenuation of the incident radiation (Maiti et al., 2013).

To our knowledge, very few studies have reported the effect of addition of conductive fillers in thermoplastic elastomers for EMI shielding applications. CB has been added to SEBS and thermoplastic polyurethane (TPU), but the efficiency of this filler is much smaller than when CNT are added. In our previous work (Kuester et al., 2015), for composites of SEBS filled with CB and EG, prepared under similar conditions, an addition of 15 wt. % fillers resulted in an SE of 17.74 dB and 10.02 dB, respectively. In the case of the TPU/CB and TPU/CNT, an EMI-SE of 12.2 dB and 21.8 dB were obtained, respectively (Ramôa et al., 2013). This difference can easily be attributed to the large aspect ratio that the CNT present as compared

to CB. Conductive polymers such as PANI (polyanyline) have also been added to thermoplastic elastomers to test their efficiency as EMI materials (Magioli et al., 2012). In their study Magioli et al (2012), when 15 wt. % of PAni.DBSA was added in SBS, the SE of the blends was around 15 dB, and the maximum SE, ranging from 35 to 40 dB, was only achieved with 30 wt. % of PAni.DBSA (Magioli et al., 2012). However, the large amount of intrinsic conductive polymers (ICP) and their difficult processing are considerable disadvantages of these materials (Thomassin et al., 2013).

Figure 2.6 presents a comparison of the experimental and the theoretical predictions of EMI-SE, as calculated using equations 3.3 and 3.4 at a frequency of 10 GHz. It can be seen that the experimental values follow the trend of the theoretical ones. The difference between them can be attributed to the fact the theoretical model does not consider some parameters, such as the intrinsic conductivity of the filler, and the volume fraction of the filler in the composite (Al-Saleh & Sundararaj, 2009).

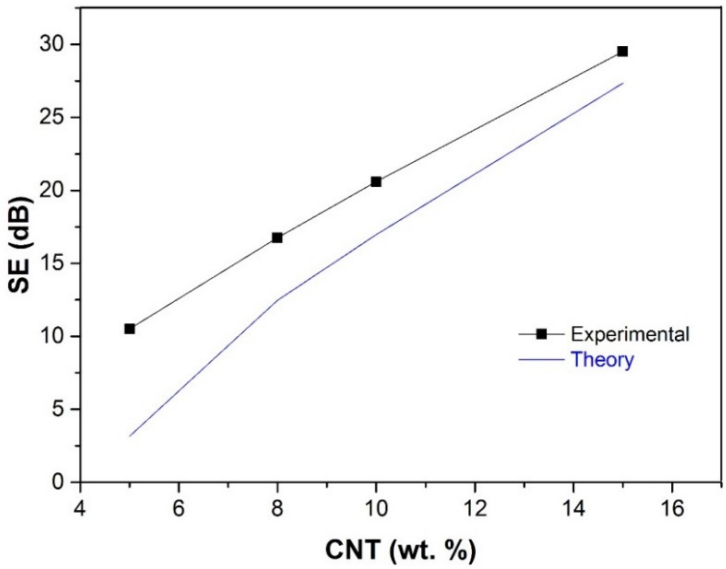

Figure 2.6 - Experimental and theoretically calculated shielding effectiveness of SEBS/CNT nanocomposites at different CNT weight fractions in the 8.2 to 12.4 GHz frequency range

Due the high reflectivity of the nanocomposites, and considering that reflection obviously occurs before absorption, most of the incident wave, as an absolute value, is blocked by reflection. However, in order to assess the intrinsic attenuation of the nanocomposites, the contribution of reflection and absorption mechanisms to the total shielding effectiveness was evaluated. Figure 2.7 shows the average shielding effectiveness by reflection (SE_R) and absorption (SE_A) mechanisms at different CNT weight fractions for the SEBS/CNT nanocomposites.

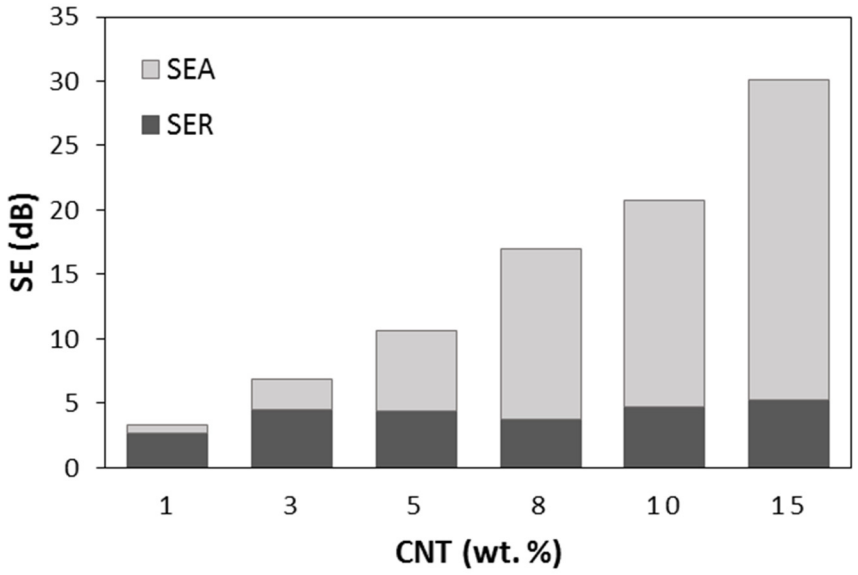

Figure 2.7 - Contribution of reflection (SE_R) and absorption mechanisms (SE_A) to the total EMI-SE (dB) at different CNT weight fractions for the SEBS/CNT nanocomposites

The contribution by SE_A mechanism increases proportionally with the increase of the CNT loading in the SEBS/CNT composites. It is known that the SE_A increases with increasing composite electrical conductivity and/or with a narrower space between the CNT. However, conversely to what obtains with single-component materials, the increase of SE_A for composite materials is non-linear. According to Al-Sahleh and Sundararaj (2009), there is no theoretical interpretation for the relation between filler connectivity, electrical conductivity, and EMI-SE presently specific for composites (Al-Saleh & Sundararaj, 2009).

Table 2.1 summarizes the EMI-SE, the total effectiveness by reflection and absorption mechanisms, and the electrical conductivity for the SEBS/CNT nanocomposites at different CNT weight fractions. As can be seen, even after the electrical conductivity leveled off, the EMI-SE continued to increase with increasing CNT concentration. A greater EMI-SE at higher amounts of CNT may be explained by the formation of a more close-packing network of CNT within the SEBS matrix. Also, absorption was the main mechanism for nanocomposites of higher electrical conductivity.

Table 2.1 - Shielding effectiveness in percentage, shielding effectiveness (dB), shielding effectiveness by reflection and absorption mechanisms (dB), and electrical conductivity of SEBS/CNT nanocomposites at different CNT weight fractions

Sample (CNT wt. %)	Attenuation (%)	SE (dB)	SE_R (dB)	SE_A (dB)	Electrical conductivity ($S.cm^{-1}$)
SEBS	13.82	0.64	0,55	0.09	1.2E-17
SEBS/CNT 1	53.07	3.28	2.67	0.61	8.4E-08
SEBS/CNT 3	79.42	6.88	4.46	2.42	1.1E-01
SEBS/CNT 5	91.30	10.67	4.44	6.23	9.4E-01
SEBS/CNT 8	98.01	17.02	3.79	13.23	1.4E+00
SEBS/CNT 10	99.16	20.78	4.75	16.03	1.8E+00
SEBS/CNT 15	99.90	30.07	5.21	24.86	2.2E+00

Besides the shielding material thickness (t), conductivity (σ), and frequency (f), other characteristics, such as electrical permittivity (ε) and magnetic permeability (μ), also strongly influence the electromagnetic shielding effectiveness (Han & Deng, 2011; Saini & Arora, 2012; Thomassin et al., 2013). Magnetic permeability quantifies the interactions between a magnetic material and the magnetic field (magnetic loss). Since carbon materials are not magnetic, only the electrical permittivity can have a role in the electromagnetic shielding effectiveness of the compounds studied here (Y. Liu, Song, Wu, & Leng, 2014). The electrical permittivity describes the manner in which the nanocomposite affects an incident electric field. The complex permittivity is composed by a real (ε') and an imaginary (ε") part, which represent the polarization loss and electric loss, respectively (Al-Saleh et al., 2013; L. Liu et al., 2010). In polymer nanocomposites, the real permittivity depends on the number of micro-capacitors

and the polarization centers (Al-Saleh et al., 2013; Yong Li et al., 2010; Yousefi et al., 2014). According to Al-Saleh, Saadeh and Sundararaj (2013), polarization centers are due to defects in the nanofiller structure, and micro-capacitors are filler nanoparticles or aggregates acting as electrodes in the insulating polymer matrix. Therefore, increases in ε' with higher CNT weight fractions are expected, once the number of micro-capacitors and structural defects in the nanocomposites is also higher. Moreover, with higher CNT loading, the gap between the CNT nanoparticles or aggregates decreases, enhancing the polarization of the material. The imaginary permittivity is related to the dissipation of the mobile charges due to the conductive paths formed in the nanocomposite. Thus, when the CNT weight fractions increase, the ε" increases because of the increase in the number of paths in the conductive network (Al-Saleh et al., 2013). Figure 2.8 shows ε' and ε" versus the frequency in the 8.2-12.4 GHz range for the SEBS/CNT nanocomposites at different weight fraction of CNT.

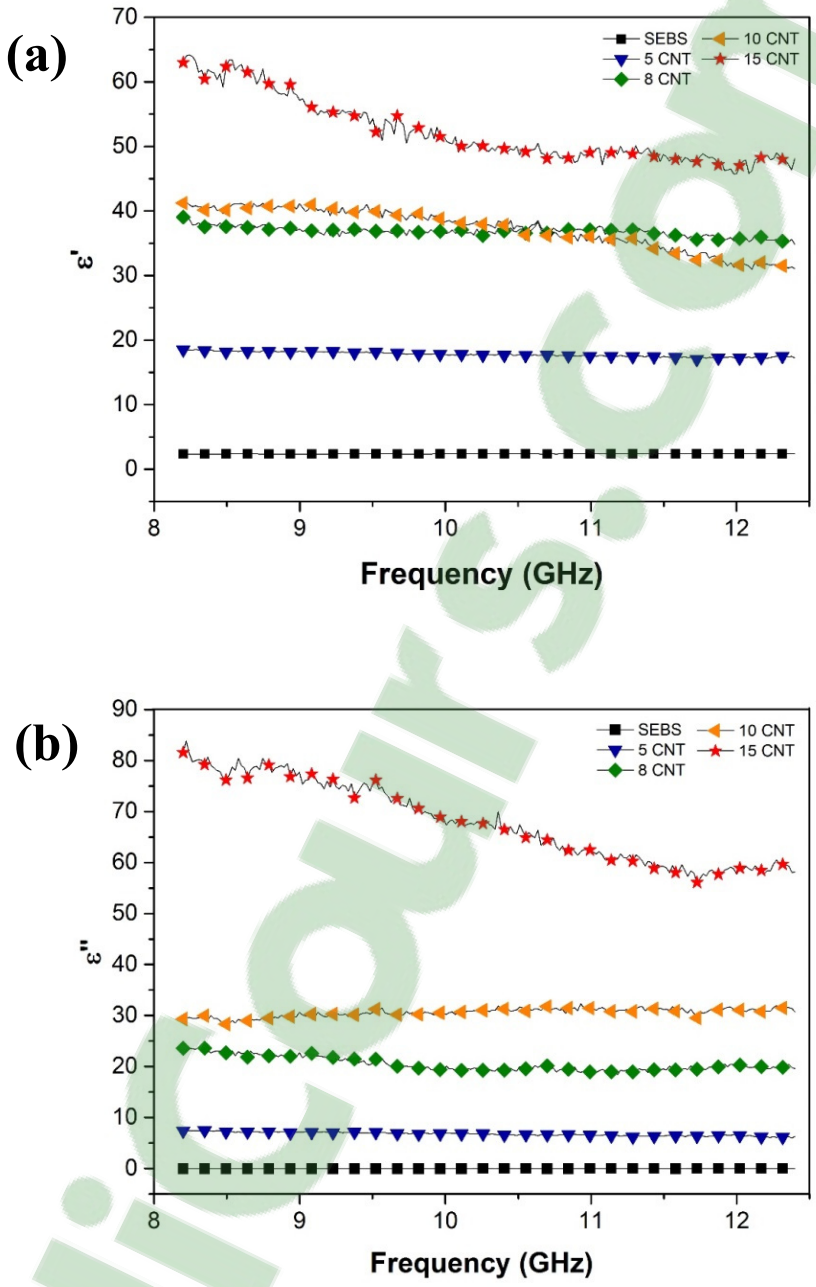

Figure 2.8 - a) Real (ε') and b) imaginary (ε") permittivity versus frequency of SEBS/CNT nanocomposites at different CNT weight fractions

For all the samples ε' and ε" enhanced as the CNT weight fractions in the SEBS/CNT nanocomposite was increased. For lower CNT loading ε' > ε", but for the nanocomposite with

15 wt. % of CNT, ε' < ε", meaning that.at this point, the mobile charge dissipation is more efficient because of the higher number of conductive paths throughout the nanocomposite.

2.4 Conclusions

Nanocomposites of SEBS/CNT prepared by melt compounding exhibited a uniform morphology, high electrical conductivity, and EMI-SE suitable for commercial applications. Experimental results demonstrated that the CNT were properly dispersed and distributed throughout the SEBS matrix, without significantly damaging their structure. SEBS/CNT presented a low electrical percolation threshold of around 1 wt. % of CNT, and a critical exponent of 1.56, indicating the formation of a three-dimensional network. The electrical conductivity was enhanced by 17 orders of magnitude, and a maximum conductivity of approximately 1 $S.cm^{-1}$ was achieved with 8.0 wt. % of CNT. EMI-SE of 30.07dB, which corresponds to a reduction of 99.9% of the incident radiation, was achieved with 15 wt. % of CNT. The EMI-SE experimental results were higher than the theoretical values. Absorption was the main shielding mechanism for all SEBS/CNT nanocomposites. Permeability results confirmed that CNT did not present significant magnetic loss. Real and imaginary permittivity increased as the CNT weight fractions were enhanced. Moreover, conversely to the nanocomposites with lower CNT loading, for the nanocomposite with 15 wt. % of CNT, ε" is higher than ε', indicating that at this point, the mobile charge dissipation is more efficient because of the higher number of conductive paths formed throughout the nanocomposite.

Acknowledgements

The authors gratefully acknowledge the financial support of Conselho Nacional de Desenvolvimento Científico e Tecnológico – CNPq, Coordenação de Aperfeiçoamento de Pessoal de Ensino Superior – CAPES, and Fundação de Amparo à Pesquisa e Inovação do Estado de Santa Catarina – FAPESC. We are also truly grateful to the Instituto de Macromoléculas Professora Eloisa Mano, Rio de Janeiro Federal University (IMA-UFRJ) for

the EMI shielding analysis, and to the Central Electron Microscopy Laboratory, Santa Catarina Federal University (LCME-UFSC) for the FEG-SEM analysis.

Clicours.COM

CHAPTER 3

This chapter presents the article concerning the results of the second part of the project regarding nanocomposites of SEBS/GnP and hybrid nanocomposites of SEBS/GnP/CNT for EMI shielding. It emphasizes the dispersion and distribution of GnP in the polymeric matrix, and the formation of an electrically conducting network and the EMI properties of the of SEBS/GnP and SEBS/GnP/CNT nanocomposites. Synergic effects of the hybrid nanocomposite are highlighted.

HYBRID NANOCOMPOSITES OF THERMOPLASTIC ELASTOMER AND CARBON NANOADDITIVES FOR ELECTROMAGNETIC SHIELDING

Scheyla Kuester[1,2], Nicole R. Demarquette[1*], José Carlos Ferreira Jr.[2], Bluma G. Soares[3], Guilherme M. O. Barra[2#]

[1*]École de technologie supérieure de Montréal, Mechanical Engineering Department, Montreal, QC, Canada

E-mail: NicoleR.Demarquette@etsmtl.ca

[2#]Universidade Federal de Santa Catarina, Departamento de Engenharia Mecânica, Florianópolis, SC, Brazil,

E-mail: g.barra@ufsc.br

[3]Universidade Federal do Rio de Janeiro, Departamento de Engenharia Metalúrgica e de Materiais, Rio de Janeiro, RJ, Brazil.

This article was published in European Polymer Journal, v. 88, p. 328–339, 2017.

ABSTRACT

Hybrid nanocomposites of poly (styrene-b-ethylene-ran-butylene-b-styrene) (SEBS), graphene nanoplatelets (GnP), and carbon nanotubes (CNT) were successfully prepared by melt compounding for electromagnetic shielding applications. The morphologies of the carbon

nanoadditives and nanocomposites were investigated by Raman spectroscopy, field emission gun scanning electron microscopy, and rheological analysis. DC electrical conductivity was assessed by two-probe and four-probe techniques. Electromagnetic interference shielding effectiveness, shielding mechanisms, and dielectric properties were conducted in the X-band microwave frequency range (8.2-12.4 GHz). The results showed that CNT had a higher affinity with the matrix, and were better dispersed than GnP. SEBS/GnP/CNT nanocomposites induced an electrical conductivity increase of 17 orders of magnitude compared to the polymer matrix. The hybrid nanocomposites presented synergic effects on EMI-SE when compared to the single-component nanocomposites (SEBS/GnP and SEBS/CNT). The maximum EMI-SE of 36.47dB (reduction of 99.98% of the incident radiation) was achieved for the SEBS/GnP/CNT nanocomposite with 5/10 wt.% of GnP/CNT, respectively. All the hybrid nanocomposites with CNT loadings equal to or higher than 8 wt.%. presented the required EMI-SE for commercial applications.

Keywords: Hybrid nanocomposites; Graphene nanoplatelets; Carbon Nanotubes; Electrical properties; Electromagnetic shielding effectiveness.

3.1 Introduction

The current information age has clearly brought deep changes to the human way of life, with nanotechnology increasingly incorporated into our daily routine, and modern society experiencing the phenomenon of technology miniaturization. Alongside the mostly beneficial changes that this new order has ushered in, the fast and growing proliferation of equipment and mobile electronic devices, such as cell phones, laptops, and tablets, have also given rise to serious problems of electromagnetic interferences (EMI), and possibly to human diseases. As a result, shielding materials, especially those based on polymer nanocomposites consisting of insulating polymer matrices and conductive carbon nanoparticles, are being widely studied in a bid to overcome these problems (Calisi et al., 2013; Cao et al., 2015; T. K. Das & Prusty, 2013; Kuilla et al., 2010; Maiti & Khatua, 2016; Micheli, Apollo, Pastore, & Marchetti, 2010; Sharma et al., 2016; Xiong et al., 2012).

Carbon nanoparticles, such as carbon nanotubes (CNTs) and graphene (GR), exhibit huge specific areas, high aspect ratios, extraordinary mechanical properties, and high thermal and electrical conductivities. For EMI shielding applications, polymer nanocomposites of CNT generally exhibit high electromagnetic interference shielding effectiveness (EMI-SE). Currently, however, CNT obtained by chemical vapor deposition (CVD) are usually expensive, leading to graphene produced from graphite being used as a cheaper alternative (Aloia, Marra, Tamburrano, Bellis, & Sarto, 2013). Recently, the search for synergic effects and cost reductions led to studies of hybrid polymer nanocomposites of carbon nanoparticles (Al-Saleh & Saadeh, 2013; M.-S. Kim et al., 2013; Lin et al., 2016; Maiti & Khatua, 2016; Maiti et al., 2013; Sharma et al., 2016). According to the literature, the combination of carbon nanoadditives of different shapes improves the conductive network in hybrid nanocomposites (Al-Saleh & Saadeh, 2013; Lin et al., 2016; Sharma et al., 2016). Hybrid nanocomposites of polystyrene (PS), CNT and graphite nanoplates, in small portions of 2/1.5 wt.% of CNT/graphite nanoplates, respectively, prepared by in situ polymerization, presented an EMI-SE of ≈ 20.2 (Maiti et al., 2013), which is the shielding effectiveness usually required for commercial applications (Al-Saleh & Saadeh, 2013; Al-Saleh et al., 2013; Cao et al., 2015; Jia et al., 2015; M.-S. Kim et al., 2013; Maiti & Khatua, 2016; Maiti et al., 2013). In another study, hybrid nanocomposites of acrylonitrile butadiene styrene (ABS), CNT, and GR, prepared by dry tumble mixing followed by hot compaction, exhibited an improvement in the EMI-SE from 7.5 to 26.8 dB by the addition of 1 wt.% of CNT to an ABS/GR nanocomposite (Sharma et al., 2016). On the other hand, ABS/CNT/Carbon black (CB) hybrid nanocomposites, prepared by solution casting followed by hot compression, did not present any synergic effects. However, the authors showed that small quantities of CNT could be replaced by CB, thereby decreasing the final cost of the nanocomposites, without impairing the EMI-SE (Al-Saleh & Saadeh, 2013).

For commercial applications of polymer composites as EMI shielding materials, the dispersion of the conductive additives is one of the most critical factors. Nevertheless, it is well known from the literature that carbon nanoparticles are very difficult to disperse in polymer matrices. Among the different compounding methods, the solvent casting technique generally provides

better dispersion, while the composites produced exhibit higher EMI-SE. However, solution casting is generally not suitable for commercial applications due to its extensive use of organic solvents, as well as to the fact that the method is not environmentally friendly. For these reasons, melt compounding is a preferred method (Lin et al., 2016), and because of that, the choice of the polymer matrix plays an important role.

Poly (styrene-b-ethylene-ran-butylene-b-styrene) (SEBS) is a thermoplastic elastomer, which exhibits the properties of an elastomer, and at the same time, has the advantage of being processed as a thermoplastic material. SEBS is basically a styrenic block copolymer comprised of three interconnected blocks, two rigid (polystyrene) in the ends, and the other, rubbery (poly (ethylene-butylene)) in the middle (Danilo J. Carastan et al., 2013; Helal et al., 2015; Yongjin Li & Shimizu, 2009; Meier et al., 2011; Rath & Li, 2011; Wang et al., 2012). Therefore, another advantage it presents relates to the fact that in systems composed of styrenic materials and carbonaceous fillers, an affinity is expected between the π electrons of both components, once their molecular structures comprise aromatic rings. These non-covalent π-π interactions may help to improve the dispersion of carbon nanoparticles inside the matrix (Bilalis, Katsigiannopoulos, Avgeropoulos, & Sakellariou, 2014; Fujigaya & Nakashima, 2015; Y.-T. Liu et al., 2011; Pöllänen, Pirinen, Suvanto, & Pakkanen, 2011; Spitalsky et al., 2010; Vasileiou et al., 2013) and enhance the EMI-SE of the final nanocomposites (Maiti & Khatua, 2016; Maiti et al., 2013; Thomassin, Huynen, Jerome, & Detrembleur, 2010).

In a previous work, we studied nanocomposites of SEBS/CNT for EMI shielding prepared by melt compounding. With 10 wt.% of CNT, we obtained the SE necessary for commercial applications, that is SE > 20 dB (reduction of 99.00% of the incident radiation); with 15 wt.% of CNT, the SE was 30 dB, representing a 99.9% reduction of the incident radiation (Kuester, Barra, Ferreira Jr, Soares, & Demarquette, 2016). In the present work, we prepared SEBS/GnP nanocomposites and hybrid nanocomposites of SEBS/GnP/CNT via the same compounding method. The nanocomposites were characterized by morphology, dispersion, polymer/carbon nanoparticle interactions, electrical conductivity, dielectric properties, and EMI shielding.

Nanocomposites of SEBS/CNT were also prepared in order to characterize the differences between the dispersion of the different carbon nanoadditives in the SEBS polymer matrix.

3.2 Experimental

Graphene nanoplatelets (GnP), (xGnP-M-25, surface area = 120 – 150 $m^2.g^{-1}$; bulk density = 0.03 – 0.1 $g.cm^{-3}$; carbon purity = 99.5%; average particle diameter = 25 μm; particle thickness = 6 – 8 nm), was purchased from XG Sciences, Inc. Multiwalled Carbon Nanotube (MWCNT) (Nanocyl™ NC 7000 series, surface area = 250 - 300 $m^2.g^{-1}$; density bulk = 0.06 $g.cm^{-3}$; carbon purity = 90 %; average diameter = 9.5 nm; average length = 1.5 μm), was obtained from Nanocyl S.A. Poly (styrene-b-ethylene-ran-butylene-b-styrene) (SEBS) (Kraton G-1650; number-average molecular weight = 94,000 $g.mol^{-1}$; polystyrene content = 30 wt.%, bulk density = 0.224 $g.cm^{-3}$, specific gravity = 0.91 $g.cm^{-3}$) was supplied by Kraton Polymers do Brasil Ind. Com. Prod. Petr. Ltda. All materials were used as received.

Polymer nanocomposites of SEBS/GnP and SEBS/GnP/CNT were obtained by melt compounding using a torque rheometer (Haake Rheocord), which was coupled to a mixing chamber (Rheomix 600p) equipped with roller rotors. The processing parameters were set as follows: temperature of 230 °C, rotational speed of 150 rpm, and total mixing time of 25 minutes. The compression molding was performed in a hydraulic press at a temperature of 230 °C, for a total of 10 minutes at a pressing pressure of approximately 20 MPa.

The morphology of the carbon nanoparticles was characterized by field emission gun scanning electron microscopy (FEG-SEM) using a JEOL JSM-6701 F field instrument at an acceleration voltage of 10 kV. For cross-sectional analysis of the nanocomposites, samples were cryogenically fractured in liquid nitrogen and placed in an aluminum sample holder containing a double-sided conductive carbon adhesive tape, and coated with gold.

Rheological measurements (Small Amplitude Oscillatory Shear analysis (SAOS)) were performed in a MCR 501 Anton Paar rheometer equipped with plate-plate geometry. The tests

were performed in the linear viscoelastic regime, at the frequency range from 0.01 to 300 rad.s^{-1}, and temperature of 230 °C.

The structural morphology of the carbon nanoparticles as-received and in the nanocomposites after processing was evaluated by Raman spectroscopy in a CRM (Confocal Raman Microscope) Alpha 300R Witec system with a 532nm laser excitation <100mW and a UHTS 300 (ultra-high throughput spectrometer), and gratings of 600 or 1800 g/mm, with a 500 blaze. The DC electrical conductivity of the SEBS and nanocomposites was characterized at room temperature by the two-probe and four-probe methods, depending on the electrical conductivity of the sample. For neat SEBS and nanocomposites of low electrical conductivity, measurements were performed using the two-probe standard method, with a Keithley 6517A electrometer connected to a Keithley 8009 test fixture. For nanocomposites of higher electrical conductivity, measures were done using the four-probe standard method, with a Keithley 6220 current source to apply the current and a Keithley 6517A electrometer to measure the difference of potential. The data presented are the average of five measurements.

The EMI-SE measurements and the dielectric analysis of the nanocomposites in the X-band microwave frequency range (8.2-12.4 GHz) were performed using a microwave network analyzer (N5230C Agilent PNA-L, Santa Clara, CA). The incident and transmitted waves were represented mathematically by complex scattering parameters S_{11} (or S_{22}) and S_{12} (or S_{21}), which are correlated with the reflectance and the transmittance. In this analysis, when the incident electromagnetic radiation collides with a shielding material, the absorbance (A), reflectivity (R), and transmittance (T) totalize 1 ($T + R + A = 1$). The coefficients of absorbance (A), reflectivity (R), and transmittance (T) were obtained using S-parameters, according to equations 1 and 2 (Al-Saleh et al., 2013; Jia et al., 2015; Maiti et al., 2013; Ramôa et al., 2013; Saini & Arora, 2012; Sharma et al., 2016).

$$T = [E_T/E_I]^2 = |S_{12}|^2 = |S_{21}|^2 \quad (1)$$

$$R = [E_R/E_I]^2 = |S_{11}|^2 = |S_{22}|^2 \quad (2)$$

EMI-SE measurements were carried out with an X-band waveguide as the sample holder, and the thickness of all samples was 2.0 mm.

3.3 Results and Discussion

3.3.1 Morphological analysis

The morphology of GnP and CNT was studied by field emission gun scanning electron microscopy (FEG-SEM). Figure 3.1 presents FEG-SEM micrographs of GnP at different magnifications. As shown in Figure 1 a), b), and c), the material exhibited some agglomerations of a few layers of graphene sheets. However, from Figure 1 d), e), and f), it can be seen that the morphology was not homogeneous, and that the material also presented some agglomerates of expanded graphite sheets.

ClicCours.com

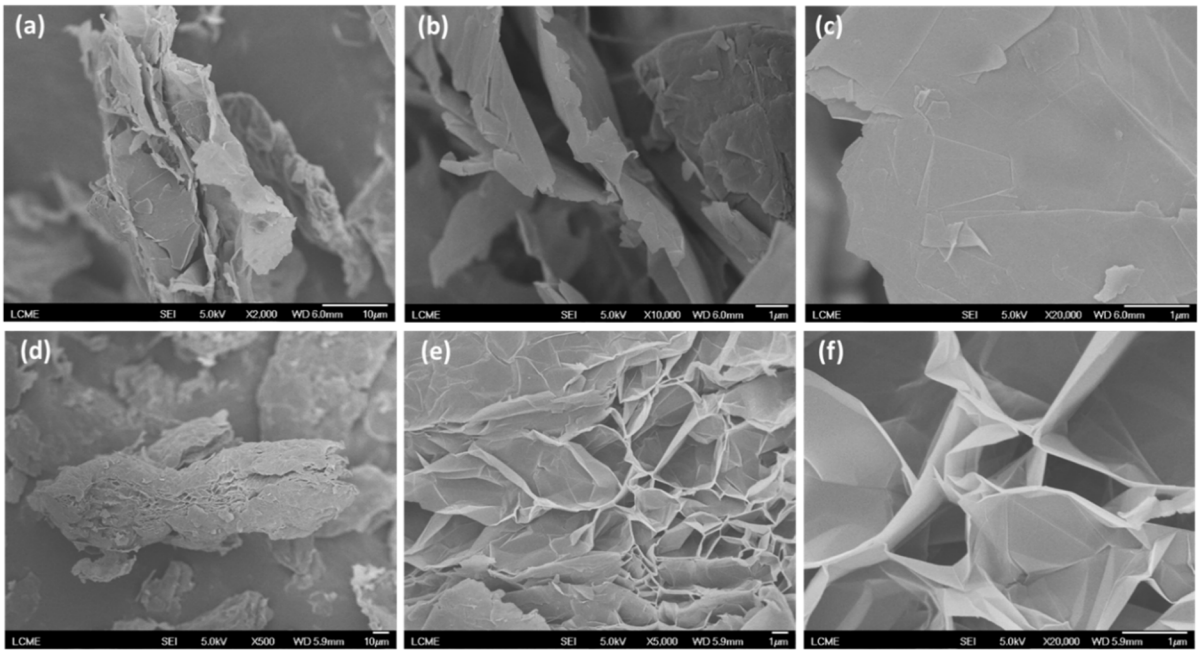

Figure 3.1 - FEG-SEM micrographs of the as-received GnP at different regions and magnifications: a) x2000, b) x10000, c) x20000, d) x500, c) x5000, and d) x20000

Figure 3.2 shows the FEG-SEM micrographs of the SEBS/GnP with 10 wt.% of GnP at different magnifications. The micrograph shown in Figure 2a) indicates that GnP was uniformly distributed in the SEBS matrix. In the micrograph with a higher magnification presented in Figure 2b), it can be observed that the nanocomposite apparently exhibited decent matrix-GnP adhesion, since there is no evidence of large voids in the interface of both phases.

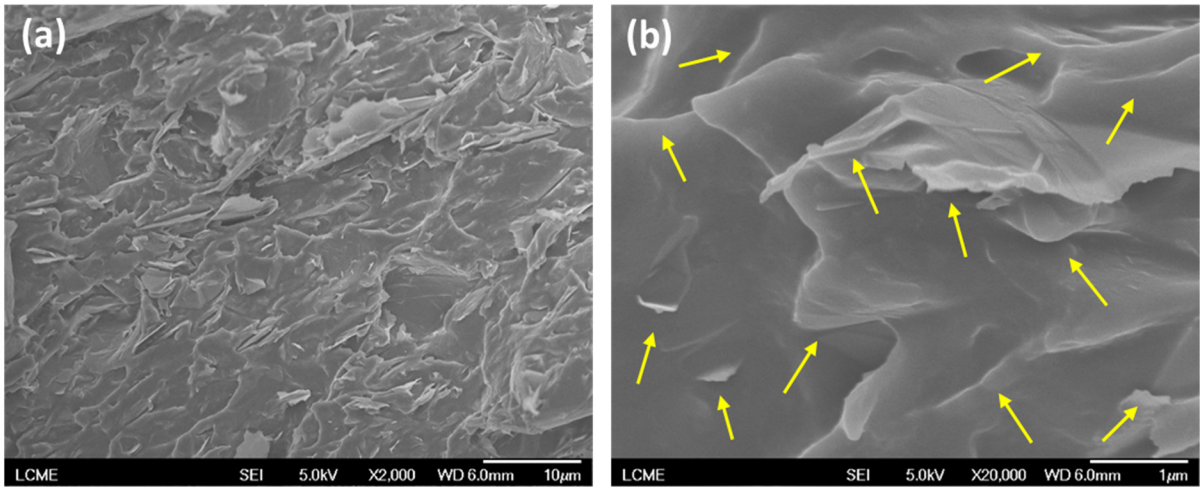

Figure 3.2 - FEG-SEM micrographs of SEBS/GnP with 10 wt.% of GnP at different magnifications: a) x2000, b) x20000

Figure 3.3 shows FEG-SEM micrographs of CNT at different magnifications. The as-received CNT a) exhibited the typical structure of large agglomerates of CNT, and b) presented tubes of different diameters.

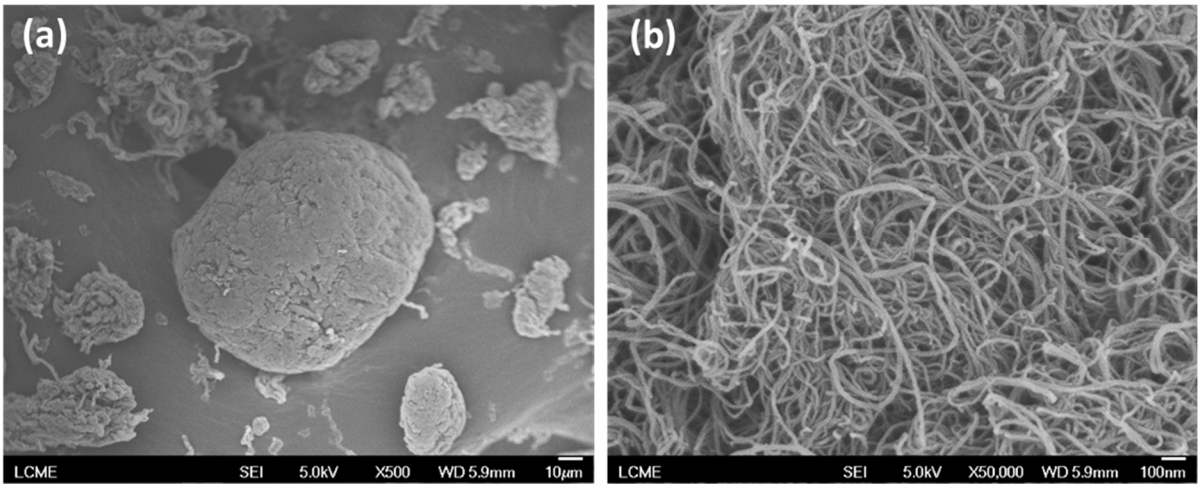

Figure 3.3 - FEG-SEM micrographs of the as-received CNT at different magnifications: a) x500, b) x50000

Figure 3.4 shows the FEG-SEM micrographs of the SEBS/CNT with 10 wt.% of CNT at different magnifications.

Clicours.COM

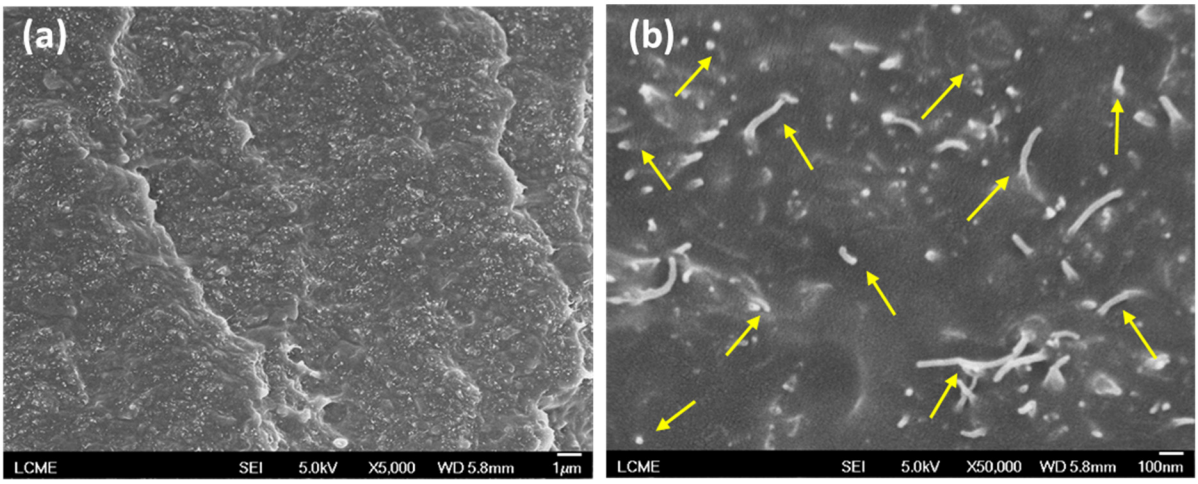

Figure 3.4 - FEG-SEM micrographs of SEBS/CNT with 10 wt.% of CNT at different magnifications: a) x5000, b) x50000

According to the micrographs, CNT (the 4a) lighter spots) seems to be satisfactorily distributed in the SEBS matrix. In figure 4b), the image of the individualized tubes suggests that the CNT agglomerates were properly disaggregated through the melt compounding process.

The dispersion of the carbon nanoparticles through the SEBS matrix, as well as the morphological structure of SEBS, were studied by rheological analysis. In the linear viscoelastic regime, small amplitude oscillatory shear (SAOS) analysis is very useful for identifying the different possible morphologies of SEBS (such as lamellar, cylindrical, spherical, or even disordered, depending on the fraction of each block in the copolymer, and on the thermodynamic interactions between the phases). Curves of log G' vs. log ω (G' = storage modulus, ω = frequency) present different slopes in the low frequency region, corresponding to differences in the relaxation times of the phase domains; these can be used to characterize the degree of the spatial order, and consequently, the SEBS morphological structure (Danilo Justino Carastan, Demarquette, Vermogen, & Masenelli-Varlot, 2008). Moreover, the study of the rheological behavior of polymer nanocomposites is also an efficient method for characterizing the dispersion of the nanoparticle into the polymeric matrix (Danilo Justino Carastan et al., 2008; N. R. Demarquette, Carastan, D.). By SAOS analysis, the influence of the addition of carbon nanoadditives on G' curves is studied via the evaluation of

changes in the low frequency slope of log G' vs. log ω curves upon variation of carbon nanoadditives loading. Figure 3.5 shows the rheological behavior (SAOS) of neat SEBS and SEBS/GnP nanocomposites at low frequencies.

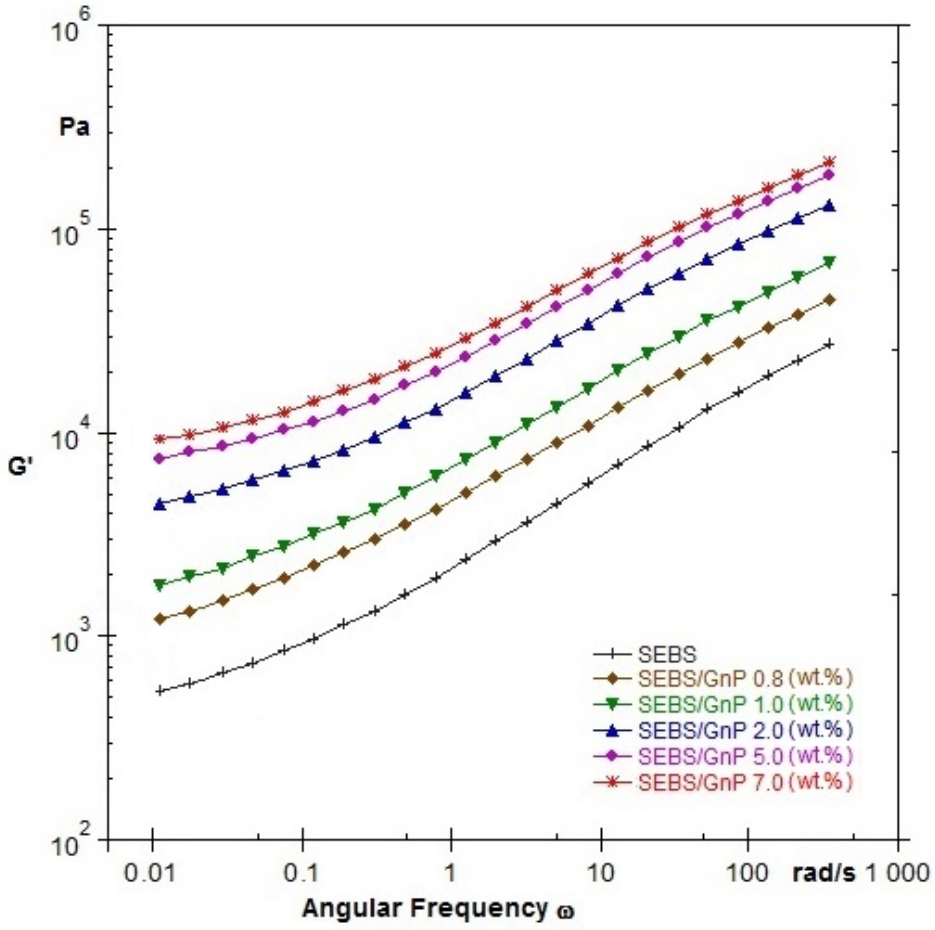

Figure 3.5 - Curves of G' as a function of frequency of neat SEBS and SEBS/GnP nanocomposites at different GnP weight fraction.

Table 3.1 - Low frequency slope of log G' vs. log ω for neat SEBS, and SEBS/GnP and SEBS/CNT nanocomposites at different carbon nanoadditive weight fractions

SEBS	Low frequency slope of log G' vs. log ω	SEBS/GnP (wt.%)	Low frequency slope of log G' vs. log ω	SEBS/CNT (wt.%)	Low frequency slope of log G' vs. log ω
0.32		0.8	0.32	0.5	0.26
		1	0.30	0.8	0.22
		2	0.27	1	0.19
		5	0.24	2	0.14
		7	0.24	3	0.11
		-	-	5	0.05

Figure 3.5 shows that the SEBS used in this work presented a terminal behavior, with a slope of 0.3 (between 1 and 0.01 rad.s^{-1}), as shown in Table 1, which is characteristic of a cylindrical morphology (Danilo Justino Carastan et al., 2008). The figure also indicates that the addition of GnP results in an increase of G' for the whole range of frequencies without a decrease in slope of log G' vs. log ω for low frequencies, showing that the GnP acts as a filler, but does not change the relaxation of the SEBS chain; this in turn indicates that it is probably not well dispersed, and does not present a significant interaction with the SEBS matrix.

Nanocomposites of SEBS/CNT were also prepared in order to characterize the difference between the dispersion of the different carbon nanoadditives in the SEBS matrix. Figure 3.6 shows the rheological behavior (SAOS) of neat SEBS and SEBS/CNT nanocomposites at low frequencies.

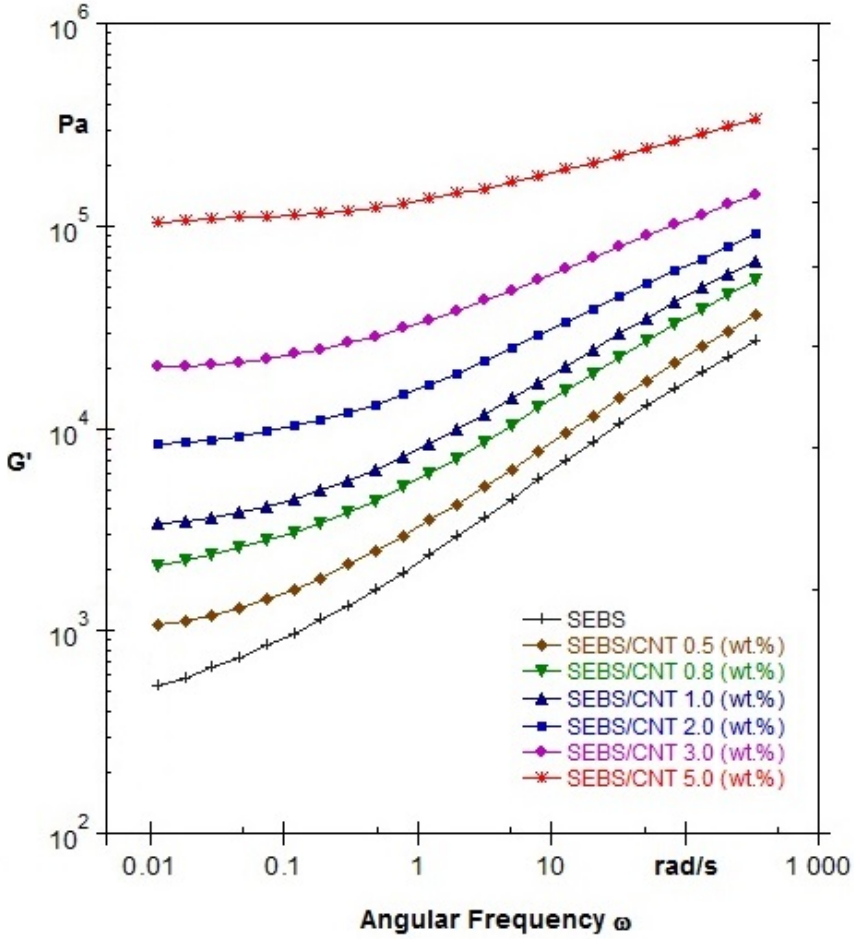

Figure 3.6 - Curves of G' as a function of frequency of neat SEBS and SEBS/CNT nanocomposites at different CNT weight fractions

It can be seen that the addition of CNT results in an increase of G' for the whole range of frequencies, but also in a decrease in slope of log G' vs log ω at low frequencies, indicating that not only does CNT act as a filler; it also reduces the mobility of SEBS chains, most likely due to the formation of a percolating network of nanoparticles (Danilo Justino Carastan et al., 2008). As shown in Figure 6, upon addition of 3.0 to 5.0 wt.% of CNT, almost horizontal non-terminal plateaus were formed in the G' curves, indicating that carbon nanoparticles hinder the low frequency relaxation processes, causing the nanocomposite to become highly solid-like. This behavior is observed for composites where particles are intercalated or exfoliated, and the degree of the effects vary depending on the microstructure and the affinity between the particle and the matrix (Danilo Justino Carastan et al., 2008).

Raman spectroscopy was used as a tool to investigate the presence of non-covalent π-π interactions between the carbon nanoparticles and the aromatic rings of polymer chains. Figure 3.7 shows Raman spectra of the pristine GnP, as well as SEBS/GnP nanocomposites with 10 wt.% of GnP.

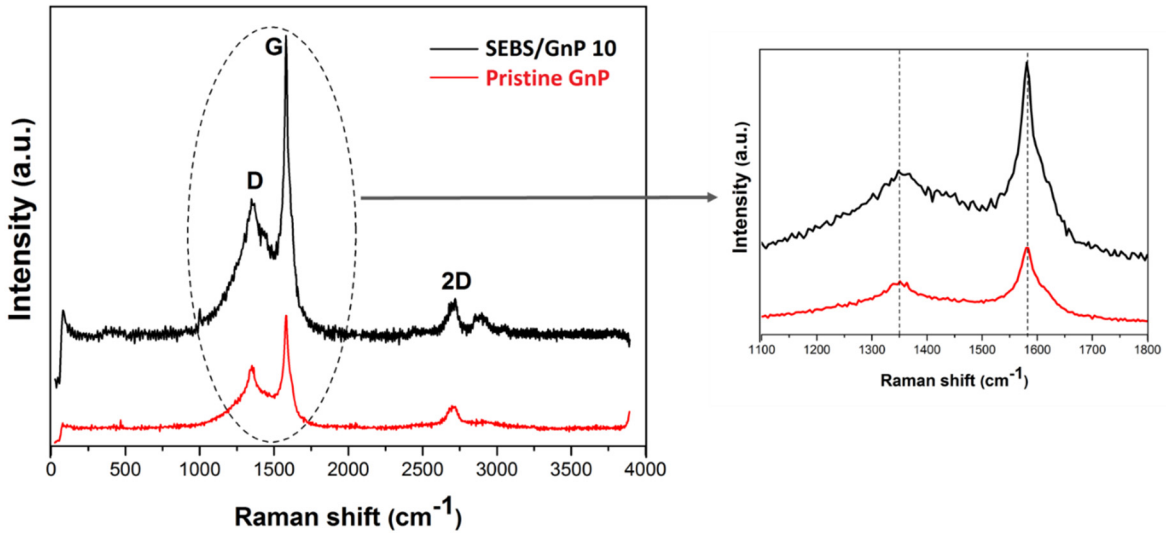

Figure 3.7 - Raman spectra of pristine GnP and SEBS/GnP nanocomposites with 10 wt.% GnP (on the left), and blow-up of the spectra in the 1100-1800 cm^{-1} region (on the right)

The pristine GnP presented the typical D peak (related to the in-plane vibration of sp^2 carbon atoms) and G peak (correlated to defects) (Zhao et al., 2012)at 1363 cm^{-1} and 1580 cm^{-1}, respectively. Compared to the pristine GnP peaks, the spectra of the SEBS/GnP nanocomposite did not present any shift in the D-band and G-band peaks. This result indicates that there is little or no interaction between the polymer matrix and the graphene nanoparticles, which is in agreement with the results exhibited by SAOS analysis.

In a previous work, we showed that the pristine CNT presented the characteristic D peak at 1335 cm^{-1}, and the G peak at 1573 cm^{-1}. When compared to the pristine CNT peaks, the spectra of the SEBS/CNT nanocomposite presented shifts of 12 cm^{-1} (1347 cm^{-1}) and 19 cm^{-1} (1592 cm^{-1}) in the D-band and G-band peaks, respectively (Kuester et al., 2016). This indicates the

existence of non-covalent interfacial interactions between CNT and the polymer matrix (Linton et al., 2010; Vasileiou et al., 2013; Zhao et al., 2012).

3.3.2 Electrical conductivity

Figure 3.8 presents the electrical conductivity of SEBS/GnP as a function of the GnP weight faction. It can be seen that the SEBS/GnP nanocomposites present a nearly constant increase in electrical conductivity with an increase in the GnP content, and do not present a sharp electrical insulating-conductor transition.

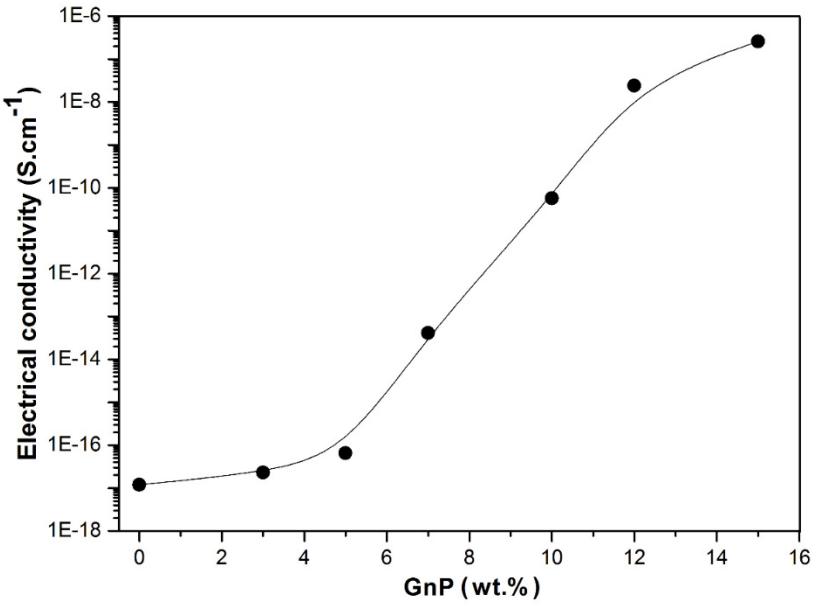

Figure 3.8 - Electrical conductivity of SEBS/GnP nanocomposites at different GnP weight fractions

Results obtained for SEBS/CNT nanocomposites prepared in our prior work, were considerably different. SEBS/CNT presented a sharp electrical insulating-conductor transition, and an electrical conductivity increase of 17 orders of magnitude, reaching ≈1 $S.cm^{-1}$ at 8 wt.% of CNT (Kuester et al., 2016).

For the hybrid nanocomposites prepared in the present work, the electrical conductivity is a function of the CNT content. In other words, hybrid nanocomposites of SEBS/GnP/CNT exhibit electrical conductivities similar to those for SEBS/CNT nanocomposites, for the same weight fraction of CNT, while the weight fraction of graphene does not contribute to enhance the electrical conductivity. This result was expected at some point, considering that the CNT presented better interaction (shown through Raman spectroscopy and rheological analysis) with the SEBS matrix than the graphene nanoplatelets. Table 3.2 shows a comparison of the electrical conductivity of SEBS/GnP, SEBS/CNT, and SEBS/GnP/CNT nanocomposites.

Table 3.2 - Comparison of the electrical conductivity of SEBS/GnP, SEBS/CNT, and SEBS/GnP/CNT nanocomposites at different weight fractions of carbon nanoadditives

SEBS/GnP (wt.%)	Electrical conductivity ($S.cm^{-1}$)	SEBS/GnP/CNT (wt.%)	Electrical conductivity ($S.cm^{-1}$)	SEBS/CNT* (wt.%)	Electrical conductivity* ($S.cm^{-1}$)
0	1.2E-17	0	1.2E-17	0	1.2E-17
3	2.3E-17	7/3	3.8E-1	3	1.1E-1
5	6.5E-17	5/5	8.4E-1	5	9.4E-01
7	4.1E-14	2/8	1.4	8	1.4
10	5.7E-11	7/8	1.5	10	1.8
15	2.6E-7	5/10	2.7	15	2.2

*Ref: (Kuester et al., 2016)

ciGuis.com

The maximum electrical conductivity of the SEBS/GnP nanocomposites was 2.6E-7 $S.cm^{-1}$ at 15 wt.% of GnP. For the hybrid nanocomposites, the electrical conductivity remained somewhat constant, between 1.4 and 2.7 $S.cm^{-1}$, for compounds with a CNT equal to or higher than 8 wt.%.

3.3.3 Electromagnetic shielding effectiveness and dielectric properties

The electromagnetic interference shielding effectiveness (EMI-SE) of the nanocomposites was established using experimental data and equations 3 and 4 (Al-Saleh et al., 2013; Al-Saleh & Sundararaj, 2009; Jia et al., 2015; Maiti et al., 2013; Ramôa et al., 2013; Sharma et al., 2016).

$$\text{EMI SE} = \text{SER} + \text{SEA} = 10\log\frac{\text{I}}{\text{I}-\text{R}} + 10\log\frac{\text{I}-\text{R}}{\text{T}} = 10\log\frac{\text{I}}{\text{T}} \quad (3)$$

$$\text{I} = 1 = \text{R} + \text{A} + \text{T} \quad (4)$$

where SE_R, and SE_A correspond to shielding mechanisms by reflection and absorption, respectively.

Figure 3.9 shows the EMI-SE of SEBS/GnP nanocomposites at different GnP weight fractions as a function of frequency.

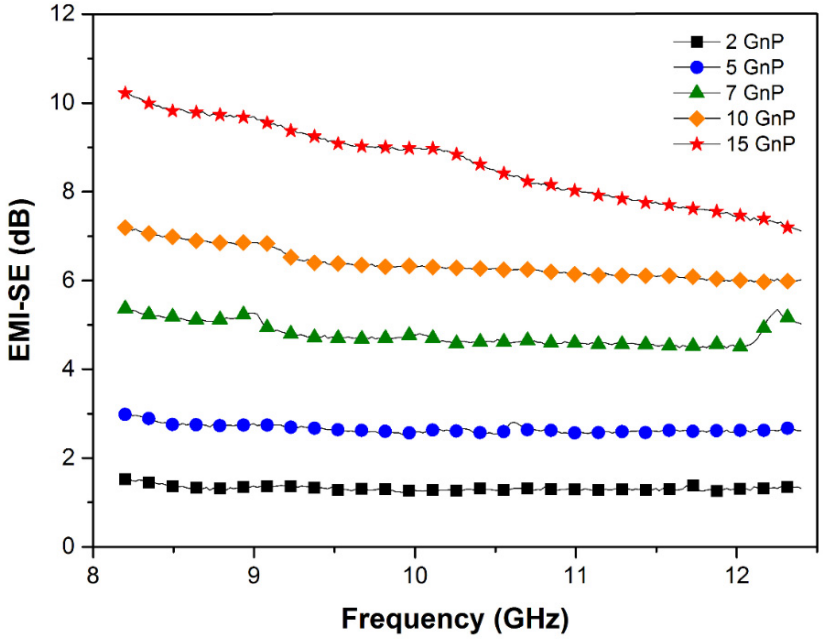

Figure 3.9 - Shielding effectiveness of SEBS/GnP nanocomposites at different GnP weight fractions as a function of frequency

For commercial applications, the minimum EMI-SE required is 20 dB, which represents a 99.00% attenuation of the incident radiation (Al-Saleh & Saadeh, 2013; Al-Saleh et al., 2013; Cao et al., 2015; Jia et al., 2015; M.-S. Kim et al., 2013; Maiti & Khatua, 2016; Maiti et al., 2013). As shown in Figure 3.9, SEBS/GnP nanocomposites do not satisfy the minimum shielding effectiveness requirement for all the compositions prepared. The EMI-SE for the nanocomposite with 15 wt.% of GnP (maximum weight fraction of nanoadditive used in this work) was 8.63 dB (86.02% attenuation) on average. However, as shown in Figure 10, hybrid nanocomposites of SEBS/GnP/CNT presented much higher EMI-SE.

Clicours.COM

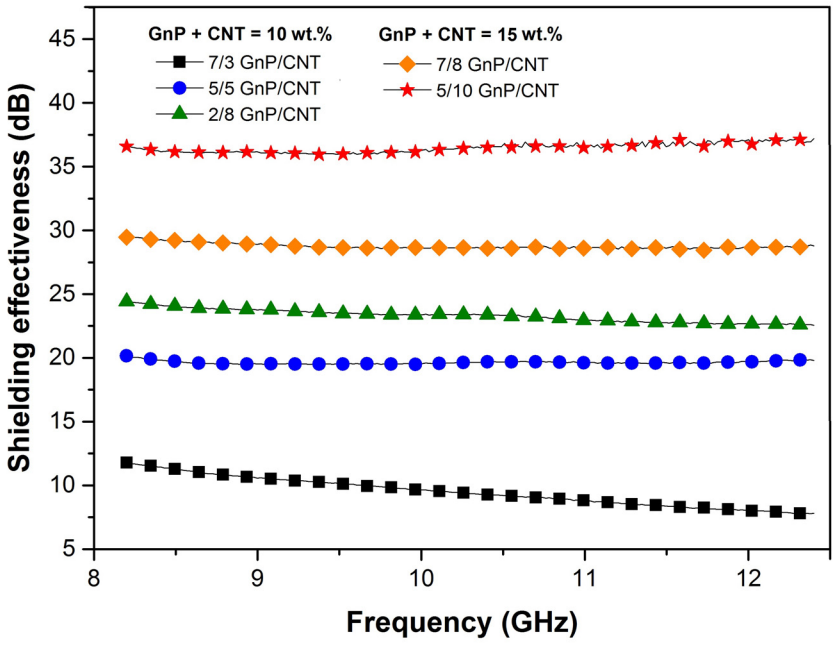

Figure 3.10 - Shielding effectiveness of SEBS/GnP/CNT nanocomposites at different GnP/CNT weight fractions as a function of frequency

At this point, it is important to consider that in a previous work, SEBS/CNT nanocomposites presented satisfactory results for nanocomposites with 10 wt.% (20.78 dB, 99.16% attenuation) and 15 wt.% (30.07 dB, 99.90% attenuation) of CNT (Kuester et al., 2016). In the present work, we prepared SEBS/GnP/CNT hybrid nanocomposites with a total loading of 10 and 15 wt.%, while varying the amount of the different nanoadditives.

For the SEBS/GnP/CNT nanocomposite at the absolute loading fraction of 10 wt.%, 7/3 wt.% of GnP/CNT, respectively, the EMI-SE was 9.48 dB (88.36% attenuation). This result was higher than the EMI-SE of 10 wt.% of GnP in SEBS/GnP nanocomposites, but still lower than the minimum requirement. However, the increase in CNT weight fractions in the nanocomposites considerably enhanced the EMI-SE. For the SEBS/GnP/CNT nanocomposite with 5/5 wt.% of GnP/CNT, the EMI-SE was 19.63 dB (98.91% attenuation). Lastly, for the nanocomposites with a minimum CNT loading equal to or higher than 8 wt.%, the shielding

effectiveness value requirement was satisfied. Table 3.3 summarizes the EMI-SE results for the different compositions.

Table 3.3 - Shielding effectiveness (dB) and percentage of attenuated radiation of SEBS/GnP, SEBS/CNT, and SEBS/GnP/CNT nanocomposites at different carbon nanoadditive weight fractions (the light gray highlights correspond to 10 wt.% of absolute carbon nanoadditive loading fraction, while the dark gray ones correspond to 15 wt.% of absolute carbon nanoadditive loading fraction)

SEBS/GnP (GnP wt.%)	EMI-SE (dB)	Radiation attenuated (%)	SEBS/CNT* (CNT wt.%)	EMI-SE* (dB)	Radiation attenuated* (%)	Total loading (GnP+CNT)	SEBS/GnP /CNT (GnP /CNT wt.%)	EMI-SE (dB)	Radiation attenuated (%)
2	1.32	26.16	3	6.88	79.42	10 wt.%	7/3	9.48	88.36
5	2.66	45.74	5	10.67	91.30		5/5	19.63	98.91
7	4.78	66.68	8	17.02	98.01		2/8	23.30	99.53
10	6.37	76.88	10	20.78	99.16	15 wt.%	7/8	28.76	99.87
15	8.63	86.02	15	30.07	99.90		5/10	36.47	99.98

*Ref: (Kuester et al., 2016)

For the SEBS/GnP/CNT nanocomposite with a total of 10 wt.% of carbon nanoadditives, in a portion of 2/8 wt.% of GnP/CNT, respectively, the EMI-SE was 23.30 dB (99.53% attenuation). This result was much higher than the EMI-SE of SEBS/GnP and SEBS/CNT nanocomposites at the same absolute loading fraction. Further, the EMI-SE was higher than the sum of the EMI-SE of SEBS/GnP with 2 wt.% of GnP and SEBS/CNT with 8 wt.% of CNT. These results show a synergic effect between the CNT and GnP regarding shielding effectiveness. A similar behavior was observed for the hybrid nanocomposites with higher weight fractions of carbon nanoadditives where the CNT >> GnP.

For the hybrid nanocomposite with an absolute carbon nanoadditive loading fraction of 15 wt.%, in a portion of 7/8 wt.% of GnP/CNT, the EMI-SE was 28.76 dB (99.87% attenuation). Finally, the higher EMI-SE of 36.47dB (99.98% attenuation) was achieved in the SEBS/GnP/CNT nanocomposite with 5/10 wt.% of GnP/CNT. Again, the EMI-SE was much higher than the effectiveness of the single nanocomposites at the same total loading fraction, i.e., greater than the sum of the EMI-SE of SEBS/GnP with 5 wt.% of GnP and SEBS/CNT with 10 wt.% of CNT, and the synergic effect was confirmed once again.

According to the literature, the advantage of preparing hybrid nanocomposites for electromagnetic shielding applications is the improvement of the conductive network due to the combination of carbon nanoadditives of different shapes, which may result in the synergic effects on the EMI-SE (Al-Saleh & Saadeh, 2013; Lin et al., 2016; Sharma et al., 2016). Sharma, S. K. et al. prepared hybrid nanocomposites of acrylonitrile butadiene styrene (ABS), CNT, and GR by dry tumble mixing followed by hot compaction. They showed that the EMI-SE of the nanocomposites increased from 7.5 to 26.8 dB with the addition of 1 wt.% of CNT to an ABS/GR nanocomposite, resulting in a synergic effect on the EMI-SE in the hybrid nanocomposite. According to the authors, the synergism was due to an improvement of the connectivity of the conductive network by the combination of the two different carbon nanoadditives (Sharma et al., 2016). Maiti, S., et al. prepared hybrid nanocomposites of polystyrene (PS), CNT, and graphite nanoplates by in situ polymerization. With a portion of 2/1.5 wt.% of CNT/Graphite nanoplate, respectively, the commercially applicable EMI-SE (≈

20.2 dB) was achieved. The authors state that the suitable EMI-SE with low amounts of nanoadditives was achieved due to the strong π-π interactions between PS and the carbon additives during in situ polymerization, and because of the interconnected conductive network formed (Maiti et al., 2013). Al-Saleh, M. H., and Saadeh, W. H. obtained nanocomposites of ABS, CNT, and carbon black by solution casting followed by hot compression. Although the hybrid nanocomposites did not present synergic effects, the authors showed that small quantities of CNT could be replaced by carbon black, decreasing the final cost of the nanocomposites, without impairing the EMI-SE (Al-Saleh & Saadeh, 2013).

In EMI shielding materials, the capacity to attenuate the incident electromagnetic radiation is the sum of the different shielding mechanisms, according the Equation 3. Thus, in order to assess the intrinsic attenuation capacity of the nanocomposites via different mechanisms, the impact of reflection (SE_R) and absorption (SE_A) mechanisms on the total shielding effectiveness was also evaluated. Table 4 shows the total EMI-SE, SE_R, and SE_A of the SEBS/GnP and SEBS/GnP/CNT nanocomposites at different carbon nanoadditive weight fractions.

Table 3.4 - Shielding effectiveness (dB), SE_R, and SE_A of the SEBS/GnP, SEBS/CNT, and SEBS/GnP/CNT nanocomposites at different carbon nanoadditive weight fractions

SEBS/GnP (GnP wt.%)	EMI-SE (dB)	SE_R	SE_A	SEBS/CNT* (CNT wt.%)	EMI-SE* (dB)	SE_R*	SE_A*	Total loading (GnP +CNT)	SEBS/GnP/CNT (GnP/CNT wt.%)	EMI-SE (dB)	SE_R	SE_A
2	1.32	1.18	0.14	3	6.88	4.46	2.42		7/3	9.48	5.08	4.40
5	2.66	2.39	0.27	5	10.67	4.44	6.23		5/5	19.63	4.61	15.02
7	4.78	4.43	0.35	8	17.02	3.79	13.23	10 wt.%	2/8	23.30	5.39	17.91
10	6.37	5.94	0.43	10	20.78	4.75	16.03		7/8	28.76	6.37	22.39
15	8.63	7.09	1.54	15	30.07	5.21	24.86	15 wt.%	5/10	36.47	6.90	29.57

*Ref: (Kuester et al., 2016)

Table 3.4 - Shielding effectiveness (dB), SE_R, and SE_A of the SEBS/GnP, SEBS/CNT, and

For all the SEBS/GnP nanocomposites prepared in the present work, the $SE_R > SE_A$. However, for the hybrid SEBS/GnP/CNT nanocomposites, the contribution by the SE_A mechanism is proportionally enhanced with increased CNT loading. More specifically, for the nanocomposite with 7/3 wt.% of GnP/CNT, $SE_R > SE_A$, while for all the other SEBS/GnP/CNT nanocomposites, $SE_A > SE_R$. These results were expected, since it is known that the SE_A increases as the nanocomposite's electrical conductivity is increased and/or with a narrower space between the carbon nanoparticles. However, unlike with single-component materials, an increase in SE_A for composite materials is non-linear, and to date, no theoretical interpretation has been established for the correlation between EMI-SE, conductive additive connectivity, electrical conductivity, and electrical permittivity specifically for composites (Al-Saleh & Sundararaj, 2009).

The complex permittivity is a useful parameter for analyzing the EMI-SE of polymeric nanocomposites based on carbon nanoparticles (Aloia et al., 2013; Cao et al., 2015; Micheli et al., 2010). According to (Al-Saleh et al., 2013; Arjmand et al., 2012; Cao et al., 2015; Theilmann et al., 2013), in polymer nanocomposites, the real permittivity (ε') (polarization) depends on the number of micro-capacitors and the polarization centers formed inside the material; here, polarization centers result from defects in the nanoadditive structure, while micro-capacitors are the carbon nanoparticles or their aggregates acting as electrodes in the insulating polymer matrix. On the other hand, the imaginary permittivity (ε") (dielectric loss) is related to the dissipation of energy due to the conductive paths formed inside the nanocomposite.

Figure 3.11 shows ε' and ε" as a function of frequency in the 8.2 - 12.4 GHz range for the a), b), SEBS/GnP and c), d), SEBS/GnP nanocomposites, respectively, at different weight fractions of carbon nanoadditives.

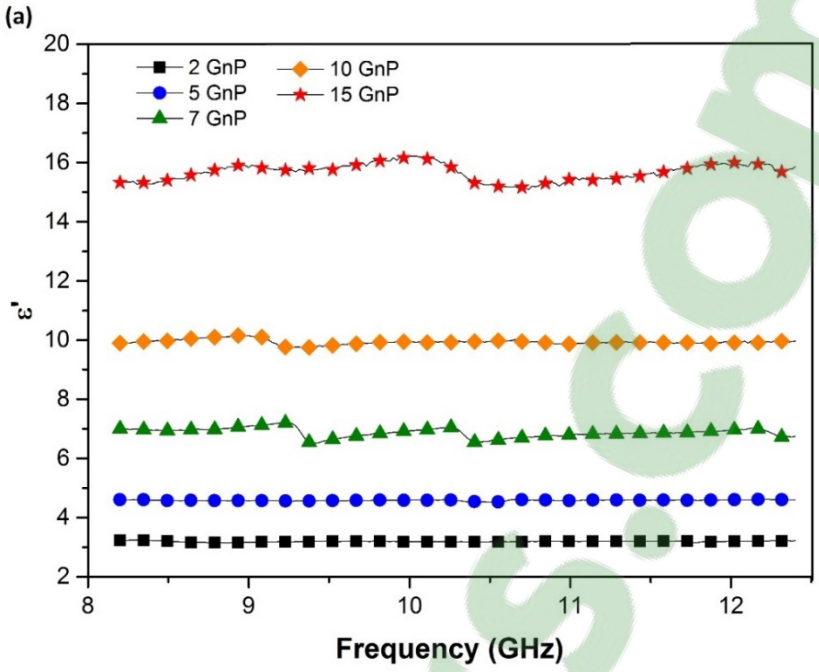
(a)
2 GnP
5 GnP
7 GnP
10 GnP
15 GnP
ε'
Frequency (GHz)

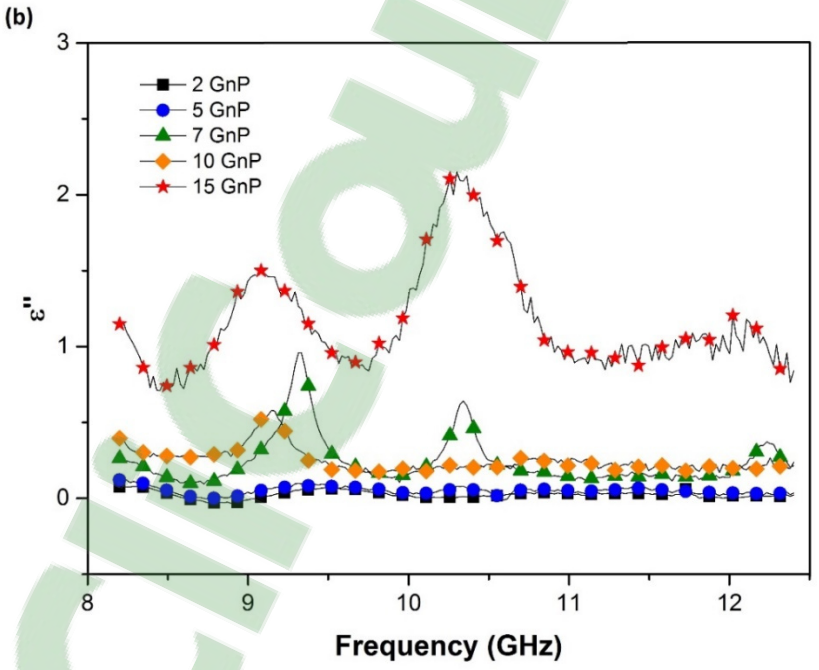
(b)
2 GnP
5 GnP
7 GnP
10 GnP
15 GnP
ε"
Frequency (GHz)

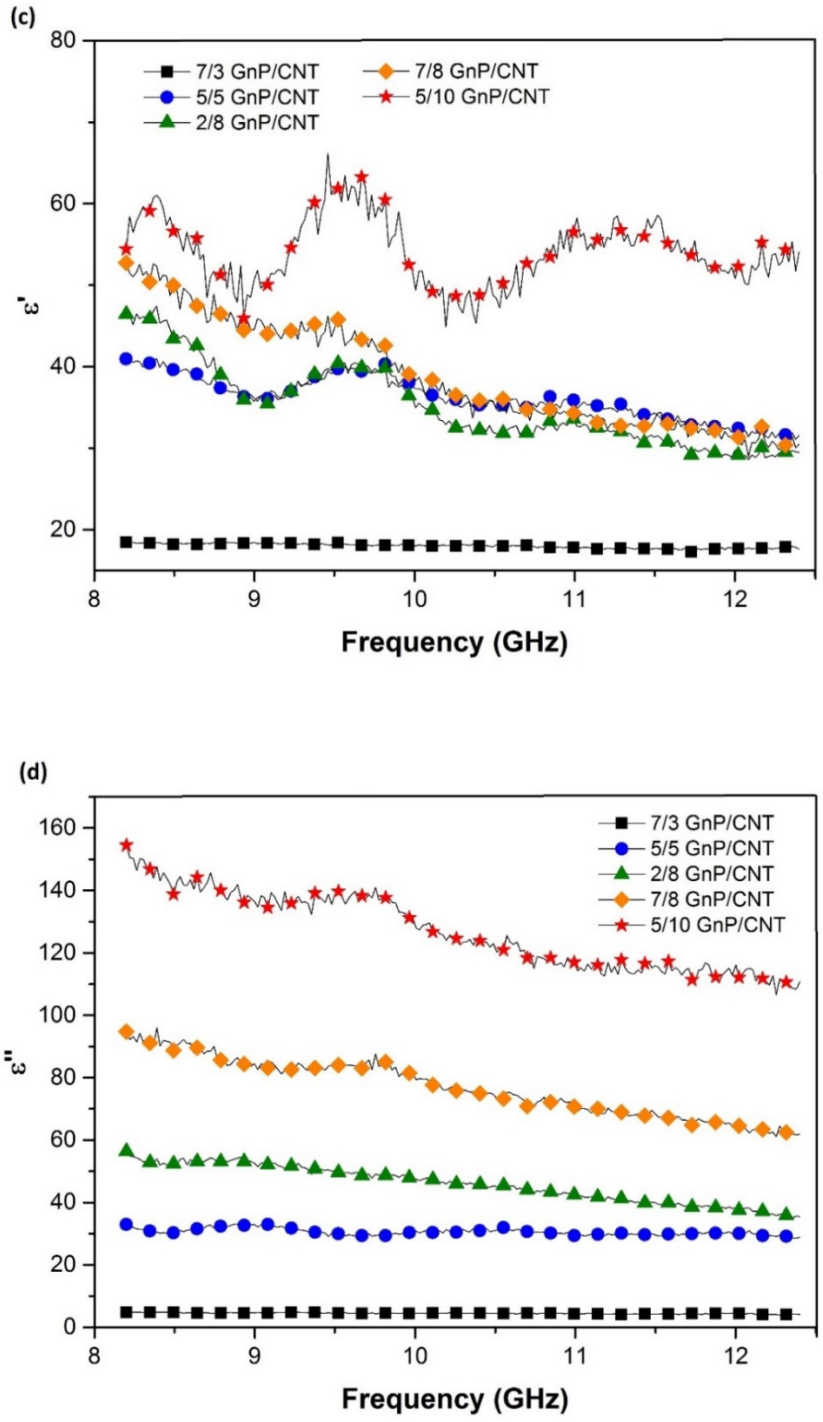

Figure 3.11 - a) c) Real (ε') and b) d) imaginary (ε") permittivity versus frequency of SEBS/GnP and SEBS/GnP/CNT nanocomposites, respectively, at different carbon nanoadditive weight fractions

For all the samples, ε' and ε" were enhanced as the weight fractions of carbon nanoadditives were increased in the nanocomposites. Increases in ε' with higher carbon nanoadditive loadings are expected since the number of structural defects and micro-capacitors inside the nanocomposites is also higher. Further, with higher amounts of carbon nanoadditives, the gap between the nanoparticles decreases, increasing the polarization inside the material. Higher values of ε" are also expected for nanocomposites with higher carbon nanoadditive loadings due to the higher amount of conductive paths inside the nanocomposites.

For all the SEBS/GnP nanocomposites, $\varepsilon' > \varepsilon''$. However, the hybrid nanocomposites presented a different behavior. For the nanocomposite with 7/3 wt.% of GnP/CNT (with a total of 10 wt.% of carbon nanoadditives), $\varepsilon' > \varepsilon''$, while for the compound of 5/5 wt.% of GnP/CNT (with a total of 10 wt.% of carbon nanoadditives), $\varepsilon' \approx \varepsilon''$, and for the nanocomposites with higher CNT loading, $\varepsilon' < \varepsilon''$, which means that at this point, the energy dissipation is more effective because of the higher number of paths forming the conductive network throughout the nanocomposite. These results justify the higher EMI-SE of the hybrid nanocomposites with CNT content higher than 8 wt.%.

3.4 Conclusions

Hybrid nanocomposites of SEBS/GnP/CNT prepared by melt compounding exhibited high electrical conductivity, as well as EMI-SE suitable for commercial applications. The electrical conductivity increased by 17 orders of magnitude when compared to that of pure matrix, reaching 1.4 $S.cm^{-1}$ at 2/8 wt.% of GnP/CNT (with a total of 10 wt.% of carbon nanoadditives). For the hybrid nanocomposites with CNT loading equal to or higher than 8 wt.%, the conductivity leveled off. The EMI-SE of the SEBS/GnP/CNT nanocomposite at the absolute loading fraction of 10 wt.% of carbon nanoadditives, in a portion of 2/8 wt.% of GnP/CNT, was 23.30 dB (99.53% attenuation). For the hybrid nanocomposite with a total of 15 wt.%, in a GnP/CNT fraction of 5/10 wt.%, the EMI-SE was 36.47dB (99.98% attenuation). These results confirm the synergic effect between the CNT and GnP regarding shielding effectiveness for the nanocomposites for which CNT >> GnP, since the EMI-SE of the hybrid

Clicours.COM

nanocomposites of SEBS/GnP/CNT was higher than the sum of the EMI-SE of the single nanocomposites of SEBS/GnP and SEBS/CNT. SEBS/GnP nanocomposites presented much lower electrical conductivity and EMI-SE than did the hybrid nanocomposites. The maximum electrical conductivity achieved with 15 wt.% of GnP was 2.6E-7 $S.cm^{-1}$, and the maximum EMI-SE was 8.63 dB. For all samples, ε' and ε" were enhanced as the weight fractions of carbon nanoadditives was increased in the nanocomposites. For all SEBS/GnP nanocomposites, ε' > ε". However, for the hybrid nanocomposite with 7/3 wt.% of GnP/CNT (with a total of 10 wt.% of carbon nanoadditives), ε' > ε"; for the 5/5 wt.% (with a total of 10 wt.% of carbon nanoadditives), ε' ≈ ε"; and for the nanocomposites with higher CNT loading, ε' < ε". These results justify the higher EMI-SE of the hybrid nanocomposites with CNT loadings higher than 8 wt.%., which is probably due to the higher number of paths in the conductive network throughout the nanocomposites, which resulted in an increase in energy dissipation. By FEG-SEM, GnP exhibited a non-homogeneous morphology, showing to be a mixture of multi-walled graphene and expanded graphite. CNT presented the characteristic morphology of MWCNT. Both carbon nanoparticles presented decent distributions throughout the matrix, as well as good adhesion due to the absence of significant voids. Rheological analyses showed that CNT could be properly dispersed into the SEBS matrix. On the other hand, it was not possible to properly disperse GnP in the matrix by melt compounding with the processing parameters used in this work. Raman spectroscopy and rheological analyses showed that SEBS/GnP nanocomposites did not present interactions with the SEBS matrix. The morphological characterization suggests that the higher electrical conductivity and EMI-SE results for the hybrid nanocomposites when compared to the SEBS/GnP nanocomposites is due to the better dispersion and higher interactions of CNT with the matrix, versus the GnP.

Acknowledgements

The authors gratefully acknowledge the financial support of the Natural Sciences and Engineering Research Council of Canada (NSERC), Conselho Nacional de Desenvolvimento Científico e Tecnológico – CNPq, Coordenação de Aperfeiçoamento de Pessoal de Ensino Superior – CAPES, and Fundação de Amparo à Pesquisa e Inovação do Estado de Santa

Catarina – FAPESC. We are also truly grateful to the Central Electron Microscopy Laboratory, Santa Catarina Federal University (LCME-UFSC), for the FEG-SEM analysis.

CHAPTER 4

This chapter presents the article corresponding to the results of the third part of the project regarding the effects of different post-processing techniques on SEBS/CNT and SEBS-MA/CNT nanocomposites. It highlights the influence of MA in the matrix, the orientation of CNT depending on the processing method, and how these factors affected the electrical, mechanical, and EMI shielding properties of the final nanocomposites. A balance between EMI shielding and mechanical properties is also presented.

MORPHOLOGY, MECHANICAL PROPERTIES AND ELECTROMAGNETIC SHIELDING EFFECTIVENESS OF SEBS/CNT NANOCOMPOSITES: EFFECTS OF MALEIC ANHYDRIDE, CNT LOADING, AND PROCESSING METHOD

Scheyla Kuester[1,2], Guilherme M. O. Barra[2*], Nicole R. Demarquette[1#]

[1#]École de technologie supérieure, Department of Mechanical Engineering

Montreal, QC, Canada

e-mail: Nicoler.Demarquette@etsmtl.ca

[2*]Universidade Federal de Santa Catarina, Departamento de Engenharia Mecânica,

Florianópolis, SC, Brazil,

e-mail: g.barra@ufsc.br

This article was submitted to Polymer International.

ABSTRACT

Nanocomposites based on poly (styrene-b-ethylene-ran-butylene-b-styrene) (SEBS) and carbon nanotubes (CNT) (SEBS/CNT), as well as SEBS grafted maleic anhydride (SEBS-MA)/CNT were successfully prepared for electromagnetic shielding applications. Both SEBS/CNT and SEBS-MA/CNT were prepared by melt compounding and post-processed using two different techniques: extrusion and compression molding. The different

nanocomposites were characterized by Raman spectroscopy and rheological analysis. Their mechanical properties, electrical (10^{-2}-10^{5} Hz) properties and electromagnetic shielding effectiveness (8.2-12.4 GHz) were also evaluated. Results showed that the CNT loading amount, the presence of MA in the matrix, and the molding technique used strongly influence the final morphologies and properties of the nanocomposites. While the nanocomposite containing 8 wt% CNT prepared by compression molding presented the highest electromagnetic shielding effectiveness (with a value of 56.73 dB, which corresponds to an attenuation of 99.9996% of the incident radiation), the nanocomposite containing 5 wt% CNT prepared by extrusion presented the best balance between electromagnetic and mechanical properties, being a good candidate to be used as an efficient flexible electromagnetic interference shielding material.

Keywords: Carbon-based polymer nanocomposites; flexible EMI shielding materials, mechanical properties, electrical properties; electromagnetic shielding effectiveness

4.1 Introduction

In all technological fields, advances in miniaturized systems and devices, and the explosion in the demand for consumer electronics increasingly require the development of more sophisticated materials. One of the challenges faced with such equipment, which generally operates at high levels of power and frequencies, is developing efficient and multifunctional electromagnetic shielding materials capable of completely sealing electromagnetic interference (EMI) emitters or receivers and fully complying with Electromagnetic Compatibility (EMC) regulations (Tong, 2009). Moreover, taking into account other parameters, such as mechanical requirements, weight, manufacture, esthetic factors, and costs, further complicates the development of suitable EMI shielding materials.

In order to meet the set of different requirements, thanks mainly to their outstanding performance/convenience ratio, electrically conductive polymer composites (ECPCs) are proving to be excellent options for high performance shielding materials. In this class of

composites, the choice of matrix and electrically conductive additives to interact with the EM waves are determinant factors, and depend on the EMI properties needed for specific applications. Currently, carbon nanotubes (CNT) are among the most popular conductive fillers. In general, CNT-based nanocomposites present great mechanical properties and high electrical conductivity at low loading amounts (low percolation threshold), more recently, many publications have also highlighted their high electromagnetic shielding properties (Thomassin et al., 2013). Regarding the matrix, while ECPCs based on conventional thermoplastic polymers generally meet most of the requirements, for some applications, however, flexible properties are also mandatory prerequisites, especially for EMI shielding gaskets and coating of flexible devices. In these cases, electrically conductive elastomers (ECEs), which are basically a subclass of ECPCs for which the polymeric matrix is an elastomer, are considered the most suitable choice (Tong, 2009).

ECE are used as EMI shielding materials in many fields, such as the electronics, electricity, telecommunications, housing, medical, and automotive industries (Tong, 2009), and many works in the literature present interesting results concerning the properties required for these applications (L. Liu et al., 2011; Merlini et al., 2017; Theilmann et al., 2013; Thomassin et al., 2013). However, most of the ECE are based on vulcanized rubbers which are difficult to process. The manufacture of devices made of conventional elastomers generally involves many steps and a vulcanization process that turn them non-recyclable and engender environmental concerns; consequently, there is an increase in both the time and cost of production. In order to overcome these problems, composites based on thermoplastic elastomers have been developed along the years (Bansala et al., 2017; Drobny, 2007b; Ramôa et al., 2013). TPEs are materials that can be manufactured as thermoplastics, while exhibiting a mechanical behavior similar to that of conventional vulcanized elastomers (Drobny, 2007a). Mostly, TPEs are phase-separated systems that present a hard phase acting as thermoreversible cross-links, as well as a soft phase that provides flexibility and elasticity. The hard phase has an upper service temperature (T_g or T_m higher than room temperature), while the soft phase exhibits a lower service temperature (T_g lower than room temperature). Thus, when the hard phase is melted or dissolved in a solvent, the material can flow and be processed as a thermoplastic material, and

by cooling or evaporation of the solvent, the elastomeric properties are recovered (Drobny, 2007a).

Currently, one of the most commonly used TPE worldwide is poly (styrene-b-ethylene-ran-butylene-b-styrene) (SEBS), which is basically a block copolymer consisting of three interconnected blocks, two rigid (polystyrene) in the ends and one rubbery (poly (ethylene-butylene)) in the middle. The remarkable advantages of SEBS include its excellent chemical resistance, UV stability, and capacity to be processed at elevated temperatures for extended periods of time without its structure sustaining damage (Drobny, 2007c; Grigorescu et al., 2016; Holden, 2000). Moreover, the presence of styrene in its structure may be advantageous for obtaining composites based on carbon additives. In these systems, an affinity between the π electrons of both components is expected once both have aromatic rings in their molecular structures (Y.-T. Liu et al., 2011; Loh et al., 2010; Maiti et al., 2013; You et al., 2014). These interactions favor the dispersion of the carbon additives, and consequently, decrease the amount of additive required to achieve the desired properties, avoid processing issues, and reduce costs.

In carbon-based polymer composites for EMI shielding in general, one of the biggest challenges lies in keeping the loading of conducting additives as low as possible; indeed, for ECEs, this condition is critical. In the case of ECEs for EMI shielding, the amount of conducting additive necessary to achieve a suitable EMI-SE may significantly decrease the resilience, strength, and ductility of the material (Chung, 2001). Consequently, the matrix loses its elastomeric properties, and as a result, its application as an EMI gasket or flexible coating, for example, is severely impaired.

Many publications in the literature report different methods for improving the engineering properties of composites with the lowest amounts of carbon additives. One of the strategies commonly applied consists in using modified polymer matrices with grafted functional groups as a means of promoting stronger physical interactions and, consequently, enhancing the dispersion of the conductive additives without decreasing their properties. One of the most

widely used multifunctional chemical intermediates is maleic anhydride (MA). As an example, Grigorescu et al. (2016) prepared nanocomposites of SEBS and SEBS-MA and graphite (G), and in their results, the SEBS-MA/CNT nanocomposites presented the best mechanical and dielectric properties. According to the authors, these improvements were due to hydrogen bonds between MA and the surface oxygen groups of G (Grigorescu et al., 2016). Other works have reported that the processing methods also could modify the morphologies of the composites and, consequently, strongly affect their final properties. As interesting example is presented by Panaitescu et al. (2014) who investigated the influence of melt processing using a two-roll mill to induce orientation on the morphology of SEBS and their composites with graphite. Their results showed that the rolling step not only modified the self-assembling architecture, but also improved the mechanical behavior of the composites (Panaitescu et al., 2014). On the other hand, the alignment induced by a processing technique may also affect the electrical properties of the composites. However, in this case, the orientation of the conductive particles generally hinders the formation of an conducting network, and thereby could decrease the electrical conductivity of the composite. Consequently, the EMI shielding effectiveness of the composites could also decrease. As an example, Arjmand et al. (2012) studied and compared the properties of PS/CNT nanocomposites for EMI-SE shielding prepared by compression and injection molding, and their results indicated that the PS/CNT compressed nanocomposites presented higher electrical conductivity, real and imaginary permittivity, and EMI-SE with lower amounts of conducting additive. According to the authors, these results had to do with the random distribution of the CNT into the PS matrix for the samples molded by compression (Arjmand et al., 2012). Therefore, considering that the main techniques used by the industry may induce orientation, which can result in opposite effects regarding the engineering properties, e.g. generally enhancing the mechanical properties while decreasing the electrical and EMI shielding properties of the composites, the effect of the distribution of the nanoparticles should be carefully analysed. Furthermore, for commercial applications of EMI shielding materials a suitable balance between mechanical properties and shielding effectiveness is critical.

In the present work, we investigated the effect of using a styrenic thermoplastic elastomer with and without MA grafting, and studied the influence of two different melt compounding processing techniques on the final morphologies and properties of carbon-based polymer nanocomposites for EMI shielding applications. SEBS/CNT and SEBS-MA/CNT with different CNT loadings were obtained by melt compounding in a mixer, followed by compression molding, and mixer followed by extrusion molding with a tape die. The nanocomposites were characterized in terms of their polymer/CNT interactions, dispersion and alignment of the CNT inside the matrices, mechanical properties, electrical properties, and EMI shielding. A balance between EMI shielding and mechanical properties is also presented.

4.2 Experimental

4.2.1 Materials

Two poly (styrene-b-ethylene-ran-butylene-b-styrene) matrices from Kraton Polymers do Brasil Ind. Com. Prod. Petr., SEBS (Kraton G-1652 M) and maleic-anhydride-grafted SEBS, identified throughout the text as SEBS-MA (Kraton FG1901 G), were used in this work. Both SEBS and SEBS-MA present a styrene/rubber content ratio of 30/70 wt% and a specific gravity of 0.91 $g.cm^{-3}$. In the case of SEBS-MA, 1.4-2.0 wt% of maleic anhydride (MA) is grafted onto the rubber midblock. The melt flow index of the copolymers (230 °C, 5000g) is 5 g/10 min for SEBS, and 22 g/10 min for SEBS-MA. Multi-walled Carbon Nanotubes (MWCNT) from Nanocyl™ (NC 7000 series) were used as the electrically conductive additives. The CNT present the following characteristics: surface area of 250-300 $m^2.g^{-1}$, bulk density of 0.06 $g.cm^{-3}$, carbon purity of 90 %, average diameter of 9.5 nm, and average length of 1.5 μm. All materials were used as received.

4.2.2 Preparation of nanocomposites

Nanocomposites of SEBS/CNT and SEBS-MA/CNT were prepared by melt compounding using a torque rheometer (Drive Unit HAAKE RheoDrive Os 4), which was coupled to a

mixing chamber (Rheomix 600p) equipped with roller rotors. The processing parameters were as follows: temperature of 220 °C, rotational speed of 150 rpm, and total mixing time of 15 minutes. Both the SEBS/CNT and SEBS-MA/CNT were further post-processed using two different techniques: extrusion and compression molding. The nanocomposites obtained by melt compounding followed by compression were molded in a hydraulic press at a temperature of 220 °C for 10 minutes under a holding pressure of approximately 5 MPa. The nanocomposites obtained by melt compounding followed by extrusion were obtained in a twin screw extruder (Extruder HAAKE PolyLab OS PTW16 OS, Drive Unit HAAKE RheoDrive OS 4) at temperature of 220 °C and a rotational speed of 150 rpm.

4.2.3 Characterization

Raman spectroscopy was used to investigate the existence of non-covalent interactions between the CNT and the SEBS and SEBS-MA matrices. Analyses were performed using a Witec Alpha 300R Plus confocal Raman microscope (CRM) with a 532nm laser excitation <100mW, and an ultra-high throughput spectrometer (UHTS 300) with gratings of 600 or 1800 g/mm with 500 blaze.

Small Amplitude Oscillatory Shear (SAOS) analysis was carried out to assess the state of dispersion of the CNT. Experiments were conducted using an Anton Paar rheometer (MCR 501C) equipped with 25 mm diameter parallel plates. The measurements were performed at 220 °C in the linear viscoelastic regime under a strain equal to 0.5% in the 0.001 to 300 $rad.s^{-1}$ frequency range.

The mechanical properties were evaluated using an STM Alliance machine, equipped with 1kN load cell, in tensile mode, according to the ASTM 412D standard. At least 5 specimens were tested for each material.

The AC electrical conductivity was assessed using a Novocontrol broadband spectrometer. Samples 20 mm in diameter were placed between two parallel brass-plated electrodes, and

Cliccours.COM

measurements were carried out at an excitation voltage of 3V, in the 10^{-2} to 10^{5} Hz frequency range, at room temperature.

The EMI-SE measurements of the nanocomposites in the X-band microwave frequency range (8.2-12.4 GHz) were performed in a vector network analyzer (E5071C, ENA series 300 kHz–20 GHz) using a WR-90 rectangular waveguide as the sample holder (22.86 mm x 10.16 mm) and the thickness of all samples was 2.0 mm.

4.3 Results and discussion

4.3.1 Morphological analysis

4.3.1.1 Raman spectroscopy

The presence of non-covalent interactions between SEBS and SEBS-MA matrices and CNT was investigated using Raman spectroscopy. Figure 4.1 shows the Raman spectra of the neat CNT and SEBS/CNT and SEBS-MA/CNT nanocomposites with 5 wt% of CNT.

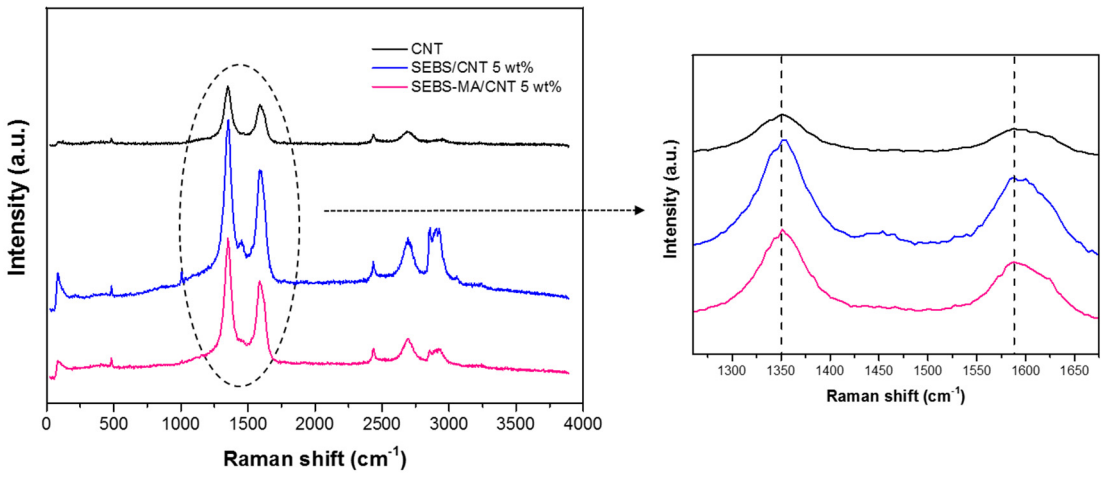

Figure 4.1 - Raman spectra of pristine CNT, and SEBS/CNT and SEBS-MA/CNT nanocomposites with 5 wt% CNT (on the left), and blow-up of the spectra in the 1250-1700 cm^{-1} region (on the right)

As shown in Figure 4.1, the characteristic D-band peak of the CNT occurred at 1351 cm^{-1}, corresponding to the in-plane vibration of sp^2 carbon atoms, while the G-band peak occurred at 1588.2 cm^{-1}, related to defects. SEBS/CNT presented a small shift of 4.4 cm^{-1} (1355.4 cm^{-1}) for the D-band peak. This shift indicates the presence of weak non-covalent π-π interfacial interactions between CNT and the aromatic rings of PS of the SEBS matrix (Rath & Li, 2011). The SEBS-MA/CNT nanocomposite presented exactly the same peaks as the pristine CNT, and no shift could be observed. This result suggests that the presence of MA in SEBS-MA chains hinders the π-π interactions between CNT and the aromatic rings of PS of the SEBS-MA matrix. Moreover, no interactions related to hydrogen bonds were observed in the SEBS-MA/CNT nanocomposites by Raman spectroscopy.

In order to assess the quantity of defects in the CNT structure, the intensity ratios of the D and G peaks, I_D/I_G, are commonly evaluated (Y.-T. Liu et al., 2011; Zhao et al., 2012). The I_D/I_G of the neat CNT was 1.03, while for the SEBS/CNT and SEBS-MA/CNT nanocomposites, it was 1.07 and 1.12, respectively. The small increase in the I_D/I_G indicated that the compounding method did not significantly damage the CNT structure.

4.3.1.2 Rheological analysis

The dispersion of CNT into the SEBS and SEBS-MA matrices was studied through rheological analysis. Small amplitude oscillatory shear (SAOS) analysis was used to characterize differences in the relaxation of polymer chains due to the presence of CNT. Through the analysis of the slopes in the curves of log G' vs. log ω (G' = storage modulus, ω = frequency) at low frequencies, it is possible to identify the formation of a physical network that hinders the polymer chains' movement (N. R. Demarquette & Carastan, 2016). Furthermore, the same analysis can be used to identify the degree of the spatial order of the phase domains, and consequently, the neat block copolymer morphological structure, which can be lamellar, cylindrical, spherical, or even disordered. Figure 4.2 shows the rheological behavior of neat SEBS and SEBS-MA matrices, and SEBS/CNT and SEBS-MA/CNT nanocomposites

prepared by melt compounding followed by extrusion molding. In order to facilitate the visualization, Table 4.1 presents the slopes of the curves of log G' vs. log ω at low frequencies.

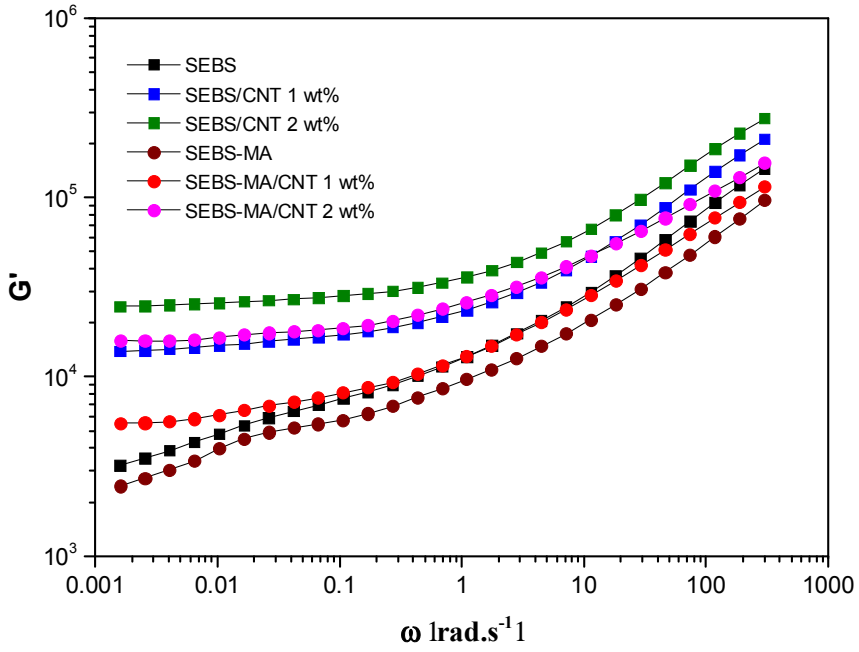

Figure 4.2 - Curves of G' as a function of frequency of neat SEBS and SEBS-MA, and nanocomposites of SEBS/CNT and SEBS-MA/CNT at different CNT weight fractions

Table 4.1. Low frequency (0.001-0.01 rad.s^{-1}) slopes of log G' vs. log ω for neat SEBS and SEBS-MA, and SEBS/CNT and SEBS-MA/CNT nanocomposites at different CNT weight fractions

SEBS SEBS/CNT (wt%)	Low frequency slope of log G' vs. log ω	SEBS-MA SEBS-MA/CNT (wt%)	Low frequency slope of log G' vs. log ω
SEBS	0.21	SEBS-MA	0.20
SEBS/CNT 1%	0.07	SEBS-MA/CNT 1%	0.13
SEBS/CNT 2%	0.05	SEBS-MA/CNT 2%	0.07

As can be seen in Figure 4.2 and Table 4.1, both neat matrices presented very similar slopes of log G' vs. log ω at low frequencies, 0.21 and 0.20 for SEBS and SEBS-MA, respectively. According to the literature, this rheological behavior at low frequencies corresponds to that of block copolymers with cylindrical structures in the ordered state (Danilo Justino Carastan et al., 2008).

For the nanocomposites, the addition of CNT increased G' for the whole range of frequencies, and decreased the slope of log G' vs. log ω at low frequencies, indicating that not only CNT acts as a filler, but it also reduces the mobility of SEBS chains. For SEBS/CNT with 1 wt% of CNT, an almost horizontal non-terminal plateau was formed in the G' curves, and the nanocomposite presented a highly solid-like behavior. For the SEBS-MA/CNT with 1 wt% of CNT, the decrease in the slope was lower. Furthermore, nanocomposites of SEBS/CNT presented a higher increase in the G' than those of SEBS-MA/CNT compared to the G' of the SEBS and SEBS-MA matrices, respectively. These results suggest that the CNT were better dispersed in SEBS than in SEBS-MA, which is in good agreement with the Raman results. For the samples with 2 wt% of CNT, a plateau was formed, and both nanocomposites presented similar slopes and highly solid-like behaviors.

There were no significant changes in rheological behavior related to the different molding techniques used, and the nanocomposites of SEBS/CNT and SEBS-MA/CNT prepared by melt compounding followed by extrusion and by compression molding (not presented) exhibited very similar rheological results. However, different characterization techniques, such as electrical and mechanical properties analysis, carried out at room temperature, can indirectly complement the morphological characterization in terms of the dispersion and orientation of carbon additives in nanocomposites.

4.3.2 Electrical conductivity

In composites based on a polymeric matrix and electrically conductive additives, the transition from insulators to conductors occurs by the formation of a connected network of the conductive

fillers inside the matrix. The critical loading amount of conductive additives from which this transition occurs is known as the electrical percolation threshold (Thomassin et al., 2013). In these materials, two distinct behaviors can be observed. Below the percolation threshold, the AC conductivity is frequency dependent and presents a slope of 1 in log-log scale. On the other hand, for nanocomposites close to or above the percolation threshold, the behavior becomes frequency-independent below a critical frequency (Stoyanov, Carthy, Kollosche, & Kofod, 2009).

The AC conductivity as a function of frequency for the SEBS/CNT and SEBS-MA/CNT nanocomposites with 1, 2, 5, and 8 wt% of CNT prepared by melt compounding followed by extrusion and by compression molding is presented in Figure 4.3.

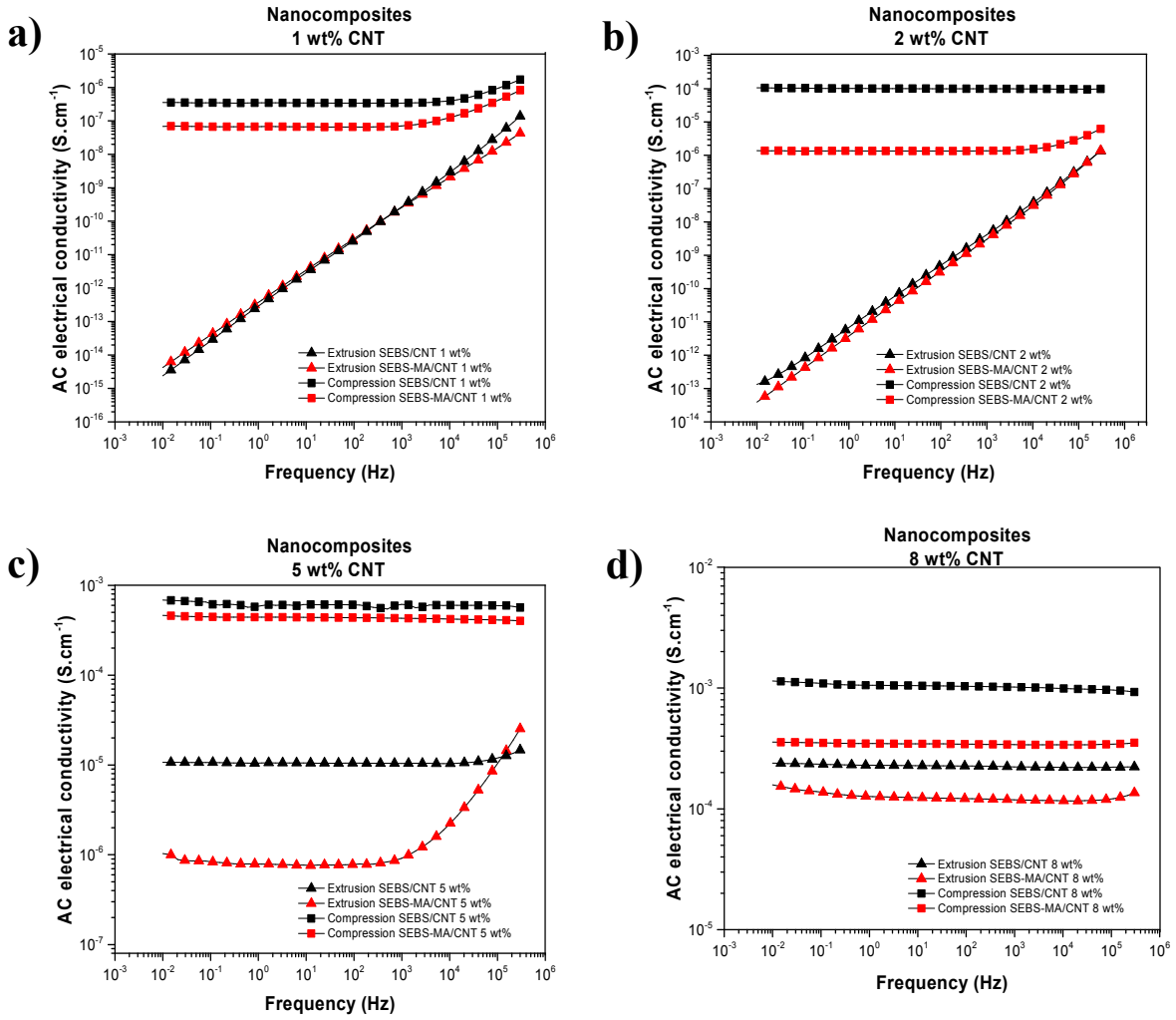

Figure 4.3 - AC conductivity as a function of frequency of the SEBS/CNT and SEBS-MA/CNT nanocomposites with a) 1, b) 2, c) 5, and d) 8 wt% of CNT

As can be seen in Figures 4.3 a-d, both the presence of MA in the matrix and the molding techniques used to prepare the nanocomposites affected the AC conductivity of the samples, although the processing methods were much more significant for the results.

For the nanocomposites of SEBS/CNT and SEBS-MA/CNT with 1 wt% of CNT prepared by extrusion, the samples presented an insulating behavior, since the AC conductivities of nanocomposites were completely frequency-dependent and similar to the pure matrices (not shown). On the other hand, for the nanocomposites with 1 wt% of CNT prepared by

compression molding, the samples presented a completely different behavior, being frequency-independent for the frequency range of around 10^{-2} to 10^{4} Hz. The AC conductivities were ≈ 3.40E-7 $S.cm^{-1}$ for SEBS/CNT at 10^{-2} to 10^{4} Hz, and ≈ 6.60E-8 $S.cm^{-1}$ for SEBS-MA/CNT at 10^{-2} to 10^{3} Hz.

The nanocomposites with CNT loading of 2 wt% presented a very similar behavior to the samples with 1 wt% of CNT. However, the SEBS/CNT nanocomposite prepared by compression molding presented a frequency-independent behavior for all the frequency ranges analyzed.

For the nanocomposites with 5 wt% of CNT, the AC conductivities were fairly frequency independent for the nanocomposites of SEBS/CNT and SEBS-MA/CNT prepared by compression molding, as well as for the sample of SEBS/CNT prepared by extrusion. These nanocomposites presented an AC of ≈ 6.10E-4 $S.cm^{-1}$, 4.40E-4 $S.cm^{-1}$, and 1.05E-5 $S.cm^{-1}$, respectively. However, the nanocomposite of SEBS-MA/CNT prepared by extrusion presented only a frequency-independent behavior between 10^{-2} to 10^{3} Hz, and an AC conductivity of ≈ 7.79E-7 $S.cm^{-1}$ in this frequency range.

Finally, all the nanocomposites with CNT loading of 8 wt% prepared by both molding techniques presented a frequency-independent behavior. Although the differences were small, the AC conductivities of the nanocomposites were ordered as follows: SEBS-MA/CNT prepared by extrusion (≈ 1.2E-4 $S.cm^{-1}$) < SEBS/CNT prepared by extrusion (2.30E-4 $S.cm^{-1}$) < SEBS-MA/CNT prepared by compression molding (3.40E-4 $S.cm^{-1}$) < SEBS/CNT prepared by compression molding (1.03E-3 S.cm-1).

In order to facilitate the comparison and highlight the different electrical conductivity behavior, Figure 4 shows the AC conductivity as a function of CNT loading of the different nanocomposites at 100 Hz.

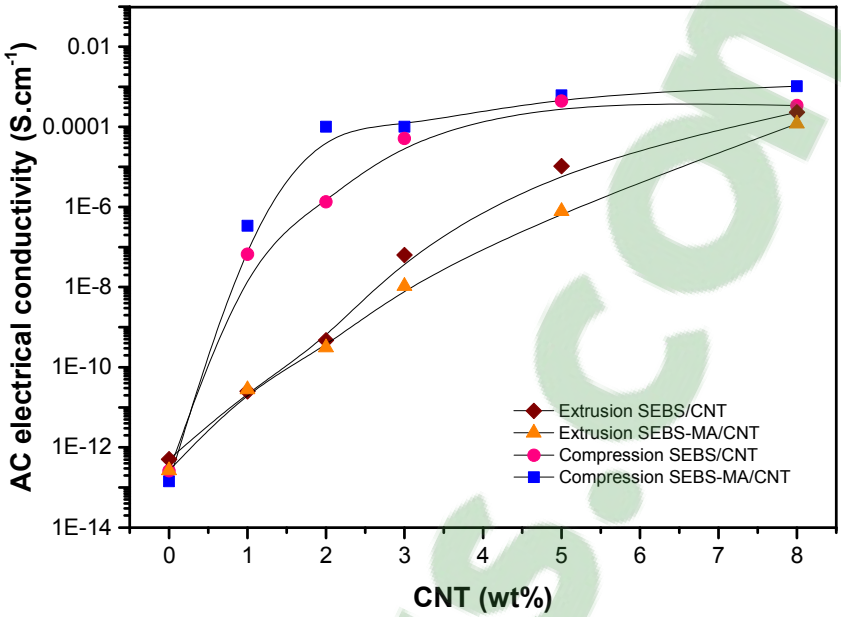

Figure 4.4 - AC conductivity of both the matrices and SEBS/CNT and SEBS-MA/CNT nanocomposites prepared by extrusion molding and by compression molding as a function of CNT loading (at 100 Hz)

It can be seen from Figure 4.4 that the presence of MA affects the electrical conductivity only slightly; on the other hand, the molding process seems to have a tremendous effect on the electrical percolation threshold of the nanocomposites: the SEBS-CNT and SEBS-MA nanocomposites prepared by compression molding present an electrical percolation threshold at around 1 wt% of CNT loading, in the case of the SEBS-CNT and SEBS-MA nanocomposites prepared by extrusion molding, there is no abrupt changes in their conductivities. The variation of the electrical conductivities of these nanocomposites was practically constant, and even with 3 wt% of CNT loading in the samples obtained by extrusion, the electrical conductivities were lower than the conductivity of the nanocomposites molded by compression with 1 wt% of CNT.

The different behaviours regarding the electrical properties can be explained considering the effects of the processing methods on the morphologies of the nanocomposites. It is well known

in the literature that some processing methods, such as extrusion, injection and roll milling, can induce an alignment of the carbon additives in polymer composites, which strongly affects their electrical properties (Arjmand et al., 2012; Mahmoodi, Arjmand, Sundararaj, & Park, 2012; Theilmann et al., 2013). A schematic representation of the effect of random and aligned distributions of CNT on the formation of the conductive networks is shown in Figure 4.5.

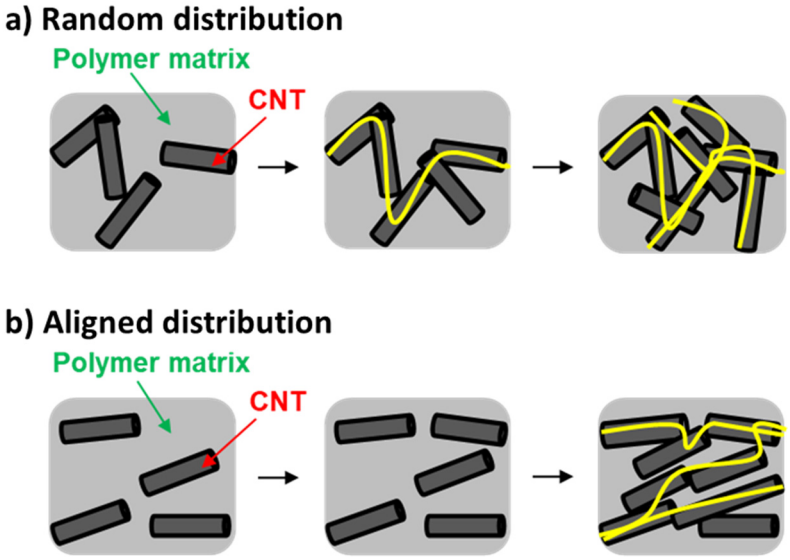

Figure 4.5 - Schematic representation of the effect of a) random and b) aligned distributions of the CNT on the formation of the conductive network of nanocomposites prepared by compression and extrusion molding, respectively

As schematically shown in Figure 4.5, for the nanocomposites prepared by compression molding, the formation of the electrically conductive network was favored by the random distribution of CNT throughout the material. Furthermore, due to the random distribution, with around 1 wt% of CNT loading, CNT-CNT connections were formed throughout the material. For the nanocomposites prepared by extrusion molding, these CNT-CNT connections were hindered by the alignment of the CNT inside the materials. In fact, the CNT do not really need to touch each other inside the matrix, but they however need to be close enough to permit the conduction of electricity upon the effect of hopping of electrons. As a consequence of the CNT

alignment, many more CNT were needed in order to get them close enough to one another to conduct electricity.

4.3.3. Mechanical properties

Carbon additives such as carbon black and graphite are traditionally used for reinforcement of thermoplastics and elastomers. However, beyond a critical loading amount, notwithstanding any enhancement of the Young's modulus that may be seen, other mechanical properties, such as the tensile strength and the elongation at break, can be severely decreased once the matrices become more brittle (Rath & Li, 2011). Furthermore, the processing method used can also affect the mechanical properties of carbon-based composites (Erik & Tsu-Wei, 2002; Panaitescu et al., 2014).

Figure 4.6 shows the stress vs. strain behavior of neat SEBS and SEBS-MA matrices, as well as SEBS/CNT and SEBS-MA/CNT nanocomposites prepared by the different processing techniques. During mechanical testing, the strain was applied along the flow direction for the materials prepared by extrusion molding.

Clicours.COM

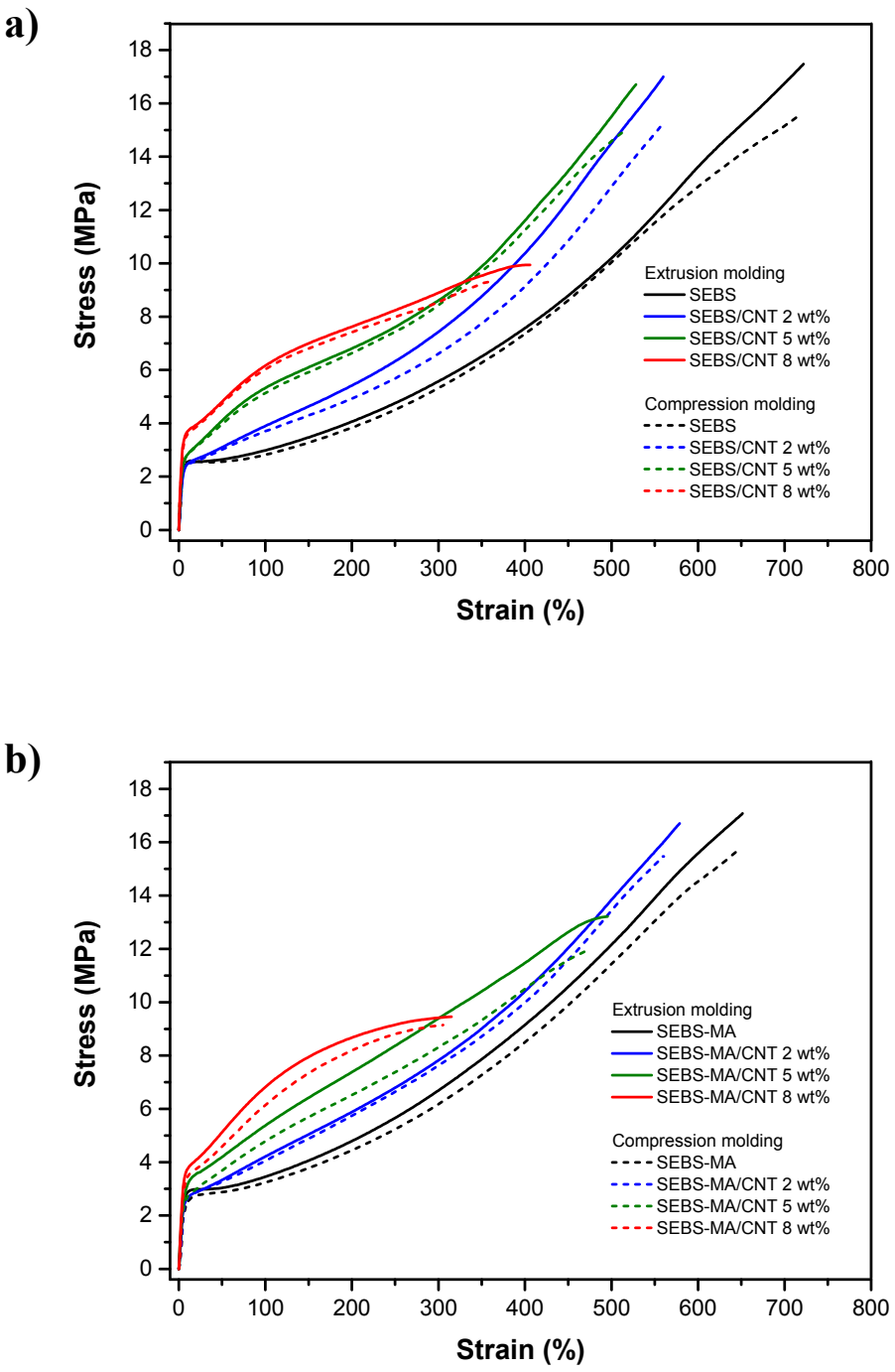

Figure 4.6 - Stress vs. strain curves for a) neat SEBS and SEBS/CNT nanocomposites, and b) neat SEBS-MA and SEBS-MA/CNT nanocomposites prepared by melt compounding followed by extrusion and by compression molding

As shown in Figure 6 for all the nanocomposites the addition of CNT resulted in an increase of the Young's modulus and stress at 100%, whereas the tensile strength and the elongation at break decreased. These effects were enhanced as the loadings of CNT in the nanocomposites increased.

For all the nanocomposites filled with 2 wt% of CNT the Young's modulus and tensile strength were quite similar to those of the neat matrix, while the elongation at break decreased. For the SEBS/CNT filled with 5 wt% of CNT the nanocomposites presented quite similar behavior to the nanocomposites filled with 2 wt% of CNT. On the other hand, for the SEBS-MA/CNT nanocomposites the addition of 5 wt% of CNT had a greater effect on the mechanical properties, and the tensile strength and elongation at break suffered a fairly significant decrease. For all the nanocomposites the addition of 8 wt% of CNT had a dramatic impact in the mechanical properties, the tensile strength decreased around 7 MPa, in average, and the elongation at break suffered a drastic decrease of more than 300% (to almost half of the elongation at break of the neat matrices).

Unlike the strong effects of the amount of CNT on the mechanical behavior of the nanocomposites, only slight differences were observed in the mechanical properties of the matrices and nanocomposites related to the different processing methods used. However, despite these differences were minor, they followed a pattern, and all the samples prepared by extrusion presented higher Young's modulus, tensile strength, stress at 100%, and elongation at break values than the samples prepared by compression. Similarly to what was observed with the AC conductivity results, the differences depending on the processing methods are related to the morphological orientation. According to the literature, when block copolymers such as SBS and SEBS are manufactured by melt methods such as extrusion, injection, and rolling molding, which induce deformation in one specific direction, the block copolymers' nanodomains are oriented in the flow direction (Danilo J. Carastan et al., 2013; Danilo Justino Carastan et al., 2008; Fang et al., 2009; Panaitescu et al., 2014). As a consequence, when stress is applied along the flow direction, the materials are stiffer because the applied force is parallel to the PS cylinders axes, and higher forces are needed for the same deformation as compared

the case with non-oriented samples (Panaitescu et al., 2014). For the nanocomposites, an analogous effect is expected regarding the nanoparticles into the matrices. The melt flow in one direction induces the orientation of the nanoparticles, and consequently, increases the forces needed to deform the material in the same direction (Panaitescu et al., 2014).

Additionally, the presence of MA in the matrix also influenced the mechanical behavior of the samples, although the Raman spectroscopy analyses showed that the presence of MA did not improve interactions between the matrix and CNT. All the samples of MA-grafted SEBS presented lower Young's modulus, tensile strength, stress at 100%, and elongation at break values. This behavior is understandable, given that the presence of MA makes the matrix more fluid, which consequently affects the distribution and alignment of CNT in the nanocomposites. These results are also in agreement with the rheological analyses.

4.3.4. Electromagnetic shielding effectiveness

For most commercial applications, the minimum electromagnetic shielding effectiveness (EMI-SE) required is 20 dB, which corresponds to an attenuation of 99.0% of the incident radiation (Jia et al., 2015; Maiti et al., 2013). The EMI-SE of the nanocomposites was experimentally established according to equations 4.1, 4.2, 4.3 and 4.4 (Saini & Arora, 2012; Thomassin et al., 2013).

$$R = [E_R/E_I]^2 = |S_{11}|^2 = |S_{22}|^2 \quad (4.1)$$

$$T = [E_T/E_I]^2 = |S_{12}|^2 = |S_{21}|^2 \quad (4.2)$$

$$I = 1 = R + A + T \quad (4.3)$$

$$\text{EMI SE} = SE_R + SE_A = 10\log\frac{I}{I-R} + 10\log\frac{I-R}{T} = 10\log\frac{I}{T} \quad (4.4)$$

where the S-parameters, S_{11} (or S_{22}) and S_{12} (or S_{21}), are correlated with the reflected (R) and the transmitted (T) power. In these analyses, when the electromagnetic radiation insides (I) the shielding material, the absorbed (A), reflected (R), and transmitted (T) power amount to 1 (Saini & Arora, 2012; Thomassin et al., 2013). The total EMI-SE is the sum of the shielding mechanisms by reflection (SE_R) and absorption (SE_A) (Saini & Arora, 2012; Thomassin et al., 2013), and a third mechanism related to multiple reflections (SE_M) may also occur. However, SE_M can be neglected if the SE_A is greater than 10 dB (Al-Saleh et al., 2013; Jia et al., 2015; Saini & Arora, 2012; Udmale V, 2013).

Figure 4.7 presents the EMI-SE of SEBS/CNT and SEBS-MA/CNT nanocomposites prepared by extrusion and by compression molding at 5 and 8 wt% of CNT in the 8.2- 12.4 GHz frequency range.

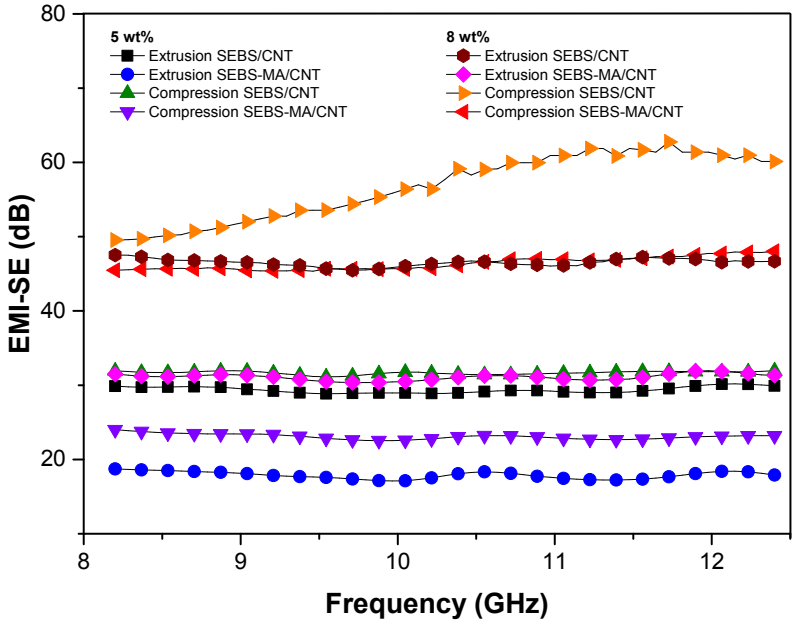

Figure 4.7 - Shielding effectiveness versus frequency of SEBS/CNT and SEBS-MA/CNT nanocomposites prepared by extrusion molding and by compression molding with 5 and 8 wt% of CNT

As can be seen in Figure 4.7, the SEBS/CNT and SEBS-MA/CNT nanocomposites prepared by compression molding and the SEBS/CNT prepared by extrusion with 5 wt% of CNT loading presented the EMI-SE required for commercial applications. Besides, all the nanocomposites with 8 wt% of CNT presented results much higher than the required shielding effectiveness. The EMI-SE for the SEBS/CNT and SEBS-MA/CNT nanocomposites with 8 wt% of CNT prepared by extrusion was 46.52 dB and 31.09 dB, and for the SEBS/CNT and SEBS-MA/CNT prepared by compression molding, it was 56.73 dB and 46.38 dB, respectively. For all the nanocomposites with 8 wt% of CNT loading, more than 99.9% of the incident electromagnetic radiation was attenuated.

In a previous work, we studied nanocomposites of SEBS/CNT for EMI shielding using a highly viscous commercial grade of SEBS (melt index <1 g/10 min (230°C, 5kg)) prepared by melt compounding followed by compression molding. In that work, the high viscosity of the matrix impaired the dispersion and distribution of the conductive additives and the maximum EMI-SE was 30.07 dB achieved with 15 wt% of CNT (Kuester et al., 2016).

Figure 4.8 shows the power balance of the incident, reflected, absorbed, and transmitted electromagnetic radiation for the SEBS/CNT nanocomposites prepared by a) extrusion and b) compression molding, and SEBS-MA/CNT prepared by c) extrusion and d) compression molding at different CNT weight fractions in the 8.2-12.4 GHz frequency range.

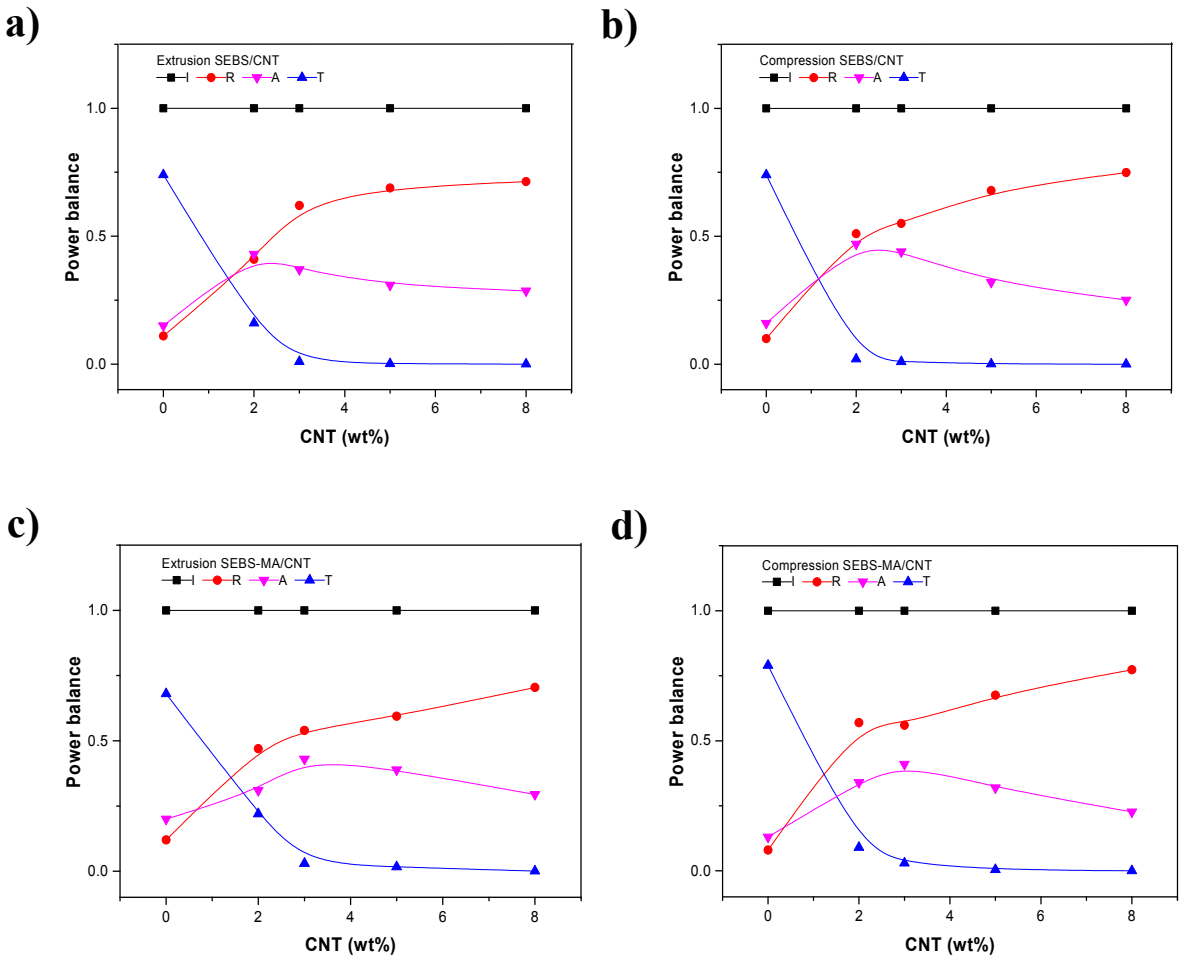

Figure 4.8 - Power balance of the incident (I), reflected (R), absorbed (A), and transmitted (T) electromagnetic radiation for the SEBS/CNT nanocomposites prepared by a) extrusion and b) compression molding, and for the SEBS-MA/CNT prepared by c) extrusion and d) compression molding at different CNT weight fractions

As shown in Figure 4.8, the transmission of most of the incident radiation, as an absolute value, is blocked by reflection. Furthermore, at this point, it is worth highlighting the difference between the concepts of shielding mechanisms and power loss. Although effective carbon-based nanocomposites generally present an SE_A higher than the SE_R mechanism and the misunderstanding in some works in the literature, in fact only a small amount of radiation is absorbed by the material. This happens because reflection obviously occurs before absorption,

and so by the time the electromagnetic radiation hits the material, most of the energy is readily reflected, and less energy is left to be absorbed or transmitted (Al-Saleh et al., 2013; Thomassin et al., 2013).

Table 4.2 summarizes the shielding behavior of the nanocomposites at different CNT weight fractions by presenting the EMI-SE (dB), the total radiation attenuated (%), the intrinsic shielding properties related to the mechanisms of reflection (SE_R) and absorption (SE_A), and the reflected (R), absorbed (A) and transmitted (T) power.

Table 4.2 - EMI-SE (dB), total radiation attenuated (%), reflection (SE_R) and absorption (SE_A) mechanisms, and reflected (R), absorbed (A) and transmitted (T) power of the nanocomposites at different CNT weight fractions

CNT	**Matrix and molding method**	**SE (dB)**	**%**	**SER (dB)**	**SEA (dB)**	**R**	**A**	**T**
0 wt%	SEBS extrusion	1.35	26.20	0.49	0.86	0.1076	0.1544	0.7380
	SEBS compression	1.36	26.33	0.47	0.89	0.1017	0.1616	0.7367
	SEBS-MA extrusion	1.68	31.64	0.54	1.14	0.1156	0.2007	0.6836
	SEBS-MA compression	1.05	21.17	0.37	0.68	0.0819	0.1298	0.7883
2 wt%	SEBS extrusion	8.12	84.33	2.34	5.78	0.4153	0.4280	0.1567
	SEBS compression	16.52	97.76	3.11	13.41	0.5104	0.4672	0.0224
	SEBS-MA extrusion	6.61	77.96	2.77	3.84	0.4699	0.3097	0.2204

	SEBS-MA compression	10.50	90.98	3.65	6.85	0.5661	0.3438	0.0901
3 wt%	SEBS extrusion	18.15	98.46	4.22	13.93	0.6182	0.3664	0.0154
	SEBS compression	19.13	98.77	3.48	15.64	0.5497	0.4380	0.0123
	SEBS-MA extrusion	15.12	96.90	3.44	11.68	0.5427	0.4263	0.0310
	SEBS-MA compression	15.54	97.17	3.56	11.97	0.5567	0.4150	0.0283
5 wt%	SEBS extrusion	29.37	99.88	5.11	24.26	0.6890	0.3098	0.0012
	SEBS compression	31.67	99.93	4.97	26.70	0.6788	0.3205	0.0007
	SEBS-MA extrusion	17.87	98.36	3.95	13.92	0.5943	0.3893	0.0164
	SEBS-MA compression	23.09	99.50	4.94	18.15	0.6755	0.3195	0.0049
8 wt%	SEBS extrusion	46.52	99.998	5.48	41.04	0.7137	0.2863	2.24E-05
	SEBS compression	56.73	99.9996	6.09	50.64	0.7491	0.2509	3.44E-06
	SEBS-MA extrusion	31.09	99.92	5.35	25.74	0.7046	0.2946	0.0008
	SEBS-MA compression	46.36	99.998	6.52	39.85	0.7731	0.2268	2.35E-05

As presented in Table 4.2, the electromagnetic shielding behavior of the different nanocomposites proved to be dependent on the presence of MA in the matrix and on the molding technique used. However, the molding method, and the consequent CNT alignment

inside the matrix, provided a more significant effect on the results. Much like the AC conductivity results, the EMI-SE increased according to the following order: SEBS-MA/CNT prepared by extrusion < SEBS/CNT prepared by extrusion < SEBS-MA/CNT prepared by compression molding < SEBS/CNT prepared by compression molding. The maximum effectiveness achieved by the SEBS/CNT nanocomposite prepared by compression molding was 56.73 dB, which represents an attenuation of 99.9996% of the incident radiation.

4.3.5. Electromagnetic shielding effectiveness vs. mechanical properties

The nanocomposites of SEBS/CNT prepared by extrusion and compression molding, and SEBS-MA/CNT prepared by compression molding with 5 wt% of CNT, as well as all nanocomposites with 8 wt% of CNT loading, presented a suitable EMI-SE (> 20 dB). However, for an elastomeric material to be used commercially, other parameters, such as the mechanical properties, must also be considered. Figure 4.9 shows a comparison of the EMI-SE and the tensile strength at break of the different nanocomposites.

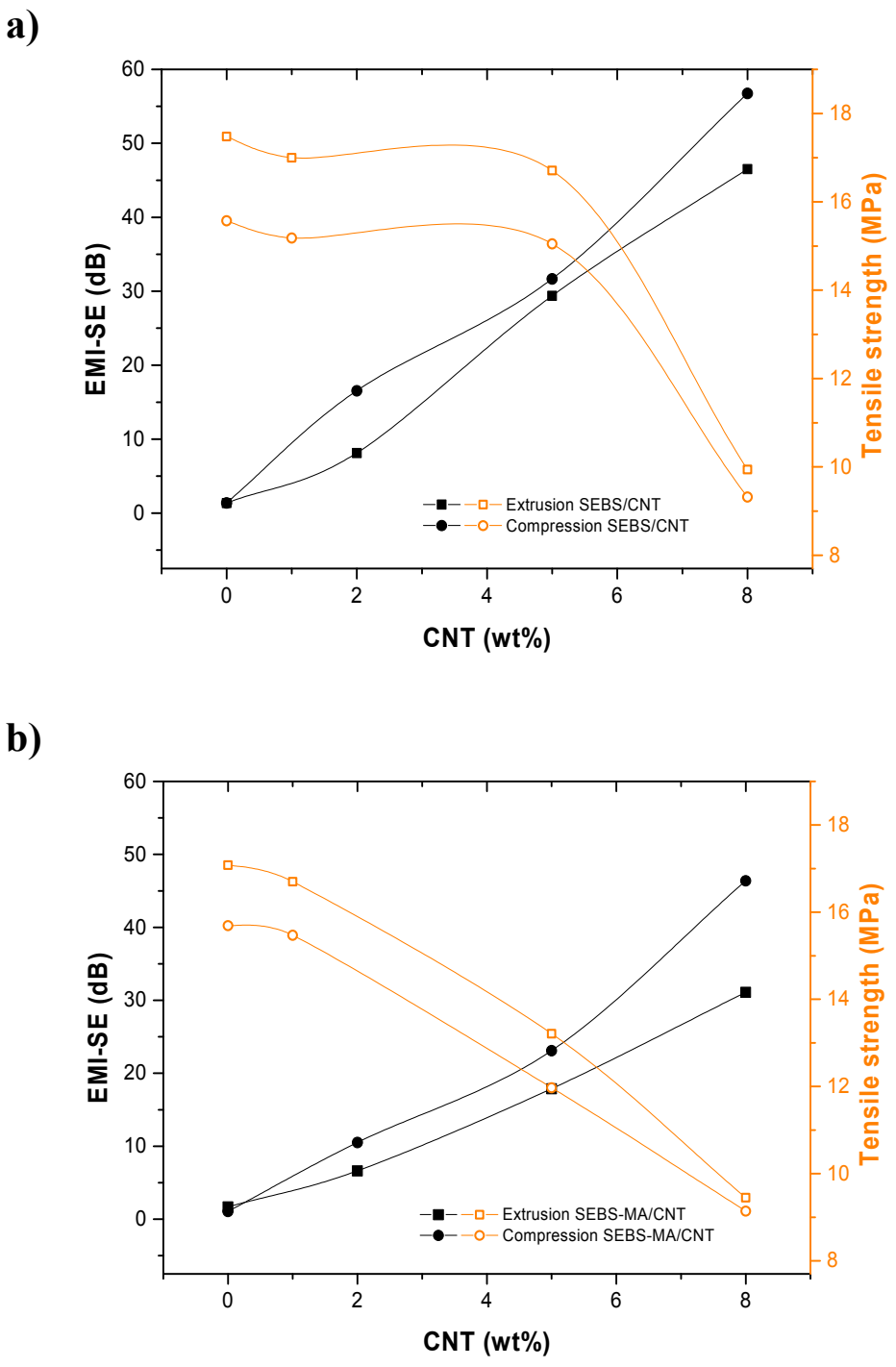

Figure 4.9 - Comparison of the EMI-SE and the tensile strength at break of the a) SEBS/CNT nanocomposites prepared by extrusion and compression molding, and b) SEBS-MA/CNT prepared by extrusion and compression molding at different CNT weight fractions

Clicours.com

As presented in Figure 4.9, although all the nanocomposites with 8 wt% of CNT loading exhibited a very high EMI-SE, the tensile strength at break decreased substantially. However, for the SEBS/CNT nanocomposites with 5 wt% of CNT loading prepared by both molding techniques, the decreases in tensile strength (Figure 9-a), as well as the elongation at break (section 4.3.3), were much less significant, while the EMI-SE remained higher than 20 dB.

In our approach, results showed excellent balances between EMI-SE, mechanical properties and processability as compared to other carbon-based flexible EMI shielding materials presented in the literature. Tanrattanakul and coworkers (2007) prepared composites of natural rubber (NR), epoxidized natural rubber (ENR), and chlorosulfonated polyethylene (CSM) filled with CB in a two-roll mill followed by the vulcanization process in a hot press. The EMI-SE of the ECEs filled with 50 phr of CB reached 18–28 dB in the 8-12 GHz frequency range. However, despite the suitable EMI-SE, results showed that the mechanical properties of the composites suffered a dramatic decrease as compared to the neat rubbers, due to the large amount of additive used. The tensile strength ranged between ≈ 15-19 MPa, and materials were stretchable ≈ 2-4 times their original length before breaking (Tanrattanakul & Bunchuay, 2007). In another work, Yuto Kato et al. (2017) prepared thin films (0.2 mm) of fluorinated rubber and "super-growth" CNTs (SG-CNTs) by solution casting. Results showed that the material presented suitable EMI-SE for commercial applications (>20 dB, attenuation of 90% of the incident radiation) at the 5.5-10 GHz frequency range with SG-CNT loading of 1 wt%. Furthermore, the tensile strength at break was 6.4 MPa and the material was flexible and stretchable to double its original length without cracking. According to the authors, their material presented a higher mechanical strength and stretchability than commercialized generic rubbers for EMI shielding (Kato et al., 2017).

In the present work, the SEBS/CNT nanocomposite with 5 wt% of CNT loading (2 mm thick) prepared by melt compounding followed by extrusion molding presented an EMI-SE of ≈ 30 dB (≈ attenuation of 99.9 % of the incident radiation) at the 8-12 GHz frequency range, a tensile strength at break of 16.7 MPa, and were stretchable to more than 5 times its original

length without cracking. Therefore, this nanocomposite can be successfully used as a flexible EMI shielding material in applications such as gaskets and device coatings.

4. Conclusions

Nanocomposites of SEBS/CNT and SEBS-MA presented different morphologies and properties depending on the presence of MA, the molding technique used, and the CNT loading amount. The presence of MA makes the matrix more fluid, which somewhat affects the dispersion and distribution of CNT. However, no MA-CNT interactions were observed, and, consequently, the effect of MA on the properties of the nanocomposites was small. On the other hand, in general, the molding process and the CNT loading amount presented significant results. The set of results from different characterization techniques clearly showed that the extrusion process induced an alignment of CNT inside the matrices. For all the nanocomposites, the AC electrical conductivity increased as the CNT loading increased. However, for the samples prepared by extrusion, the CNT-CNT connections were hindered due to the alignment of CNT and, consequently, higher loadings were necessary to get the CNT close enough to conduct electricity as compared to the samples with random orientation prepared by compression molding. Consequently, samples with 1wt% of CNT prepared by compression molding presented a higher electrical conductivity than nanocomposites prepared by extrusion with 3 times this CNT loading amount. For all the nanocomposites, the addition of CNT increased the Young's modulus and stress at 100%, whereas they decreased the tensile strength and the elongation at break. The amount of CNT had a greater influence on the mechanical behavior of the nanocomposites than the processing methods. Decreases in the tensile strength and in the elongation at break were notably dramatic for the samples with 8 wt% of CNT, once the matrices became more brittle. Concerning the shielding properties, the SEBS/CNT nanocomposite with 8 wt% of CNT loading prepared by compression molding achieved a very high EMI-SE of 56.73 dB, which represents an attenuation of 99.9996% of the incident radiation. However, the combination of different results plainly demonstrated that the SEBS/CNT nanocomposite with 5 wt% of CNT loading prepared by melt compounding followed by extrusion presented an outstanding balance between shielding effectiveness,

mechanical properties and processability. Therefore, it can be concluded that the latter can be successfully used as a flexible high performance EMI shielding material.

Acknowledgements

The authors gratefully acknowledge the financial support of the Natural Sciences and Engineering Research Council of Canada (NSERC), Conselho Nacional de Desenvolvimento Científico e Tecnológico – CNPq, Coordenação de Aperfeiçoamento de Pessoal de Ensino Superior – CAPES, and Fundação de Amparo à Pesquisa e Inovação do Estado de Santa Catarina – FAPESC. We are also truly grateful to Professor Dr. Uttandaraman Sundararaj and Dr. Mohammad Arjmand from the University of Calgary for the EMI shielding analysis.

CHAPTER 5

DISCUSSION

This chapter summarizes the main findings of each article exposed in chapters 2 to 4. Some observations are also presented.

5.1 Summary of the main results

This thesis investigated the relationship between structure, properties, processing, and performance of carbon-based thermoplastic elastomer nanocomposites prepared by different compounding techniques for the development an efficient flexible EMI shielding material. Besides the two different carbon nanoadditives, CNT and GnP, and the two post-processing, extrusion and compression molding, three different commercial grades of SEBS with styrene/rubber ratio of 30/70 were used in this study. The SEBS matrices were SEBS Kraton G1650 (melt index <1 g/10 min (230°C, 5kg)) used in the first and second phases of the project, and SEBS Kraton G1652 (melt index 5 g/10 min (230°C, 5kg)) and SEBS-MA Kraton FG1901 (melt index 22 g/10 min (230°C, 5kg)) used in the third phase of the project. The differences on melt index are related to the molecular weight of the three matrices, and the presence of MA. Results showed that all the different aspects involved in this work affected the final morphology, properties and performance of the nanocomposites.

i) In the first phase (chapter 2), nanocomposites were prepared by melt compounding followed by compression molding. CNT were properly dispersed into the SEBS matrix without significantly damaging their structure. SEBS/CNT nanocomposites exhibited non-covalent π-π interactions between CNT and the aromatic rings of the matrix. SEBS/CNT presented a low electrical percolation threshold of around 1 wt. % of CNT. The maximum electrical conductivity, reached for the sample with 8 wt% of CNT, was around 1 $S.cm^{-1}$, which was 17 orders of magnitude higher than the conductivity of the neat SEBS. For samples with higher CNT loading amounts

the electrical conductivity leveled off. Regarding the EMI shielding performance, experimental results showed to be higher than the theoretical predicted values. For the sample with 15 wt% of CNT, EMI-SE was 30.07dB, which corresponded to a reduction of 99.9% of the incident radiation in the frequency range of 8-12 GHz. In this frequency range, real and imaginary permittivity increased as the CNT weight fractions were enhanced. For the nanocomposites with 15 wt% of CNT, ε" was higher than ε', which indicated that from this point, mobile charge dissipation was more efficient because of the higher number of conductive paths formed throughout the sample.

ii) In the second part of the project (chapter 3), SEBS/GnP and hybrid SEBS/GnP/CNT nanocomposites were prepared using the same processing techniques as the ones employed in the first part. Morphologies, properties and shielding performances of the different nanocomposites were compared among themselves and the shielding properties were also compared to the results obtained by the SEBS/CNT nanocomposites prepared in the first phase of this work. The morphological characterization showed that GnP was non-homogeneous, showing to be a mixture of multi-walled graphene and expanded graphite. SEBS/GnP nanocomposites did not exhibit non-covalent interactions between GnP and the SEBS. GnP presented decent distribution throughout the matrix, however it was not possible to properly disperse the GnP particles into the matrix by melt compounding with the processing parameters used in this work. For the SEBS/GnP nanocomposites, the maximum electrical conductivity achieved with 15 wt.% of GnP was 2.6E-7 $S.cm^{-1}$. For SEBS/GnP/CNT samples with 2/8 wt.% of GnP/CNT (with a total of 10 wt.% of carbon nanoadditives) the electrical conductivity was 1.4 $S.cm^{-1}$. For the hybrid nanocomposites with CNT loading equal to or higher than 8 wt.%, the conductivity leveled off. Concerning the shielding properties, the maximum EMI-SE for SEBS/GnP nanocomposites was 8.63 dB reached by the sample with 15 wt% of GNP. For all SEBS/GnP samples ε' were higher than ε". For the hybrid SEBS/GnP/CNT nanocomposite at the absolute loading fraction of

15 wt.% of carbon nanoadditives, in a portion of 5/10 wt.% of GnP/CNT, the EMI-SE was 36.47dB, which represents an attenuation of 99.98% of the incident radiation. For the sample with 7/3 wt.% of GnP/CNT (with a total of 10 wt.% of carbon nanoadditives), $\varepsilon' > \varepsilon''$; for the 5/5 wt.% (with a total of 10 wt.% of carbon nanoadditives), $\varepsilon' \approx \varepsilon''$; and for the nanocomposites with higher CNT loading, $\varepsilon' < \varepsilon''$. These results pointed out that for samples with CNT loading amounts higher than 8 wt% a higher number of paths was formed in the conductive network, which resulted in an increase in energy dissipation. These results are in agreement to the results of electrical conductivity, and justified the higher EMI-SE of the hybrid nanocomposites compared to the SEBS/GnP nanocomposites. Comparing the properties of SEBS/GnP, SEBS/GnP/CNT, and SEBS/CNT (from the first part of the project), results indicated synergic effects between CNT and GnP regarding shielding effectiveness for the nanocomposites where CNT >> GnP. The synergism was evidenced by the fact that the EMI-SE of the hybrid nanocomposites of SEBS/GnP/CNT were higher than the sum of the EMI-SE of the single nanocomposites of SEBS/GnP and SEBS/CNT with the same total amount of conducting additive.

iii) In the last phase (chapter 4), nanocomposites of SEBS/CNT and SEBS-MA/CNT were prepared by melt compounding followed by two different post-processing, extrusion and compression molding. The nanocomposites presented different morphologies and properties depending on the amount of CNT, presence of MA, and the molding technique used. Regarding the samples of SEBS grafted maleic anhydride, no MA-CNT interactions were observed, and, consequently, the effect of MA on the properties of the nanocomposites was small. However, the presence of MA makes the matrix more fluid, which somewhat affects the dispersion and distribution of CNT. For all the nanocomposites AC electrical conductivity increased as the CNT loading increased. The presence of MA affected the electrical properties of the nanocomposites slightly. On the other hand, the effect of the molding technique in the conductivity of the nanocomposites were very strong.

Nanocomposites prepared by compression molding presented much higher AC electrical conductivity, as well as lower electrical percolation threshold. The different behaviours regarding the processing methods can be explained considering that the extrusion process induced an alignment of the CNT along the flow direction. Whereas, for the nanocomposites prepared by compression molding the CNT were randomly distributed. Due to this random distribution, the formation of CNT-CNT connections throughout the material was favored with lower CNT loading amount. As a consequence, nanocomposites with 1wt% of CNT prepared by compression molding presented higher electrical conductivity than samples prepared by extrusion with 3 times this CNT loading amount. For nanocomposites with 8 wt% of CNT the values levelled off, suggesting a saturation of the system related to the AC electrical conductivity. Regarding the mechanical properties, the effect of the molding technique used was not substantial. The presence of MA modifies the flow index which, consequently, affected the distribution and alignment of CNT in the nanocomposites, and all the SEBS-MA/CNT nanocomposites presented lower Young`s modulus, stress at 100%, tensile strength, and elongation at break than the SEBS/CNT nanocomposites. The effect of CNT loading amount was very strong, and for all the nanocomposites the addition of CNT increased the Young`s modulus and stress at 100%, whereas decreased the tensile strength and elongation at break. The decreases on the tensile strength and elongation at break were notably dramatic for the samples with 8 wt% of CNT, once the matrices became more brittle. In respect to shielding properties, the EMI-SE of the nanocomposites presented similar behaviour to the AC electrical conductivity and the higher effectiveness followed the order: SEBS-MA/CNT prepared by extrusion < SEBS/CNT prepared by extrusion < SEBS-MA/CNT prepared by compression molding < SEBS/CNT prepared by compression molding. The higher EMI-SE, achieved by the SEBS/CNT prepared by compression molding with 8 wt% of CNT, was very remarkable, reaching 56.73 dB that represents an attenuation of 99.9996% of the incident radiation. However, as a final point, the combination of the different results demonstrated that the SEBS/CNT with 5 wt%

of CNT loading prepared by melt compounding followed by extrusion presented an outstanding balance between shielding effectiveness, mechanical properties and processability. Therefore, the latter can be successfully used as a flexible high performance EMI shielding material.

ClicCours.com

CONCLUSION AND RECOMENDATIONS

This chapter presents the general conclusion and some recommendations for future work.

6.1 Conclusions

In this work carbon-based thermoplastic elastomer nanocomposites were obtained and studied regarding the correlation between their structures, properties, melt processing methods, and performances for EMI shielding applications. The nanocomposites presented different morphologies and properties depending on the type and amount of conducting additive, presence of MA, and the processing conditions used. The dispersion and distribution of the conducting additives in the polymeric matrix, as well as the additive-matrix interactions strongly influenced the formation of the electrically conducting network and the EMI shielding properties of the nanocomposites. It was found that hybrid nanocomposites of different carbon nanoparticles resulted in synergic effects regarding EMI shielding. Results pointed out that special attention must be given to the loading amount of carbon additives, once from a certain amount of carbon additives in the polymer matrices, the mechanical properties of the nanocomposites suffered a drastic decrease. Over the course of the development of the project, different aspects combined showed that it was possible to obtain materials with outstanding balances between shielding effectiveness, mechanical properties, and processability. Therefore, it can be concluded that some nanocomposites prepared in this work have great potential as high performance flexible EMI shielding materials.

6.2 Recommendations

In order to extend the findings of this work, and consolidate and expand the range of applications of the flexible EMI shielding materials prepared, many additional studies might be worth investigation. Suggestions for further research procedures are listed bellow.

Clicours.COM

i) Evaluate the molecular weight of the different commercial grades of SEBS by Gel Permeation Chromatography (GPC) and characterize the microstructure of the neat matrices and nanocomposites by Transmission Electron Microscope (TEM) and Small Angle X-ray scattering (SAXS) in order to deeper understand the influence of the morphology of these materials in their key properties for EMI shielding applications.

ii) Characterize the mechanical properties concerning compression set, resilience, tear resistance, abrasion resistance, adhesion peel, and hardness, and investigate the aging effects on the properties of the nanocomposites, for better estimate potential applications of the nanocomposites as EMI shielding coating and EMI shielding gaskets.

iii) Investigate the properties of carbon-filled nanocomposites based on SEBS with different PS/rubber ratios for preparing an ample class of EMI shielding materials with the suitable properties to satisfy a wider range of applications.

iv) Characterize the EMI shielding properties at different frequency bands in order to analyse the possibility of using the nanocomposites in a wide frequency range.

v) Prepare SEBS/CNT and SEBS/GnP multi-layer nanocomposites with a gradient morphology by an additive manufacturing technique as an attempt for better controlling and tailoring the morphology and the critical properties for EMI shielding materials.

APPENDIX I

LIST OF SOME COMPANIES THAT PRODUCE AND COMMERCIALIZE MATERIALS FOR EMI SHIELDING

- 3M

http://www.3m.com

- Chomerics

https://www.chomerics.com

- Comtest engineering B.V.

http://www.comtest.eu/products/anechoic-chambers/absorbers.html

- Creavac-creative Vakuumbeschichtung GmbH

http://www.creavac.de

- DEM Manufacturing

http://www.dem-uk.com

- ERA Technology LTD.

www.era.co.uk

- ETS-Lindgren

http://www.ets-lindgren.com

- HEICO Corporation

http://www.heico.com

- HITEK Electronic Materials Ltd

https://www.hitek-ltd.co.uk

- Kemtron Ltd

http://www.kemtron.co.uk

- KITAGAWA Industries Co., LTD (KG)

http://kgs-ind.com/products/emc

- Laird Plc.

http://www.laird-plc.com

- Leader Tech

https://leadertechinc.com

- Marktek Inc.

http://www.marktek-inc.com

- NTD Shielding Services Ltd

http://www.ntdshielding.co.uk

- Omega Shielding Products

http://www.omegashielding.com

- RTP Company

https://www.rtpcompany.com

- Schaffner Group

https://www.schaffner.com

- Schlegel Electronic Materials

http://www.schlegelemi.com/en/index.php

- Tech-Etch, Inc.

http://www.tech-etch.com

APPENDIX II

VITA

EDUCATION

- Dual-degree Doctorate - Doctor in Materials Science and Engineering from Federal University of Santa Catarina (UFSC), Florianopolis, BR, and Doctor of Philosophy from École de technologie supérieure (ÉTS), Montreal, CA. Supervisors: Prof. Guilherme Mariz de Oliveira Barra (UFSC) and Prof. Nicole Raymonde Demarquette (ÉTS). From July 2013 to December 2017.

- Master in Materials Science and Engineering –Federal University of Santa Catarina (UFSC), Florianopolis, BR. Supervisor: Prof. Guilherme Mariz de Oliveira Barra. From July 2011 to July 2013.

- Specialist in Science Education (Graduate Certificate Program) – Federal Institute of Santa Catarina (IFSC), Florianopolis, BR. Supervisor: Prof. Andreia de Bem Machado. From July 2010 to December 2011.

- Bachelor in Industrial Chemistry – University of Southern Santa Catarina (UNISUL), Tubarao, BR. From January 2004 to December 2008.

SCHOLARSHIPS AND AWARDS

- Conference travel award – Coordination for Improvement of Higher Education Staff (Coordenação de Aperfeiçoamento de Pessoal de Nível Superior - CAPES)/UFSC, BR, 2017.

- Scholarship from National Counsel of Technological and Scientific Development (Conselho Nacional de Desenvolvimento Científico e Tecnológico – CNPq), BR. From February 2013 to June 2017.

- Conference travel award – École de Technologie Supérieure (ÉTS), CA, 2016.

- Conference travel award – Society of Plastics Engineers (SPE), CA, 2016.

- Internal scholarship from ÉTS, CA, 2016

- Scholarship from Science Without Borders Program – CNPq. Internship at École de technologie supérieure, CA. From January 2005 to December 2015.

- Scholarship from CAPES, BR. From July 2013 to February 2013.

- Scholarship from CAPES, BR. From July 2011 to June 2013.

- Scholarship from Unisul Program of Scientific Initiation (Programa Unisul de Iniciação Científica – PUIC), BR. From July 2005 to June 2006.

TEACHING AND ADVISING EXPERIENCE

- Teaching Assistant – École de technologie supérieure – Structure and properties of polymers, Fall Term 2015.

- Undergraduate dissertation co-advisor – Federal University of Santa Catarina (UFSC), Florianopolis, BR. Obtaining and characterization of electricity conducting composites of poly (styrene-b-(ethylene-co-butylene)-b-styrene and carbon nanotubes for electromagnetic shielding, José Carlos Ferreira Júnior, 2015

- Member of undergraduate dissertation examining committee – Federal University of Santa Catarina (UFSC), Florianopolis, BR. Synthesis of polypyrrole in the presence of different surfactants and their use as a thermoplastic polyurethane matrix additive, Adriana Silveira, 2014.

PUBLICATIONS

Articles Submitted to Scientific Journals

- KUESTER, S.; BARRA, G. M. O.; DEMARQUETTE, N. R. Morphology, mechanical properties and electromagnetic shielding effectiveness of SEBS/CNT nanocomposites: effects of maleic anhydride, CNT loading, and processing method. Submitted to Polymer International.

Articles Published in Scientific Journals

- KUESTER, S.; DEMARQUETTE, N. R.; FERREIRA JUNIOR, J. C.; SOARES, B. G.; BARRA, G. M. O. Hybrid nanocomposites of thermoplastic elastomer and carbon nanoadditives for electromagnetic shielding. European Polymer Journal, v. 88, p. 328–339, 2017.

- KUESTER, S.; BARRA, G. M. O.; FERREIRA JUNIOR, J. C.; SOARES, B. G.; DEMARQUETTE, N. R. Electromagnetic interference shielding and electrical properties of nanocomposites based on poly (styrene-b-ethylene-ran-butylene-b-styrene) and carbon nanotubes. European Polymer Journal, v.77, p.43 -53, 2016.

clicours.com

- KUESTER, S.; MERLINI, C.; BARRA, G. M. O.; FERREIRA JUNIOR, J. C.; SOUZA, A. C.; LUCAS, A. A.; SOARES, B. G. Processing and characterization of conductive composites based on poly (styrene-b-ethylene-ran-butylene- b-styrene) (SEBS) and carbon additives: A comparative study of expanded graphite and carbon black. Composites Part B: Engineering, v.84, p.236 - 247, 2016.

- POTTMAIER, D.; MELO, C.R.; SARTOR, M.N.; KUESTER, S.; AMADIO, T.M.; FERNANDES, C.A.H.; MARINHA, D.; ALARCON, O.E. The Brazilian energy matrix: From a materials science and engineering perspective. Renewable & Sustainable Energy Reviews, v.19, p.678 - 691, 2013.

- KUESTER, S.; Pottmaier, D; Machado, A. B.; Alarcon, O. E. Conectividade na construção de conhecimentos: adequação da grade curricular no curso de engenharia de materiais. Revista Gestao Universitaria na America Latina - GUAL. , v.4, p.195 - 207, 2012.

CONFERENCE PRESENTATIONS

- KUESTER, S.; BARRA, G. M. O.; DEMARQUETTE, N. R. Nanocomposites of SEBS/CNT for electromagnetic shielding: effect of processing method and maleic anhydride. Oral presentation delivered at the ANTEC Anaheim, USA, 2017.

- KUESTER, S.; BARRA, G. M. O.; DEMARQUETTE, N. R. Electrically conductive polymer nanocomposites based on poly(styrene-b-(ethylene-co-butylene)-b- styrene) and carbon nanoadditives for electromagnetic shielding. Polymer Processing Society Conference Abstracts, p.17., 2015. Oral presentation delivered at the Polymer Processing Society Conference Graz, Austria, 2015.

- KUESTER, S.; BARRA, G. M. O.; DEMARQUETTE, N. R. Hybrid nanocomposites based on poly (styrene-b-(ethylene-cobutylene)-b-styrene)/carbon nanotubes/graphene for electromagnetic shielding. Graphene & 2D Materials International Conference and Exhibition Abstracts. Poster presentation delivered at the Graphene & 2D Materials International Conference and Exhibition, Montreal, Canada, 2015.

- KUESTER, S.; SOUZA, A. C.; LUCAS, A. A.; BARRA, G. M. O. Electrical percolation and rheology of polymeric composites of poly (styrene-b-(ethylene-cobutylene)-b-styrene) and expanded graphite and conductive carbon black. Latin American Symposium on Polymers/XII Ibero American Congress on Polymers Abstracts. Poster presentation delivered at the XIV Latin American Symposium on Polymers/XII Ibero American Congress on Polymers, Porto de Galinhas, Brazil, 2014.

- KUESTER, S.; LUCAS, A. A.; SOARES, B. G.; BARRA, G. M. O. Preparation and characterization of composites of poly (styrene-b-(ethylene-cobutylene)-b-styrene and expanded graphite and conductive carbon black. 12° Congresso Brasileiro de Polímeros Abstracts. Poster presentation delivered at the 12° Congresso Brasileiro de Polímeros, Florianópolis, Brazil, 2013.

MISCELLANEOUS

- Article published in a scientific magazine - Interactive platform KUESTER, S.; BARRA, G. M. O.; DEMARQUETTE, N. R. Did you Know that your Mobile Devices Cause Electromagnetic Interference? Substance – ÉTS, CA, 2015.

Clicours.COM

- Affiliation

Member of Society of Plastics Engineers (SPE)

- Personal interests

Nanotechnology, electromagnetic shielding, energy storage, mechanical sensors…

LIST OF BIBLIOGRAPHICAL REFERENCES

Abraham, J., Arif P, M., Xavier, P., Bose, S., George, S. C., Kalarikkal, N., & Thomas, S. (2017). Investigation into dielectric behaviour and electromagnetic interference shielding effectiveness of conducting styrene butadiene rubber composites containing ionic liquid modified MWCNT. *Polymer, 112*, 102-115. doi: http://dx.doi.org/10.1016/j.polymer.2017.01.078

Al-Hartomy, O. A., Al-Ghamdi, A. A., Al-Solamy, F. R., Dishovsky, N., Slavcheva, D., Iliev, V., & El-Tantawy, F. (2013). Dielectric and microwave properties of natural rubber-based composites tailored by the fillers specific features. *Proceedings of the Institution of Mechanical Engineers, Part L: Journal of Materials: Design and Applications, 227*(2), 168-176. doi: doi:10.1177/1464420712463850

Al-Hartomy, O. A., Al-Solamy, F., Al-Ghamdi, A., Dishovsky, N., Iliev, V., & El-Tantawy, F. (2011). Dielectric and Microwave Properties of Siloxane Rubber/Carbon Black Nanocomposites and Their Correlation. *International Journal of Polymer Science, 2011*, 7. doi: 10.1155/2011/837803

Al-Saleh, M. H., Gelves, G. A., & Sundararaj, U. (2011). Copper nanowire/polystyrene nanocomposites: Lower percolation threshold and higher EMI shielding. *Composites Part A: Applied Science and Manufacturing, 42*(1), 92-97. doi: http://dx.doi.org/10.1016/j.compositesa.2010.10.003

Al-Saleh, M. H., & Saadeh, W. H. (2013). Hybrids of conductive polymer nanocomposites. *Materials & Design (1980-2015), 52*, 1071-1076. doi: http://dx.doi.org/10.1016/j.matdes.2013.06.072

Al-Saleh, M. H., Saadeh, W. H., & Sundararaj, U. (2013). EMI shielding effectiveness of carbon based nanostructured polymeric materials: A comparative study. *Carbon, 60*(0), 146-156. doi: http://dx.doi.org/10.1016/j.carbon.2013.04.008

Al-Saleh, M. H., & Sundararaj, U. (2009). Electromagnetic interference shielding mechanisms of CNT/polymer composites. *Carbon, 47*(7), 1738-1746. doi: http://dx.doi.org/10.1016/j.carbon.2009.02.030

Alig, I., Pötschke, P., Lellinger, D., Skipa, T., Pegel, S., Kasaliwal, G. R., & Villmow, T. (2012). Establishment, morphology and properties of carbon nanotube networks in polymer melts. *Polymer, 53*(1), 4-28. doi: http://dx.doi.org/10.1016/j.polymer.2011.10.063

Alig, I., Skipa, T., Lellinger, D., & Pötschke, P. (2008). Destruction and formation of a carbon nanotube network in polymer melts: Rheology and conductivity spectroscopy. *Polymer, 49*(16), 3524-3532. doi: http://dx.doi.org/10.1016/j.polymer.2008.05.037

Aloia, A. G. D., Marra, F., Tamburrano, A., Bellis, G. D., & Sarto, M. S. (2013, 2-6 Sept. 2013). *Synthesis and characterization of graphene-based nanocomposites for EM shielding applications.* Paper presented at the 2013 International Symposium on Electromagnetic Compatibility.

Anh Son, H. (2011). Electrical conductivity and electromagnetic interference shielding characteristics of multiwalled carbon nanotube filled polyurethane composite films. *Advances in Natural Sciences: Nanoscience and Nanotechnology, 2*(2), 025007.

Anupama, J., Anil, B., Rajvinder, S., Alegaonkar, P. S., Balasubramanian, K., & Suwarna, D. (2013). Graphene nanoribbon–PVA composite as EMI shielding material in the X band. *Nanotechnology, 24*(45), 455705.

Arenhart, R. G., Barra, G. M. O., & Fernandes, C. P. (2016). Simulation of percolation threshold and electrical conductivity in composites filled with conductive particles: Effect of polydisperse particle size distribution. *Polymer Composites, 37*(1), 61-69. doi: 10.1002/pc.23155

Arjmand, M., Apperley, T., Okoniewski, M., & Sundararaj, U. (2012). Comparative study of electromagnetic interference shielding properties of injection molded versus compression molded multi-walled carbon nanotube/polystyrene composites. *Carbon, 50*(14), 5126-5134. doi: http://dx.doi.org/10.1016/j.carbon.2012.06.053

Arjmand, M., Mahmoodi, M., Gelves, G. A., Park, S., & Sundararaj, U. (2011). Electrical and electromagnetic interference shielding properties of flow-induced oriented carbon nanotubes in polycarbonate. *Carbon, 49*(11), 3430-3440. doi: http://dx.doi.org/10.1016/j.carbon.2011.04.039

Bansala, T., Joshi, M., Mukhopadhyay, S., Doong, R.-a., & Chaudhary, M. (2017). Electrically conducting graphene-based polyurethane nanocomposites for microwave shielding applications in the Ku band. *Journal of Materials Science, 52*(3), 1546-1560. doi: 10.1007/s10853-016-0449-8

Basu, S., Singhi, M., Satapathy, B. K., & Fahim, M. (2013). Dielectric, electrical, and rheological characterization of graphene-filled polystyrene nanocomposites. *Polymer Composites, 34*(12), 2082-2093. doi: 10.1002/pc.22617

Bauhofer, W., & Kovacs, J. Z. (2009). A review and analysis of electrical percolation in carbon nanotube polymer composites. *Composites Science and Technology, 69*(10), 1486-1498. doi: http://dx.doi.org/10.1016/j.compscitech.2008.06.018

Benson, V. S., Pirie, K., Schüz, J., Reeves, G. K., Beral, V., Green, J., & Collaborators, f. t. M. W. S. (2013). Mobile phone use and risk of brain neoplasms and other cancers: prospective study. *International Journal of Epidemiology*. doi: 10.1093/ije/dyt072

Bhadra, S., Singha, N. K., & Khastgir, D. (2009). Dielectric properties and EMI shielding efficiency of polyaniline and ethylene 1-octene based semi-conducting composites. *Current Applied Physics, 9*(2), 396-403. doi: http://dx.doi.org/10.1016/j.cap.2008.03.009

Bhawal, P., Ganguly, S., Das, T. K., Mondal, S., & Das, N. C. Mechanically robust conductive carbon clusters confined ethylene methyl acrylate–based flexible composites for superior shielding effectiveness. *Polymers for Advanced Technologies*, n/a-n/a. doi: 10.1002/pat.4092

Bilalis, P., Katsigiannopoulos, D., Avgeropoulos, A., & Sakellariou, G. (2014). Non-covalent functionalization of carbon nanotubes with polymers. *RSC Advances, 4*(6), 2911-2934. doi: 10.1039/C3RA44906H

Bilotti, E., Zhang, H., Deng, H., Zhang, R., Fu, Q., & Peijs, T. (2013). Controlling the dynamic percolation of carbon nanotube based conductive polymer composites by addition of secondary nanofillers: The effect on electrical conductivity and tuneable sensing

behaviour. *Composites Science and Technology, 74*(0), 85-90. doi: http://dx.doi.org/10.1016/j.compscitech.2012.10.008

Bokobza, L. (2007). Multiwall carbon nanotube elastomeric composites: A review. *Polymer, 48*(17), 4907-4920. doi: http://dx.doi.org/10.1016/j.polymer.2007.06.046

Brigandi, P. J., Cogen, J. M., & Pearson, R. A. (2014). Electrically conductive multiphase polymer blend carbon-based composites. *Polymer Engineering & Science, 54*(1), 1-16. doi: 10.1002/pen.23530

Calisi, N., Giuliani, A., Alderighi, M., Schnorr, J. M., Swager, T. M., Di Francesco, F., & Pucci, A. (2013). Factors affecting the dispersion of MWCNTs in electrically conducting SEBS nanocomposites. *European Polymer Journal, 49*(6), 1471-1478. doi: http://dx.doi.org/10.1016/j.eurpolymj.2013.03.029

Cao, M.-S., Wang, X.-X., Cao, W.-Q., & Yuan, J. (2015). Ultrathin graphene: electrical properties and highly efficient electromagnetic interference shielding. *Journal of Materials Chemistry C, 3*(26), 6589-6599. doi: 10.1039/C5TC01354B

Carastan, D. J., Amurin, L. G., Craievich, A. F., Gonçalves, M. d. C., & Demarquette, N. R. (2013). Morphological evolution of oriented clay-containing block copolymer nanocomposites under elongational flow. *European Polymer Journal, 49*(6), 1391-1405. doi: http://dx.doi.org/10.1016/j.eurpolymj.2013.02.036

Carastan, D. J., Amurin, L. G., Craievich, A. F., Gonçalves, M. d. C., & Demarquette, N. R. (2014). Clay-containing block copolymer nanocomposites with aligned morphology prepared by extrusion. *Polymer International, 63*(2), 184-194. doi: 10.1002/pi.4480

Carastan, D. J., Demarquette, N. R., Vermogen, A., & Masenelli-Varlot, K. (2008). Linear viscoelasticity of styrenic block copolymers–clay nanocomposites. *Rheologica Acta, 47*(5), 521-536. doi: 10.1007/s00397-008-0283-2

Castro Neto, A. H., Guinea, F., Peres, N. M. R., Novoselov, K. S., & Geim, A. K. (2009). The electronic properties of graphene. *Reviews of Modern Physics, 81*(1), 109-162.

Chatterjee, S., Nafezarefi, F., Tai, N. H., Schlagenhauf, L., Nüesch, F. A., & Chu, B. T. T. (2012). Size and synergy effects of nanofiller hybrids including graphene nanoplatelets and carbon nanotubes in mechanical properties of epoxy composites. *Carbon, 50*(15), 5380-5386. doi: http://dx.doi.org/10.1016/j.carbon.2012.07.021

Choudhary, V., & Gupta, A. (2011). *Polymer/Carbon Nanotube Nanocomposites*: InTech.

Chung, D. D. L. (2000). Materials for electromagnetic interference shielding. *Journal of Materials Engineering and Performance, 9*(3), 350-354. doi: 10.1361/105994900770346042

Chung, D. D. L. (2001). Electromagnetic interference shielding effectiveness of carbon materials. *Carbon, 39*(2), 279-285. doi: 10.1016/s0008-6223(00)00184-6

Coleman, J. N., Khan, U., Blau, W. J., & Gun'ko, Y. K. (2006). Small but strong: A review of the mechanical properties of carbon nanotube–polymer composites. *Carbon, 44*(9), 1624-1652. doi: http://dx.doi.org/10.1016/j.carbon.2006.02.038

Dai, H. (2002). Carbon Nanotubes: Synthesis, Integration, and Properties. *Accounts of Chemical Research, 35*(12), 1035-1044. doi: 10.1021/ar0101640

Das, N. C., Chaki, T. K., Khastgir, D., & Chakraborty, A. (2001). Electromagnetic interference shielding effectiveness of conductive carbon black and carbon fiber-filled composites based on rubber and rubber blends. *Advances in Polymer Technology, 20*(3), 226-236. doi: 10.1002/adv.1018

Das, N. C., Khastgir, D., Chaki, T. K., & Chakraborty, A. (2000). Electromagnetic interference shielding effectiveness of carbon black and carbon fibre filled EVA and NR based composites. *Composites Part A: Applied Science and Manufacturing, 31*(10), 1069-1081. doi: http://dx.doi.org/10.1016/S1359-835X(00)00064-6

Das, N. C., & Maiti, S. (2008). Electromagnetic interference shielding of carbon nanotube/ethylene vinyl acetate composites. *Journal of Materials Science, 43*(6), 1920-1925. doi: 10.1007/s10853-008-2458-8

Das, T. K., & Prusty, S. (2013). Graphene-Based Polymer Composites and Their Applications. *Polymer-Plastics Technology and Engineering, 52*(4), 319-331. doi: 10.1080/03602559.2012.751410

Demarquette, N. R., & Carastan, D. J. (2016). Rheological Behavior of Nanocomposites *Nanocomposite Materials* (pp. 233-264): CRC Press.

Demarquette, N. R., Carastan, D. Rheological Behavior of Nanocomposites.

Drobny, J. G. (2007a). 1 - Introduction *Handbook of Thermoplastic Elastomers* (pp. 1-8). Norwich, NY: William Andrew Publishing.

Drobny, J. G. (2007b). 3 - Additives *Handbook of Thermoplastic Elastomers* (pp. 13-27). Norwich, NY: William Andrew Publishing.

Drobny, J. G. (2007c). 5 - Styrenic Block Copolymers *Handbook of Thermoplastic Elastomers* (pp. 161-177). Norwich, NY: William Andrew Publishing.

El-Tantawy, F. (2005). Development of novel functional conducting elastomer blends containing butyl rubber and low-density polyethylene for current switching, temperature sensor, and EMI shielding effectiveness applications. *Journal of Applied Polymer Science, 97*(3), 1125-1138. doi: 10.1002/app.21778

El Achaby, M., Arrakhiz, F.-E., Vaudreuil, S., el Kacem Qaiss, A., Bousmina, M., & Fassi-Fehri, O. (2012). Mechanical, thermal, and rheological properties of graphene-based polypropylene nanocomposites prepared by melt mixing. *Polymer Composites, 33*(5), 733-744. doi: 10.1002/pc.22198

Electromagnetic Compatibility (EMC) Shielding Market - Global Industry Analysis, Market Size, Share, Trends, Analysis, Growth and Forecast, 2013 - 2019. Retrieved August 9th, 2017, from http://www.transparencymarketresearch.com/electromagnetic-compatibility-shielding-market.html

EMI and RFI shielding materials and technologies - a global strategic business report. (2016). Retrieved August 8th, 2017, from http://www.strategyr.com/pressMCP-7873.asp

EMI Shielding Market (Materials Type - Conductive Polymers, Conductive Coatings and Paints, Metal Shielding Products, and EMI/EMC Filters; End-use Industry - Telecommunication and IT, Healthcare, Aerospace and Defense, Automotive, and Consumer Electronics) - Global Industry Analysis, Size, Share, Growth, Trends, and Forecast 2017 - 2025. (2017). Retrieved August 9th, 2017, from http://www.transparencymarketresearch.com/emi-shielding-market.html

EMI Shielding Market by Component (EMI Shielding Tapes & Laminates, Conductive Coatings and Paints, Metal Shielding Products, Conductive Polymers, EMI Filters), Method (Radiation, Conduction), Industry (Consumer Electronics, Telecom & IT, Automotive, Healthcare, Defense & Aerospace), and Geography - Global Forecast to 2022. (2017). Retrieved August 8th, 2017, from

http://www.marketsandmarkets.com/Market-Reports/emi-shielding-market-105681800.html

EMI Shielding Materials - Global Market Outlook (2017-2023). (2017). Retrieved August 9th, 2017, from http://www.strategymrc.com/report/emi-shielding-materials-market

EMI/RFI: Materials and Technologies. (2016). Retrieved August 9th, 2017, from https://www.electronics.ca/store/emi-rf-shielding-technologies-and-markets.html

Erik, T. T., & Tsu-Wei, C. (2002). Aligned multi-walled carbon nanotube-reinforced composites: processing and mechanical characterization. *Journal of Physics D: Applied Physics, 35*(16), L77.

Estrada Moreno, I. A., Díaz Diaz, A., Mendoza Duarte, M. E., & Ibarra Gómez, R. (2009). Strain Effect on the Electrical Conductivity of CB/SEBS and GP/SEBS Composites. *Macromolecular Symposia, 283–284*(1), 361-368. doi: 10.1002/masy.200950943

Fang, L., Wei, M., Shang, Y., Jimenez, L., Kazmer, D., Barry, C., & Mead, J. (2009). Surface morphology alignment of block copolymers induced by injection molding. *Polymer, 50*(24), 5837-5845. doi: http://dx.doi.org/10.1016/j.polymer.2009.09.013

Fletcher, A., Gupta, M. C., Dudley, K. L., & Vedeler, E. (2010). Elastomer foam nanocomposites for electromagnetic dissipation and shielding applications. *Composites Science and Technology, 70*(6), 953-958. doi: http://dx.doi.org/10.1016/j.compscitech.2010.02.011

Fujigaya, T., & Nakashima, N. (2015). Non-covalent polymer wrapping of carbon nanotubes and the role of wrapped polymers as functional dispersants. *Science and Technology of Advanced Materials, 16*(2), 024802. doi: 10.1088/1468-6996/16/2/024802

Gargama, H., Thakur, A. K., & Chaturvedi, S. K. (2016). Polyvinylidene fluoride/nanocrystalline iron composite materials for EMI shielding and absorption applications. *Journal of Alloys and Compounds, 654*, 209-215. doi: http://dx.doi.org/10.1016/j.jallcom.2015.09.059

Geetha, S., Satheesh Kumar, K. K., Rao, C. R. K., Vijayan, M., & Trivedi, D. C. (2009). EMI shielding: Methods and materials—A review. *Journal of Applied Polymer Science, 112*(4), 2073-2086. doi: 10.1002/app.29812

Gelves, G. A., Al-Saleh, M. H., & Sundararaj, U. (2011). Highly electrically conductive and high performance EMI shielding nanowire/polymer nanocomposites by miscible mixing and precipitation. *Journal of Materials Chemistry, 21*(3), 829-836. doi: 10.1039/C0JM02546A

Genuis, S. J. (2008). Fielding a current idea: exploring the public health impact of electromagnetic radiation. *Public Health, 122*(2), 113-124. doi: http://dx.doi.org/10.1016/j.puhe.2007.04.008

Gherardini, L., Ciuti, G., Tognarelli, S., & Cinti, C. (2014). Searching for the Perfect Wave: The Effect of Radiofrequency Electromagnetic Fields on Cells. *International Journal of Molecular Sciences, 15*(4), 5366-5387. doi: 10.3390/ijms15045366

Ghosh, P., & Chakrabarti, A. (2000). Conducting carbon black filled EPDM vulcanizates: assessment of dependence of physical and mechanical properties and conducting character on variation of filler loading. *European Polymer Journal, 36*(5), 1043-1054. doi: https://doi.org/10.1016/S0014-3057(99)00157-3

Göldel, A., Marmur, A., Kasaliwal, G. R., Pötschke, P., & Heinrich, G. (2011). Shape-Dependent Localization of Carbon Nanotubes and Carbon Black in an Immiscible

Polymer Blend during Melt Mixing. *Macromolecules, 44*(15), 6094-6102. doi: 10.1021/ma200793a

Gooch, J. W., & Daher, J. K. (2007). EMI Gaskets *Electromagnetic Shielding and Corrosion Protection for Aerospace Vehicles* (pp. 103-106). New York, NY: Springer New York.

Grigorescu, R. M., Ciuprina, F., Ghioca, P., Ghiurea, M., Iancu, L., Spurcaciu, B., & Panaitescu, D. M. (2016). Mechanical and dielectric properties of SEBS modified by graphite inclusion and composite interface. *Journal of Physics and Chemistry of Solids, 89*, 97-106. doi: http://doi.org/10.1016/j.jpcs.2015.10.008

Guanghua, G., Tahir, Ç., & William, A. G., III. (1998). Energetics, structure, mechanical and vibrational properties of single-walled carbon nanotubes. *Nanotechnology, 9*(3), 184.

Gupta, T. K., Singh, B. P., Dhakate, S. R., Singh, V. N., & Mathur, R. B. (2013). Improved nanoindentation and microwave shielding properties of modified MWCNT reinforced polyurethane composites. *Journal of Materials Chemistry A, 1*(32), 9138-9149. doi: 10.1039/C3TA11611E

Gupta, T. K., Singh, B. P., Teotia, S., Katyal, V., Dhakate, S. R., & Mathur, R. B. (2013). Designing of multiwalled carbon nanotubes reinforced polyurethane composites as electromagnetic interference shielding materials. *Journal of Polymer Research, 20*(6), 169. doi: 10.1007/s10965-013-0169-6

Han, M., & Deng, L. (2011). High Frequency Properties of Carbon Nanotubes and Their Electromagnetic Wave Absorption Properties. *Carbon Nanotubes Applications on Electron Devices*, 299-314. doi: 10.5772/16629

Hardell, L., & Sage, C. (2008). Biological effects from electromagnetic field exposure and public exposure standards. *Biomedicine & Pharmacotherapy, 62*(2), 104-109. doi: http://dx.doi.org/10.1016/j.biopha.2007.12.004

Heaney, M. B. (1999). *The Measurement, Instrumentation and Sensors Handbook* Crc Press

Helal, E., Demarquette, N. R., Amurin, L. G., David, E., Carastan, D. J., & Fréchette, M. (2015). Styrenic block copolymer-based nanocomposites: Implications of nanostructuration and nanofiller tailored dispersion on the dielectric properties. *Polymer, 64*, 139-152. doi: http://dx.doi.org/10.1016/j.polymer.2015.03.026

Hoenlein, W., Kreupl, F., Duesberg, G. S., Graham, A. P., Liebau, M., Seidel, R., & Unger, E. (2003). Carbon nanotubes for microelectronics: status and future prospects. *Materials Science and Engineering: C, 23*(6), 663-669. doi: http://dx.doi.org/10.1016/j.msec.2003.09.153

Holden, G. (2000). Thermoplastic Elastomers *Kirk-Othmer Encyclopedia of Chemical Technology*: John Wiley & Sons, Inc.

Hossmann, K. A., & Hermann, D. M. (2003). Effects of electromagnetic radiation of mobile phones on the central nervous system. *Bioelectromagnetics, 24*(1), 49-62. doi: 10.1002/bem.10068

Huang, J.-C. (1995). EMI shielding plastics: A review. *Advances in Polymer Technology, 14*(2), 137-150. doi: 10.1002/adv.1995.060140205

International Electrotechnical Commission. Retrieved February 7, 2016, from http://www.iec.ch/

Jalali, M., Dauterstedt, S., Michaud, A., & Wuthrich, R. (2011). Electromagnetic shielding of polymer–matrix composites with metallic nanoparticles. *Composites Part B:*

Engineering, 42(6), 1420-1426. doi: http://dx.doi.org/10.1016/j.compositesb.2011.05.018

Jalali, M., Molière, T., Michaud, A., & Wuthrich, R. (2013). Multidisciplinary characterization of new shield with metallic nanoparticles for composite aircrafts. *Composites Part B: Engineering, 50*, 309-317. doi: http://dx.doi.org/10.1016/j.compositesb.2013.02.043

Jana, P. B., Mallick, A. K., & De, S. K. (1991). Electromagnetic interference shielding by carbon fibre-filled polychloroprene rubber composites. *Composites, 22*(6), 451-455. doi: http://dx.doi.org/10.1016/0010-4361(91)90204-T

Jia, L.-C., Yan, D.-X., Cui, C.-H., Jiang, X., Ji, X., & Li, Z.-M. (2015). Electrically conductive and electromagnetic interference shielding of polyethylene composites with devisable carbon nanotube networks. *Journal of Materials Chemistry C, 3*(36), 9369-9378. doi: 10.1039/C5TC01822F

Joseph, N., & Thomas Sebastian, M. (2013). Electromagnetic interference shielding nature of PVDF-carbonyl iron composites. *Materials Letters, 90*, 64-67. doi: http://dx.doi.org/10.1016/j.matlet.2012.09.014

Kato, Y., Horibe, M., Ata, S., Yamada, T., & Hata, K. (2017). Stretchable electromagnetic-interference shielding materials made of a long single-walled carbon-nanotube-elastomer composite. *RSC Advances, 7*(18), 10841-10847. doi: 10.1039/C6RA25350D

Kilbride, B. E., Coleman, J. N., Fraysse, J., Fournet, P., Cadek, M., Drury, A., . . . Blau, W. J. (2002). Experimental observation of scaling laws for alternating current and direct current conductivity in polymer-carbon nanotube composite thin films. *Journal of Applied Physics, 92*(7), 4024-4030. doi: 10.1063/1.1506397

Kim, E., Lim, D. Y., Kang, Y., & Yoo, E. (2016). Fabrication of a stretchable electromagnetic interference shielding silver nanoparticle/elastomeric polymer composite. *RSC Advances, 6*(57), 52250-52254. doi: 10.1039/C6RA04765C

Kim, H., Abdala, A. A., & Macosko, C. W. (2010). Graphene/Polymer Nanocomposites. *Macromolecules, 43*(16), 6515-6530. doi: 10.1021/ma100572e

Kim, M.-S., Yan, J., Joo, K.-H., Pandey, J. K., Kang, Y.-J., & Ahn, S.-H. (2013). Synergistic effects of carbon nanotubes and exfoliated graphite nanoplatelets for electromagnetic interference shielding and soundproofing. *Journal of Applied Polymer Science, 130*(6), 3947-3951. doi: 10.1002/app.39605

Kim, Y. A., Hayashi, T., Endo, M., Gotoh, Y., Wada, N., & Seiyama, J. (2006). Fabrication of aligned carbon nanotube-filled rubber composite. *Scripta Materialia, 54*(1), 31-35. doi: http://dx.doi.org/10.1016/j.scriptamat.2005.09.014

Kuester, S., Barra, G. M. O., Ferreira Jr, J. C., Soares, B. G., & Demarquette, N. R. (2016). Electromagnetic interference shielding and electrical properties of nanocomposites based on poly (styrene-b-ethylene-ran-butylene-b-styrene) and carbon nanotubes. *European Polymer Journal, 77*, 43-53. doi: http://dx.doi.org/10.1016/j.eurpolymj.2016.02.020

Kuester, S., Merlini, C., Barra, G. M. O., Ferreira Jr, J. C., Lucas, A., de Souza, A. C., & Soares, B. G. (2015). Processing and characterization of conductive composites based on poly(styrene-b-ethylene-ran-butylene-b-styrene) (SEBS) and carbon additives: A comparative study of expanded graphite and carbon black. *Composites Part B: Engineering, 84*, 236-247. doi: http://dx.doi.org/10.1016/j.compositesb.2015.09.001

Kuilla, T., Bhadra, S., Yao, D., Kim, N. H., Bose, S., & Lee, J. H. (2010). Recent advances in graphene based polymer composites. *Progress in Polymer Science, 35*(11), 1350-1375. doi: http://dx.doi.org/10.1016/j.progpolymsci.2010.07.005

Kumar, G. S., Vishnupriya, D., Chary, K. S., & Patro, T. U. (2016). High dielectric permittivity and improved mechanical and thermal properties of poly(vinylidene fluoride) composites with low carbon nanotube content: effect of composite processing on phase behavior and dielectric properties. *Nanotechnology, 27*(38), 385702.

Lee, S. S., Park, C. Y., & Lee, D. S. (2008). Properties of nanocomposites based on sulfonated poly(styrene-b-ethylenebutylene-b-styrene) and multiwalled carbon nanotubes. *Colloids and Surfaces A: Physicochemical and Engineering Aspects, 313–314*, 239-241. doi: http://dx.doi.org/10.1016/j.colsurfa.2007.04.101

Li, C., Thostenson, E. T., & Chou, T.-W. (2007). Dominant role of tunneling resistance in the electrical conductivity of carbon nanotube–based composites. *Applied Physics Letters, 91*(22), 223114. doi: 10.1063/1.2819690

Li, J., & Kim, J.-K. (2007). Percolation threshold of conducting polymer composites containing 3D randomly distributed graphite nanoplatelets. *Composites Science and Technology, 67*(10), 2114-2120. doi: http://dx.doi.org/10.1016/j.compscitech.2006.11.010

Li, Y., Chen, C., Li, J.-T., Zhang, S., Ni, Y., Cai, S., & Huang, J. (2010). Enhanced Dielectric Constant for Efficient Electromagnetic Shielding Based on Carbon-Nanotube-Added Styrene Acrylic Emulsion Based Composite. *Nanoscale Research Letters, 5*(7), 1170-1176. doi: 10.1007/s11671-010-9621-2

Li, Y., & Shimizu, H. (2009). Toward a Stretchable, Elastic, and Electrically Conductive Nanocomposite: Morphology and Properties of Poly[styrene-b-(ethylene-co-butylene)-b-styrene]/Multiwalled Carbon Nanotube Composites Fabricated by High-Shear Processing. *Macromolecules, 42*(7), 2587-2593. doi: 10.1021/ma802662c

Lin, J.-H., Lin, Z.-I., Pan, Y.-J., Chen, C.-K., Huang, C.-L., Huang, C.-H., & Lou, C.-W. (2016). Improvement in Mechanical Properties and Electromagnetic Interference Shielding Effectiveness of PVA-Based Composites: Synergistic Effect Between Graphene Nano-Sheets and Multi-Walled Carbon Nanotubes. *Macromolecular Materials and Engineering, 301*(2), 199-211. doi: 10.1002/mame.201500314

Linton, D., Driva, P., Sumpter, B., Ivanov, I., Geohegan, D., Feigerle, C., & Dadmun, M. D. (2010). The importance of chain connectivity in the formation of non-covalent interactions between polymers and single-walled carbon nanotubes and its impact on dispersion. *Soft Matter, 6*(12), 2801-2814. doi: 10.1039/B921170E

Liu, L., Kong, L. B., Yin, W. Y., Chen, Y., & Matitsine, S. (2010). *Microwave Dielectric Properties of Carbon Nanotube Composites*: InTech.

Liu, L., Kong, L. B., Yin, W. Y., & Matitsine, S. (2011). Characterization of Single- and Multiwalled Carbon Nanotube Composites for Electromagnetic Shielding and Tunable Applications. *IEEE Transactions on Electromagnetic Compatibility, 53*(4), 943-949. doi: 10.1109/TEMC.2011.2159798

Liu, Y.-T., Xie, X.-M., & Ye, X.-Y. (2011). High-concentration organic solutions of poly(styrene-co-butadiene-co-styrene)-modified graphene sheets exfoliated from graphite. *Carbon, 49*(11), 3529-3537. doi: http://dx.doi.org/10.1016/j.carbon.2011.04.052

Liu, Y., Song, D., Wu, C., & Leng, J. (2014). EMI shielding performance of nanocomposites with MWCNTs, nanosized Fe3O4 and Fe. *Composites Part B: Engineering, 63*(0), 34-40. doi: http://dx.doi.org/10.1016/j.compositesb.2014.03.014

Liu, Z., Bai, G., Huang, Y., Ma, Y., Du, F., Li, F., . . . Chen, Y. (2007). Reflection and absorption contributions to the electromagnetic interference shielding of single-walled carbon nanotube/polyurethane composites. *Carbon, 45*(4), 821-827. doi: http://dx.doi.org/10.1016/j.carbon.2006.11.020

Loh, K. P., Bao, Q., Ang, P. K., & Yang, J. (2010). The chemistry of graphene. *Journal of Materials Chemistry, 20*(12), 2277-2289. doi: 10.1039/B920539J

Lu, W., Lin, H., & Chen, G. (2006). Nonuniversal transport behavior in heterogeneous high-density polyethylene/graphite nanosheet composites. *Journal of Polymer Science Part B: Polymer Physics, 44*(13), 1846-1852. doi: 10.1002/polb.20842

M. Y. Koledintseva, J. L. D., R. E. DuBroff, K. N. Rozanov, and B. Archambeault. (2009). Modeling of shielding composite materials and structures for microwave frequencies. *Progress In Electromagnetics Research B, 15*, 197-215.

Madani, M. (2009). Conducting carbon black filled NR/ IIR blend vulcanizates: Assessment of the dependence of physical and mechanical properties and electromagnetic interference shielding on variation of filler loading. *Journal of Polymer Research, 17*(1), 53. doi: 10.1007/s10965-009-9289-4

Madhu, B. J., Ashwini, S. T., Shruthi, B., Divyashree, B. S., Manjunath, A., & Jayanna, H. S. (2014). Structural, dielectric and electromagnetic shielding properties of Ni–Cu nanoferrite/PVP composites. *Materials Science and Engineering: B, 186*, 1-6. doi: http://dx.doi.org/10.1016/j.mseb.2014.02.018

Magioli, M., Soares, B. G., Sirqueira, A. S., Rahaman, M., & Khastgir, D. (2012). EMI shielding effectiveness and dielectrical properties of SBS/PAni.DBSA blends: Effect of blend preparation. *Journal of Applied Polymer Science, 125*(2), 1476-1485. doi: 10.1002/app.36338

Mahmoodi, M., Arjmand, M., Sundararaj, U., & Park, S. (2012). The electrical conductivity and electromagnetic interference shielding of injection molded multi-walled carbon nanotube/polystyrene composites. *Carbon, 50*(4), 1455-1464. doi: http://dx.doi.org/10.1016/j.carbon.2011.11.004

Maiti, S., & Khatua, B. B. (2016). Graphene nanoplate and multiwall carbon nanotube–embedded polycarbonate hybrid composites: High electromagnetic interference shielding with low percolation threshold. *Polymer Composites, 37*(7), 2058-2069. doi: 10.1002/pc.23384

Maiti, S., Shrivastava, N. K., Suin, S., & Khatua, B. B. (2013). Polystyrene/MWCNT/Graphite Nanoplate Nanocomposites: Efficient Electromagnetic Interference Shielding Material through Graphite Nanoplate–MWCNT–Graphite Nanoplate Networking. *ACS Applied Materials & Interfaces, 5*(11), 4712-4724. doi: 10.1021/am400658h

Markham, D. (1999). Shielding: quantifying the shielding requirements for portable electronic design and providing new solutions by using a combination of materials and design. *Materials & Design, 21*(1), 45-50. doi: http://dx.doi.org/10.1016/S0261-3069(99)00049-7

Clicours.COM

Matzeu, G., Pucci, A., Savi, S., Romanelli, M., & Di Francesco, F. (2012). A temperature sensor based on a MWCNT/SEBS nanocomposite. *Sensors and Actuators A: Physical, 178*(0), 94-99. doi: http://dx.doi.org/10.1016/j.sna.2012.02.043

McColl, N., Auvinen, A., Kesminiene, A., Espina, C., Erdmann, F., de Vries, E., . . . Schüz, J. (2015). European Code against Cancer 4th Edition: Ionising and non-ionising radiation and cancer. *Cancer Epidemiology, 39, Supplement 1*, S93-S100. doi: http://dx.doi.org/10.1016/j.canep.2015.03.016

McLachlan, D. S., Chiteme, C., Park, C., Wise, K. E., Lowther, S. E., Lillehei, P. T., . . . Harrison, J. S. (2005). AC and DC percolative conductivity of single wall carbon nanotube polymer composites. *Journal of Polymer Science Part B: Polymer Physics, 43*(22), 3273-3287. doi: 10.1002/polb.20597

Meier, J. G., Crespo, C., Pelegay, J. L., Castell, P., Sainz, R., Maser, W. K., & Benito, A. M. (2011). Processing dependency of percolation threshold of MWCNTs in a thermoplastic elastomeric block copolymer. *Polymer, 52*(8), 1788-1796. doi: http://dx.doi.org/10.1016/j.polymer.2011.02.024

Merhi, Z. r. O. (2012). Challeng ing cell phone impact on reproduction: A Review. *Journal of Assisted Reproduction and Genetics, 29*, 293–297. doi: 10.1007/s10815-012-9722-1

Merlini, C., Pegoretti, A., Vargas, P. C., da Cunha, T. F., Ramôa, S. D. A. S., Soares, B. G., & Barra, G. M. O. (2017). Electromagnetic interference shielding effectiveness of composites based on polyurethane derived from castor oil and nanostructured carbon fillers. *Polymer Composites*, n/a-n/a. doi: 10.1002/pc.24501

Micheli, D., Apollo, C., Pastore, R., & Marchetti, M. (2010). X-Band microwave characterization of carbon-based nanocomposite material, absorption capability comparison and RAS design simulation. *Composites Science and Technology, 70*(2), 400-409. doi: https://doi.org/10.1016/j.compscitech.2009.11.015

Mohammed, H. A.-S., & Uttandaraman, S. (2013). X-band EMI shielding mechanisms and shielding effectiveness of high structure carbon black/polypropylene composites. *Journal of Physics D: Applied Physics, 46*(3), 035304.

Mohanraj, G. T., Chaki, T. K., Chakraborty, A., & Khastgir, D. (2006). AC impedance analysis and EMI shielding effectiveness of conductive SBR composites. *Polymer Engineering & Science, 46*(10), 1342-1349. doi: 10.1002/pen.20593

Nazıroglu, M., Yuksel, M., Kose, S. A., & Ozkaya, M. O. (2013). Recent Reports of Wi-Fi and Mobile Phone-Induced Radiation on Oxidative Stress and Reproductive Signaling Pathways in Females and Males. *The Journal of Membrane Biology, 246*, 869–875.

Odom, T. W., Huang, J.-L., Kim, P., & Lieber, C. M. (2000). Structure and Electronic Properties of Carbon Nanotubes. *The Journal of Physical Chemistry B, 104*(13), 2794-2809. doi: 10.1021/jp993592k

Ounaies, Z., Park, C., Wise, K. E., Siochi, E. J., & Harrison, J. S. (2003). Electrical properties of single wall carbon nanotube reinforced polyimide composites. *Composites Science and Technology, 63*(11), 1637-1646. doi: http://dx.doi.org/10.1016/S0266-3538(03)00067-8

Panaitescu, D. M., Gabor, R. A., Nicolae, C. A., Ghiurea, M., Mihailescu, M., & Grigorescu, R. M. (2014). Influence of melt processing induced orientation on the morphology and mechanical properties of poly(styrene-b-ethylene/butylene-b-styrene) block

copolymers and their composites with graphite. *Materials & Design, 64*, 694-705. doi: http://dx.doi.org/10.1016/j.matdes.2014.08.049

Park, S. H., Theilmann, P. T., Asbeck, P. M., & Bandaru, P. R. (2010). Enhanced Electromagnetic Interference Shielding Through the Use of Functionalized Carbon-Nanotube-Reactive Polymer Composites. *IEEE Transactions on Nanotechnology, 9*(4), 464-469. doi: 10.1109/TNANO.2009.2032656

Pavlovsky, S., & Siegmann, A. (2009). Chemical sensing materials. I. Electrically conductive SEBS copolymer systems. *Journal of Applied Polymer Science, 113*(5), 3322-3329. doi: 10.1002/app.30310

Peponi, L., Tercjak, A., Verdejo, R., Lopez-Manchado, M. A., Mondragon, I., & Kenny, J. M. (2009). Confinement of Functionalized Graphene Sheets by Triblock Copolymers. *The Journal of Physical Chemistry C, 113*(42), 17973-17978. doi: 10.1021/jp9074527

Pöllänen, M., Pirinen, S., Suvanto, M., & Pakkanen, T. T. (2011). Influence of carbon nanotube–polymeric compatibilizer masterbatches on morphological, thermal, mechanical, and tribological properties of polyethylene. *Composites Science and Technology, 71*(10), 1353-1360. doi: https://doi.org/10.1016/j.compscitech.2011.05.009

Potts, J. R., Dreyer, D. R., Bielawski, C. W., & Ruoff, R. S. (2011). Graphene-based polymer nanocomposites. *Polymer, 52*(1), 5-25. doi: http://dx.doi.org/10.1016/j.polymer.2010.11.042

Ramôa, S. D. A. S., Barra, G. M. O., Oliveira, R. V. B., de Oliveira, M. G., Cossa, M., & Soares, B. G. (2013). Electrical, rheological and electromagnetic interference shielding properties of thermoplastic polyurethane/carbon nanotube composites. *Polymer International, 62*(10), 1477-1484. doi: 10.1002/pi.4446

Rath, T., & Li, Y. (2011). Nanocomposites based on polystyrene-b-poly(ethylene-r-butylene)-b-polystyrene and exfoliated graphite nanoplates: Effect of nanoplatelet loading on morphology and mechanical properties. *Composites Part A: Applied Science and Manufacturing, 42*(12), 1995-2002. doi: http://dx.doi.org/10.1016/j.compositesa.2011.09.002

Rubin, Z., Sunshine, S. A., Heaney, M. B., Bloom, I., & Balberg, I. (1999). Critical behavior of the electrical transport properties in a tunneling-percolation system. *Physical Review B, 59*(19), 12196-12199.

Sachdev, V. K., Patel, K., Bhattacharya, S., & Tandon, R. P. (2011). Electromagnetic interference shielding of graphite/acrylonitrile butadiene styrene composites. *Journal of Applied Polymer Science, 120*(2), 1100-1105. doi: 10.1002/app.33248

Sahoo, B. P., Naskar, K., & Tripathy, D. K. (2012). Conductive carbon black-filled ethylene acrylic elastomer vulcanizates: physico-mechanical, thermal, and electrical properties. *Journal of Materials Science, 47*(5), 2421-2433. doi: 10.1007/s10853-011-6065-8

Saini, P., & Arora, M. (2012). Microwave Absorption and EMI Shielding Behavior of Nanocomposites Based on Intrinsically Conducting Polymers, Graphene and Carbon Nanotubes. *New Polymers for Special Applications*, 71-112. doi: 10.5772/48779

Schettini, A. R. A., Khastgir, D., & Soares, B. G. (2012). Microwave dielectric properties and EMI shielding effectiveness of poly(styrene-b-styrene- butadiene-styrene) copolymer filled with PAni.Dodecylbenzenesulfonic acid and carbon black. *Polymer Engineering & Science, 52*(9), 2041-2048. doi: 10.1002/pen.23090

Schettini, A. R. A., & Soares, B. G. (2011). Study of Microwave Absorbing Properties of Polyaniline/STF Conducting Composites Prepared by in Situ Polymerization. *Macromolecular Symposia, 299-300*(1), 164-174. doi: 10.1002/masy.200900106

Sharma, S. K., Gupta, V., Tandon, R. P., & Sachdev, V. K. (2016). Synergic effect of graphene and MWCNT fillers on electromagnetic shielding properties of graphene-MWCNT/ABS nanocomposites. *RSC Advances, 6*(22), 18257-18265. doi: 10.1039/C5RA23418B

Singh, K., Ohlan, A., & Dhawan, S. K. (2012). *Polymer-Graphene Nanocomposites: Preparation, Characterization, Properties, and Applications*.

Soldano, C., Mahmood, A., & Dujardin, E. (2010). Production, properties and potential of graphene. *Carbon, 48*(8), 2127-2150. doi: http://dx.doi.org/10.1016/j.carbon.2010.01.058

Spitalsky, Z., Tasis, D., Papagelis, K., & Galiotis, C. (2010). Carbon nanotube–polymer composites: Chemistry, processing, mechanical and electrical properties. *Progress in Polymer Science, 35*(3), 357-401. doi: http://dx.doi.org/10.1016/j.progpolymsci.2009.09.003

Srivastava, S., & Mittal, V. (2017). *Advanced Nanostructured Materials in Electromagnetic Interference Shielding: Advances in Energy, Environment and Polymer Nanocomposites*.

Stanley, H. E. (1977). Cluster shapes at the percolation threshold: and effective cluster dimensionality and its connection with critical-point exponents. *Journal of Physics A: Mathematical and General, 10*(11), L211.

Stoyanov, H., Carthy, D. M., Kollosche, M., & Kofod, G. (2009). Dielectric properties and electric breakdown strength of a subpercolative composite of carbon black in thermoplastic copolymer. *Applied Physics Letters, 94*(23), 232905. doi: 10.1063/1.3154553

Sun, Y., Guo, Z.-X., & Yu, J. (2010). Effect of ABS Rubber Content on the Localization of MWCNTs in PC/ABS Blends and Electrical Resistivity of the Composites. *Macromolecular Materials and Engineering, 295*(3), 263-268. doi: 10.1002/mame.200900242

Tanrattanakul, V., & Bunchuay, A. (2007). Microwave absorbing rubber composites containing carbon black and aluminum powder. *Journal of Applied Polymer Science, 105*(4), 2036-2045. doi: 10.1002/app.26303

Theilmann, P., Yun, D.-J., Asbeck, P., & Park, S.-H. (2013). Superior electromagnetic interference shielding and dielectric properties of carbon nanotube composites through the use of high aspect ratio CNTs and three-roll milling. *Organic Electronics, 14*(6), 1531-1537. doi: http://dx.doi.org/10.1016/j.orgel.2013.02.029

Thomassin, J.-M., Huynen, I., Jerome, R., & Detrembleur, C. (2010). Functionalized polypropylenes as efficient dispersing agents for carbon nanotubes in a polypropylene matrix; application to electromagnetic interference (EMI) absorber materials. *Polymer, 51*(1), 115-121. doi: https://doi.org/10.1016/j.polymer.2009.11.012

Thomassin, J.-M., Jérôme, C., Pardoen, T., Bailly, C., Huynen, I., & Detrembleur, C. (2013). Polymer/carbon based composites as electromagnetic interference (EMI) shielding materials. *Materials Science and Engineering: R: Reports, 74*(7), 211-232. doi: http://dx.doi.org/10.1016/j.mser.2013.06.001

Tong, X. C. (2009). *Advanced Materials and Design for Electromagnetoc Interference Shielding*: CRC Press.

Udmale V, M. D., Gadhave R, Pinjare D, Yamgar R. (2013). Development trends in Conductive Nano-Composites for Radiation Shielding. *Orient J Chem, 29(3)*, 927-936. doi: http://dx.doi.org/10.13005/ojc/290310

Valentini, M., Piana, F., Pionteck, J., Lamastra, F. R., & Nanni, F. (2015). Electromagnetic properties and performance of exfoliated graphite (EG) – Thermoplastic polyurethane (TPU) nanocomposites at microwaves. *Composites Science and Technology, 114*, 26-33. doi: https://doi.org/10.1016/j.compscitech.2015.03.006

Vargas-Bernal, R., Herrera-Perez, G., Calixto-Olalde, M. E., & Tecpoyotl-Torres, M. (2013). Analysis of DC Electrical Conductivity Models of Carbon Nanotube-Polymer Composites with Potential Application to Nanometric Electronic Devices. *Journal of Electrical and Computer Engineering, 2013*, 14. doi: 10.1155/2013/179538

Vasileiou, A. A., Docoslis, A., Kontopoulou, M., Xiang, P., & Ye, Z. (2013). The role of non-covalent interactions and matrix viscosity on the dispersion and properties of LLDPE/MWCNT nanocomposites. *Polymer, 54*(19), 5230-5240. doi: http://dx.doi.org/10.1016/j.polymer.2013.07.034

Wang, D., Nakajima, K., Fujinami, S., Shibasaki, Y., Wang, J.-Q., & Nishi, T. (2012). Characterization of morphology and mechanical properties of block copolymers using atomic force microscopy: Effects of processing conditions. *Polymer, 53*(9), 1960-1965. doi: http://dx.doi.org/10.1016/j.polymer.2012.02.046

Wode, F., Tzounis, L., Kirsten, M., Constantinou, M., Georgopanos, P., Rangou, S., . . . Stamm, M. (2012). Selective localization of multi-wall carbon nanotubes in homopolymer blends and a diblock copolymer. Rheological orientation studies of the final nanocomposites. *Polymer, 53*(20), 4438-4447. doi: http://dx.doi.org/10.1016/j.polymer.2012.08.004

Wu, M., & Shaw, L. (2006). Electrical and mechanical behaviors of carbon nanotube-filled polymer blends. *Journal of Applied Polymer Science, 99*(2), 477-488. doi: 10.1002/app.22255

Wu, Z., Wang, H., Tian, X., Ding, X., Zhou, H., & Ye, X. (2014). Fabrication and properties of carbon nanotube/styrene–ethylene–butylene–styrene composites via a sequential process of (electrostatic adsorption aided dispersion)-plus-(melt mixing). *Journal of Applied Polymer Science, 131*(9), n/a-n/a. doi: 10.1002/app.40227

Xiong, Y., Xie, Y., Zhang, F., Ou, E., Jiang, Z., Ke, L., . . . Xu, W. (2012). Reduced graphene oxide/hydroxylated styrene–butadiene–styrene tri-block copolymer electroconductive nanocomposites: Preparation and properties. *Materials Science and Engineering: B, 177*(14), 1163-1169. doi: http://dx.doi.org/10.1016/j.mseb.2012.05.012

Yonglai, Y., Mool, C. G., & Kenneth, L. D. (2007). Towards cost-efficient EMI shielding materials using carbon nanostructure-based nanocomposites. *Nanotechnology, 18*(34), 345701.

You, F., Wang, D., Cao, J., Li, X., Dang, Z.-M., & Hu, G.-H. (2014). In situ thermal reduction of graphene oxide in a styrene–ethylene/butylene–styrene triblock copolymer via melt blending. *Polymer International, 63*(1), 93-99. doi: 10.1002/pi.4528

Yousefi, N., Sun, X., Lin, X., Shen, X., Jia, J., Zhang, B., . . . Kim, J.-K. (2014). Highly Aligned Graphene/Polymer Nanocomposites with Excellent Dielectric Properties for High-

Performance Electromagnetic Interference Shielding. *Advanced Materials, 26*(31), 5480-5487. doi: 10.1002/adma.201305293

Yue, L., Pircheraghi, G., Monemian, S. A., & Manas-Zloczower, I. (2014). Epoxy composites with carbon nanotubes and graphene nanoplatelets – Dispersion and synergy effects. *Carbon, 78*, 268-278. doi: http://dx.doi.org/10.1016/j.carbon.2014.07.003

Zha, J.-W., Li, W.-K., Liao, R.-J., Bai, J., & Dang, Z.-M. (2013). High performance hybrid carbon fillers/binary-polymer nanocomposites with remarkably enhanced positive temperature coefficient effect of resistance. *Journal of Materials Chemistry A, 1*(3), 843-851. doi: 10.1039/C2TA00429A

Zhang, C.-S., Ni, Q.-Q., Fu, S.-Y., & Kurashiki, K. (2007). Electromagnetic interference shielding effect of nanocomposites with carbon nanotube and shape memory polymer. *Composites Science and Technology, 67*(14), 2973-2980. doi: http://dx.doi.org/10.1016/j.compscitech.2007.05.011

Zhang, Q., Xiong, H., Yan, W., Chen, D., & Zhu, M. (2008). Electrical conductivity and rheological behavior of multiphase polymer composites containing conducting carbon black. *Polymer Engineering & Science, 48*(11), 2090-2097. doi: 10.1002/pen.21079

Zhang, S., Yin, S., Rong, C., Huo, P., Jiang, Z., & Wang, G. (2013). Synergistic effects of functionalized graphene and functionalized multi-walled carbon nanotubes on the electrical and mechanical properties of poly(ether sulfone) composites. *European Polymer Journal, 49*(10), 3125-3134. doi: http://dx.doi.org/10.1016/j.eurpolymj.2013.07.011

Zhao, L., Li, Y., Qiu, J., You, J., Dong, W., & Cao, X. (2012). Reactive bonding mediated high mass loading of individualized single-walled carbon nanotubes in an elastomeric polymer. *Nanoscale, 4*(20), 6613-6621. doi: 10.1039/C2NR31401K

Zhu, Y., Murali, S., Cai, W., Li, X., Suk, J. W., Potts, J. R., & Ruoff, R. S. (2010). Graphene and Graphene Oxide: Synthesis, Properties, and Applications. *Advanced Materials, 22*(35), 3906-3924. doi: 10.1002/adma.201001068

Zucolotto, V., Avlyanov, J., & Mattoso, L. H. C. (2004). Elastomeric conductive composites based on conducting polymer–modified carbon black. *Polymer Composites, 25*(6), 617-621. doi: 10.1002/pc.20056